A Fundamental Study of Refrigerant Line Transients

J. C. Shelton and A. M. Jacobi

ACRC CR-4 March 1995

For additional information:

Air Conditioning and Refrigeration Center
University of Illinois
Mechanical & Industrial Engineering Dept.
1206 West Green Street
Urbana, IL 61801

(217) 333-3115

The Air Conditioning and Refrigeration Center was founded in 1988 with a grant from the estate of Richard W. Kritzer, the founder of Peerless of America Inc. A State of Illinois Technology Challenge Grant helped build the laboratory facilities. The ACRC receives continuing support from the Richard W. Kritzer Endowment and the National Science Foundation. The following organizations have also become sponsors of the Center.

Acustar Division of Chrysler
Amana Refrigeration, Inc.
Brazeway, Inc.
Carrier Corporation
Caterpillar, Inc.
Delphi Harrison Thermal Systems
E. I. du Pont de Nemours & Co.
Eaton Corporation
Electric Power Research Institute
Ford Motor Company
Frigidaire Company
General Electric Company
Lennox International, Inc.
Modine Manufacturing Co.
Peerless of America, Inc.
U. S. Army CERL
U. S. Environmental Protection Agency
Whirlpool Corporation

For additional information:

Air Conditioning & Refrigeration Center
Mechanical & Industrial Engineering Dept.
University of Illinois
1206 West Green Street
Urbana IL 61801

217 333 3115

Executive Summary

Dangerous pressure excursion incidents in industrial refrigeration systems have been attributed to condensation-induced shock and vapor-propelled liquid slugging. Because of industry trends towards the use of alternate refrigerants and centralized systems and the resulting higher localized volumes of potentially dangerous refrigerants, the occurrence of hydraulic shocks in refrigeration systems has become a critical issue. Although the initiating mechanisms of condensation-induced shock and vapor-propelled liquid slugging are not well understood, these transients have important implications on system maintenance, repair costs, system down-time, and public safety. The purpose of this research was to provide system designers and operators with methods for avoiding these transients. This objective was accomplished through the review of two-phase flow regimes, the analysis of the generic causes and resulting pressure surges of condensation-induced shock and vapor-propelled liquid slugging, and by the study of the critical flow regimes that occur in industrial refrigeration systems.

After an introduction in Chapter 1, a review of two-phase flow regimes is presented in Chapter 2. This survey includes a study of variations in flow patterns due to flow configurations, alternate fluids, and refrigerant-oil effects. In Chapter 3 the characteristics of condensation-induced shock, including the effects of various flow properties on the magnitude of the shock, are discussed. A similar review of vapor-propelled liquid slugging is presented in Chapter 4, where a discussion of the initiating mechanisms is followed by an example analysis of the potential shock due to slug impact. Critical flow regimes are discussed in the context of industrial refrigeration systems in Chapter 5. In Chapter 6, the results are applied to develop flow models and shock maps that indicate what design and operating conditions are susceptible to hydraulic shocks. Finally, in Chapter 7, we summarize recommendations for avoiding condensation-induced shock and vapor-propelled liquid slugging in refrigeration systems. These recommendations are given in condensed form below:

- Install valves or valve combinations that allow the gradual release of flow from high to low pressure pipes.
- Do not depend on pressure relief valves for the prevention of hydraulic shock because the transient is too fast to trigger the opening of the valve.
- Avoid piping configurations that trap liquid in hot-gas or suction lines. Do not allow refrigerant to condense and stand in the hot-gas main.
- Carefully and completely pump out evaporators before the initiation of hot-gas defrost.
- Do not position check valves so that liquid can become trapped between the check valve and any other device.
- Do not operate a refrigeration system in the "susceptible" region of the flow and shock maps provided in this report.
- Check the mechanical integrity of the piping system (e.g., welds) to reduce the possibility of a system failure during a hydraulic shock.

The appendices of this report present the details of the flow model, a derivation of the handbook approach for predicting flow through a valve and graphical representations of the results, shock maps valid for a wide range of designs, a detailed annotated bibliography, and a discussion of experiments that can be used to verify this theoretical study.

Through this research we have developed a rational method for predicting and preventing the occurrence of condensation-induced shock and vapor-propelled liquid slugging in refrigeration systems. This contribution was achieved by developing a detailed understanding of the two-phase flow and operating conditions, by developing a theoretical model based on this understanding, and by applying this model to relevant system scenarios.

Table of Contents

Nomenclature iii

1. Introduction 1

2. Two-Phase Flow 3

2.1 A Description of Two-Phase Flow Regimes 3

2.1.1 Horizontal Fluid Flows 3

2.1.2 Vertical Flow Regimes 5

2.2 Flow Regime Maps 8

2.2.1 Horizontal Flow Maps 8

2.2.2 Vertical Flow Maps 13

2.3 Countercurrent Flow Transitions 18

2.4 Applicability of Flow Maps 20

2.5 Oil Concentration Effects 23

3. Condensation-Induced Shock 26

3.1 Liquid Inertia Limits 26

3.1.1 Incompressible Limit 26

3.1.2 Compressibility Effects 27

3.2 Heat Transfer Effects 28

4. Vapor-Propelled Liquid Slugging 30

4.1 Influences on Vapor-Propelled Liquid Slug Initiation 30

4.1.1 Fluid Flow Effects 30

4.1.2 Fluid Property Effects 31

4.1.3 Piping Configuration Effects 33

4.2 Pressure Calculations 34

5. Critical Flow Regimes in Refrigerant Piping 38

5.1 Hot Gas Defrost 38

5.2 Hydraulic Shock During Hot Gas Defrost 40

6. Flow Analysis 42
6.1 Flow Model 42
6.2 Handbook Method 45
6.3 Shock Maps 47
6.4 Use of the Shock Maps 49

7. Conclusions and Recommendations 50

References 54

Appendix A: Flow Model Derivation 57
Appendix B: Handbook Method for Flow Calculations 62
Appendix C: Handbook Maps 67
Appendix D: Shock Maps 77
Appendix E: Experimental Design for the Study of Hydraulic Shocks 86
Appendix F: Annotated Bibliography 90

Nomenclature

a	speed of sound or acceleration	ft / s, ft / s^2
A	flow cross-sectional area	ft^2
c	specific heat	Btu / (lbm·° F)
c_p	constant pressure specific heat	Btu / (lbm·° F)
c_v	constant volume specific heat	Btu / (lbm·° F)
C_v	flow coefficient	dimensionless
D	diameter	ft
f	friction factor	dimensionless
F	force or modified Froude number [Eq. (2.2)]	lbf, dimensionless
F_K	ratio of specific heats factor [Eq. (B.23)]	dimensionless
F_P	piping geometry factor [Eq. (B.27)]	dimensionless
g	gravity	ft / s^2
G	gas specific gravity at standard conditions; = 1for air at standard conditions (also defined as the ratio of molecular weights of gas over air)	dimensionless
h	heat transfer coefficient	Btu / (hr·ft^2·° R)
h_G	vapor depth	ft
h_L	liquid depth	ft
h_{fg}	latent heat	Btu / lbm
h_l	head loss	ft^2 / s^2
i	enthalpy	Btu / lbm
Ja	Jakob number [Eq. (3.3)]	dimensionless
k	head loss coefficient [Eq. (B.3)]	dimensionless
K	product of the modified Froude number and the square root of the superficial Reynolds number [Eq. (2.4)]	dimensionless

l_E	entry length	ft
m	mass	lbm
$\dot{m}$	mass flow rate	lbm / s
M	Mach number [Eq. (A.9)]	dimensionless
P	pressure	lbf / in^2
Q	volumetric flow rate	ft^3 / s
Q	condensation rate	lbm / s
r	radius	ft
R	gas constant or radius of vapor / liquid interface	ft·lbf / lbm·° R, ft
Re	Reynolds number	dimensionless
s	Jeffrey's sheltering coefficient [Eq. (2.7)]	dimensionless
S	perimeter	ft
T	temperature or ratio of turbulent to gravitational forces [Eq. (2.3)]	° R, dimensionless
U	velocity	ft / s
U_{GS}	superficial vapor velocity; velocity of the vapor phase if it were traveling alone in the pipe	ft / s
U_{LS}	superficial liquid velocity; velocity of the liquid phase if it were traveling alone in the pipe	ft / s
x	distance or pressure drop ratio [Eq. (B.24)]	ft, dimensionless
x_T	pressure drop ratio factor [Eq. (B.22)]	dimensionless
X	Lockhart-Martinelli parameter [Eq. (2.1)]	dimensionless
Y	expansion factor [Eq. (B.22)]	dimensionless
Z	compressibility factor [Eq. (B.27)]	dimensionless

Greek

α	pipe inclination	degrees
γ	ratio of specific heats, c_p / c_v	dimensionless
Φ	volume fraction of liquid in slugs	dimensionless
ρ	density	lbm / ft^3
σ	interfacial tension	lbf
τ	time	s
υ	kinematic viscosity	ft^2 / s

Subscripts and Superscripts

a	air
c	critical; property of the fluid at the critical point
G	vapor
i	interfacial
L	liquid
M	mixture
n	exponent [Eq. (2.11)]
orf	orifice
r	reduced
S	superficial; phase velocity if only that phase existed in the pipe
t	stagnation; thermodynamic reference state reached when the fluid is isentropically brought to a state of zero velocity and zero potential
w	water
1	valve inlet
2	valve exit
o	initial condition
~	dimensionless parameter

Chapter 1

Introduction

Several pressure excursion incidents in industrial refrigeration systems have been attributed to two mechanisms of hydraulic shock: condensation-induced shock and vapor-propelled liquid slugging. As the refrigeration industry moves toward the use of alternate refrigerants and centralized systems, the occurrence of hydraulic shocks in refrigeration systems becomes a critical issue. Although the initiating mechanisms of condensation-induced shock and vapor-propelled liquid slugging are not well understood, these transients have important implications on system maintenance, repair costs, system down-time, and public safety.

The purpose of this work is to provide system designers and operators with methods for avoiding these transients. The main objectives are accomplished by reviewing two-phase flow regimes, by analyzing the generic causes and resulting pressure surges of condensation-induced shock and vapor-propelled liquid slugging, and by studying the critical flow regimes that occur in industrial refrigeration systems. In Chapter 2, an overview of two-phase flow regimes is presented. This review includes the variations in flow patterns due to flow configurations, alternate fluids, and refrigerant-oil mixtures. The ability of flow maps to predict flow regimes under these various situations is also discussed.

Chapters 3 and 4 focus on the occurrences of hydraulic shocks. Chapter 3 analyzes the characteristics of condensation-induced shock, including the effects that various flow properties have on the magnitude of the shock. A similar review of vapor-propelled liquid slugging is presented in Chapter 4. Besides examining the initiating mechanisms of the shock, this chapter also analyzes the pressure surges that may result in a refrigeration system.

The remaining chapters apply the hydraulic shock analyses to refrigeration systems. Chapter 5 establishes the parts of industrial refrigeration systems that are susceptible to condensation-induced shock and vapor-propelled liquid slugging. A theoretical model of the initiation of these

shocks is developed in Chapter 6. Flow maps are developed from this model to provide a graphical tool for determining the flow conditions present in a system. To make this tool more applicable, maps are also created using a handbook method that is currently used in industry. Shock maps are developed to establish the flow conditions necessary for shock initiation. The flow and shock maps are used together to determine when a system is susceptible to hydraulic shock. Supplemental to this graphical analysis method, suggestions for system and operation changes are given in Chapter 7. The combination of these recommendations and the flow analysis provides an effective method with which to avoid hydraulic shocks.

Chapter 2

Two-Phase Flow

2.1 A Description of Two-Phase Flow Regimes

In a two-phase liquid-vapor flow, many variations in the pattern of the flow are possible. Observations indicate, however, that these flow patterns may be naturally grouped by the relative location and behavior of the fluid phases within the flow. The defining of flow regimes is an attempt to establish the unique characteristics of each significant flow pattern. Many descriptions of flow patterns have been proposed in the literature. Therefore, for the sake of clarity, it is necessary to define the flow regimes that will be use in this study.

2.1.1 Horizontal Fluid Flows

Forces such as gravity and interfacial shear play significant roles in determining the flow regime in horizontal two-phase flows (Manwell, 1989). At low liquid and vapor velocities, the liquid phase flows continuously along the bottom of the conduit and the vapor phase flows in a similar manner along the top. Due to the low phase velocities and the stabilizing affect of gravity, there is generally a smooth interface between the two phases. This flow pattern is called *stratified* or *stratified-smooth* flow. As the velocity of the vapor phase is increased, finite disturbances occur at the liquid-vapor interface. These disturbances create waves on the liquid surface. The flow pattern, however, is still characterized by the vertical separation of the two phases. This regime is therefore referred to as *stratified-wavy* flow. The combination of stratified-smooth and stratified-wavy flows makes up the stratified flow regime, as shown in Figure 2.1.

During stratified-wavy flow, the increased vapor velocity reduces the vapor pressure over the waves on the liquid-vapor interface, creating a Bernoulli lifting force (Taitel and Dukler, 1976).

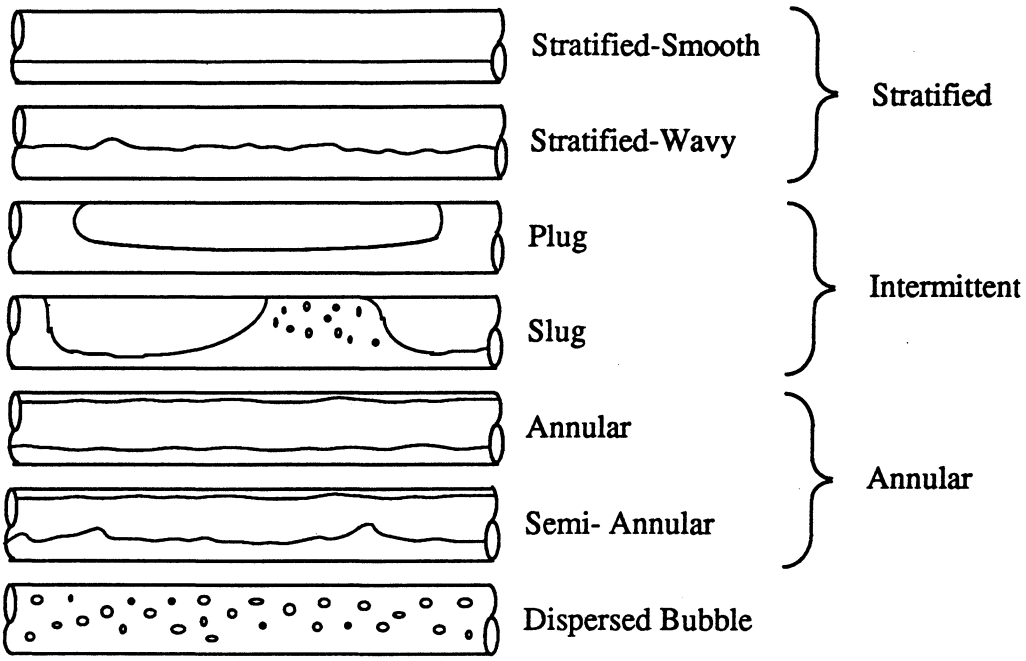

Figure 2.1. Diagrams of various two-phase flow regimes for horizontal fluid flows (Dukler and Taitel, 1986).

This lifting force on the waves is countered by the stabilizing effect of gravity. Therefore, the growth of a wave depends on the balance of these two forces. As the velocity of the vapor phase is increased the Bernoulli lifting force increases until it overcomes the stabilizing effects of gravity. When this occurs, the wave will grow to bridge the conduit and the stratified-wavy flow will undergo transition to either *intermittent* or *annular* flow, depending on the amount of liquid present.

In order for intermittent flow to occur, there must be enough liquid in the conduit to completely bridge the pipe. The intermittent flow regime is characterized by a nonuniform distribution of the liquid phase in the axial direction and consists of *slug* and *plug* flow (see Figure 2.1). During slug flow, waves of liquid bridge the conduit and are propelled downstream by the vapor phase. These slugs are separated by regions of vapor flowing over a stratified liquid layer. An important characteristic of the slugs is the degree of aeration of the liquid phase. Plug flow is considered to be the limiting case when there are no entrained vapor bubbles in the liquid.

This flow pattern appears similar to slug flow and consists of large, elongated bubbles located in the upper portion of the conduit and separated by regions of liquid. The other limiting case is when the degree of aeration of the liquid causes the slug to become unstable. This flow pattern is called *pseudo-slug* flow because the slug is no longer capable of continually bridging the conduit. Such a flow is very close to a transition to annular flow.

When the amount of liquid in the conduit is insufficient to completely bridge the pipe, transition to *annular* flow occurs. During annular flow the liquid phase flows as a film around the pipe perimeter. The film surrounds a core of high velocity vapor which may contain entrained liquid droplets. During annular flow, the liquid phase is equally distributed about the pipe wall. The annular regime also consists of *semi-annular* or *wavy-annular* flow. Semi-annular often occurs during the transition from the stratified-wavy to the annular flow regime. The physical features of this flow pattern are therefore a combination of these two flow regimes. In semi-annular flow, the liquid phase covers the entire circumference of the pipe; however, the majority of the liquid flows along the bottom of the pipe and maintains a wavy interface with the vapor phase.

The final flow pattern for horizontal two-phase flows is the dispersed bubble regime. As its name indicates, the dispersed bubble flow regime consists of vapor bubbles distributed throughout the liquid phase in the pipe, as shown in Figure 2.1. Dispersed bubble flow occurs when the liquid flow rate is much higher than the vapor flow rate. Dukler and Taitel (1986) suggest that transition to dispersed bubble flow from intermittent flow occurs when the turbulent fluctuations are strong enough to overcome the buoyant forces that keep the vapor phase at the top of the conduit.

2.1.2 Vertical Flow Regimes

The various types of flow regimes that occur in vertical two-phase flows are similar to the regimes presented for horizontal two-phase flows. The physical characteristics of vertical flows are inherently different, however, since the force of gravity acts as a tangential force rather than as a normal force as it does for horizontal flows. Therefore, the various flow regimes and the

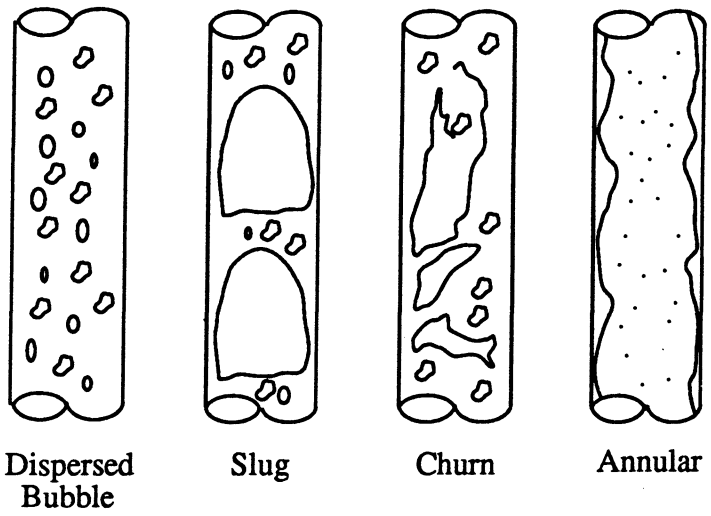

Figure 2.2. Diagram of various two-phase flow regimes for vertical fluid flows (Dukler and Taitel, 1986).

conditions that cause them are dependent upon whether the fluid flow is in the upward or downward direction. The simplest type of vertical flow pattern is the *bubble* flow regime. This regime resembles horizontal dispersed bubble flow in that it consists of a continuous liquid phase containing vapor bubbles distributed throughout the flow. The smaller bubbles are spherical and flow in a rectilinear motion. Larger bubbles, however, may become deformed and therefore follow a random path. Sometimes smaller bubbles intermittently coalesce to form larger bubbles with spherical caps, but with diameters insufficient to bridge the entire pipe. An example of this flow regime is shown in Figure 2.2. For concurrent upflows, bubble flow exists at low vapor velocities. As the liquid velocity is increased, the flow remains in the bubble flow regime, and turbulence in the liquid phase breaks up the larger bubbles in the flow so that only small bubbles are present. This type of bubble flow is known as *dispersed bubble* flow. In concurrent downflow, dispersed bubble flow occurs at high liquid velocities where the turbulent effects of the liquid phase are sufficient to break apart the slugs in the flow. Therefore, even though bubble flow is present in both concurrent upflow and downflow, the characteristic phase velocities of the flows are substantially different.

A second type of flow pattern that occurs in vertical two-phase flow is the slug flow regime.

Although this regime is similar in appearance to the slug flow pattern that occurs in horizontal piping systems, the physical characteristics are distinctly different. In vertical slug flow, the vapor phase flows mostly in large bullet-shaped bubbles that occupy most of the pipe's cross-sectional area and can vary in length from one tube diameter to over a hundred diameters. These bubbles are sometimes referred to as "Taylor bubbles" (Taitel, *et al.*, 1980). The Taylor bubbles are separated radially from the wall by a thin liquid film that flows in the opposite direction of the bubbles. Axially, successive Taylor bubbles are separated by slugs of liquid that form stable bridges across the conduit. Therefore, as in horizontal slug flows, the velocity of the slugs is equal to that of the superficial vapor velocity. In concurrent upflows, transition from bubble to slug flow occurs when the vapor velocity is sufficient to cause the unrestricted coalescence of small bubbles into the larger Taylor bubbles. In concurrent downward flows, however, the slug flow regime is reached by increasing the liquid phase velocity until there is a sufficient amount of liquid to bridge the pipe.

A third type of flow pattern, *churn* flow, is actually considered an entry length phenomenon that precedes the existence of slug flow (Dukler and Taitel, 1986). Churn flow resembles a chaotic version of slug flow because the slugs of liquid are too short to maintain a stable bridge between two successive Taylor bubbles. As a slug deteriorates, the liquid from the slug falls down in a film around the bubble. The falling film causes the bubble to become narrow and distorted. The liquid from the film then accumulates in the following slug, causing a large degree of aeration in that slug. As a result, the bridge of the pipe becomes unstable and the slug begins to deteriorate in the same manner as the previous slug. With each successive breaking up of a liquid slug, the lengths of the following slugs and Taylor bubbles become longer and thus more stable. Eventually, the length of the slug is large enough that a competent, stable bridge is formed between the two Taylor bubbles. At this point, transition to slug flow occurs. In concurrent upflows, churn flow occurs at vapor velocities higher than those associated with slug flow. This is because the increased amount of vapor aerates and destabilizes the slugs. In downward vertical flows, though, the vapor phase does not lift the liquid slug. Therefore,

increases in vapor velocity only serve to increase the velocity of the slugs and churn flow does not exist.

The final type of vertical two-phase flow pattern is annular flow. This flow regime resembles annular flow in horizontal configurations in that the liquid flows as a film on the pipe walls and surrounds a vapor core. However, since gravity acts axially rather than normally, the liquid film is more evenly distributed about the pipe circumference. Furthermore, since there is no longer a normal force to retain the liquid phase against the piping wall, there is a higher concentration of liquid droplets in the vapor core, and larger waves on the surface of the liquid phase. Annular flow occurs at substantially different vapor flow rates for vertical upflow and downflow. For concurrent vertical upflow, annular flow occurs at high vapor velocities sufficient to lift the liquid phase. In concurrent vertical downflow, however, annular flow occurs at low liquid and vapor velocities.

2.2 Flow Regime Maps

The physical characteristics of each two-phase flow pattern are significantly different. These differences directly affect the heat transfer and pressure drop associated with each flow regime. This makes the determination of the type of flow in a pipe crucial to two-phase flow analyses. The flow pattern in a pipe is determined by the characteristics of the flow, the properties of working fluid, and the physical properties of the piping system. Within each flow regime, however, the same approximate empirical laws govern the flow (Shah, 1975). Flow regime maps attempt to use these laws to establish correlations or theoretical relationships that predict which flow regime will occur for given fluid, piping, and flow conditions.

2.2.1 Horizontal Flow Maps

One of the first flow regime maps created for horizontal pipes was developed by Baker (1954). Since Baker's map, most flow regime maps have been based on experimental data. These correlations are completely empirical and are without any basis in the mechanisms responsible for flow transition (Dukler and Taitel, 1986). Therefore, although most of these

correlations accurately predict the data upon which they are based, the maps are only good for a narrow range of parameters. Present flow maps are sensitive to changes in pipe diameter, fluid properties, and pipe inclination (Andritsos, *et al.*, 1992). There is a need for generalized flow maps that can predict flow patterns for a variety of parameters and flow conditions.

The mechanistic approaches to developing flow maps can be divided into four groups (Kordyban, 1990). The first type of flow map relies on an analysis of Kelvin-Helmholtz instabilities of the interfacial waves based on the wave motion equations. These analyses indicate that slug formation is heavily dependent on wave length. The second approach also considers Kelvin-Helmholtz instabilities, but evaluates stability using the Bernoulli equation rather than wave motion. This theory offers a better explanation of experimental results by showing slug initiation to be dependent on the proximity of the wave to the top of the pipe and independent of wavelength. The third approach is based on a kinetic energy analysis of the fluid flow. Slug transition is shown to be a function of the energy flux between the high and low liquid levels. While this method seems unique in its approach, it has been proposed that this energy analysis and the Kelvin-Helmholtz analysis are two separate descriptions of the same physical phenomenon (Kordyban, 1990). The most recent method for developing a flow map consists of introducing a linear instability into a flow model that includes the effects of friction and inertia. This final correlation technique is considered by some to be an advancement over previous analyses (Kordyban, 1990).

As will be discussed in subsequent chapters, the onset of liquid slugging is directly related to the occurrence of vapor-propelled liquid slugging and condensation-induced shock. Each flow map must have a defined criterion for slug transition. Most predictions of transition are based on a Kelvin-Helmholtz instability analysis of liquid waves. In this case, the height of the liquid in the pipe is the limiting factor for transition. An alternative criterion is that transition occurs due to Kelvin-Helmholtz instabilities at the crest of the liquid waves (Kordyban, 1990). Under this assumption, transition is limited by the proximity of the wave crest to the top of the pipe (Kordyban and Okleh, 1992). Another alternate approach involves assuming that slug transition

occurs when the energy flux between the high and low liquid levels reaches a maximum; this is believed to be identical to the first (Kordyban, 1990). A third approach is to compare the gas stagnation pressure at the base of a wave pushing up a lump of liquid and the Bernoulli lift forces acting at the wave's crest to the restoring hydrostatic forces of the flow (Wallis and Dobson, 1973).

A flow regime map that many researchers use as a standard for comparison is the flow regime map by Taitel and Dukler (1976), shown in Figure 2.3. Unlike other flow maps, the Taitel and Dukler map uses three separate coordinate systems to plot the transition criteria between the various flow regimes. The argument for using multiple variables is that different parameters control each flow transition. Therefore, more than one coordinate system is required to accurately describe the various transitions. The coordinates of the Taitel and Dukler map are defined as:

$$X = \left[\frac{(dP/dx)_{LS}}{(dP/dx)_{GS}}\right]^{\frac{1}{2}} \tag{2.1}$$

$$F = \sqrt{\frac{\rho_G}{(\rho_G - \rho_L)}}\left[\frac{U_{GS}}{\sqrt{Dg\cos\alpha}}\right] \tag{2.2}$$

$$T = \left[\frac{|(dP/dx)_{LS}|}{(\rho_L - \rho_G)g\cos\alpha}\right]^{\frac{1}{2}} \tag{2.3}$$

$$K = \left[\frac{\rho_G (U_{GS})^2 U_{LS}}{(\rho_L - \rho_G)g\,\upsilon_L \cos\alpha}\right]^{\frac{1}{2}} \tag{2.4}$$

where X is the Lockhart-Martinelli number, F is the Froude number modified by a density ratio, T is a ratio of turbulent to gravitational forces, and K is the product of the modified Froude number and the square root of the superficial Reynolds number. Each of the transition criterion has been nondimensionalized in terms of these coordinates. The specific coordinates that correspond to each transition are given in Figure 2.3. In order for the transition from stratified-wavy flow to occur there must be sufficient energy input into the liquid surface to cause rapid

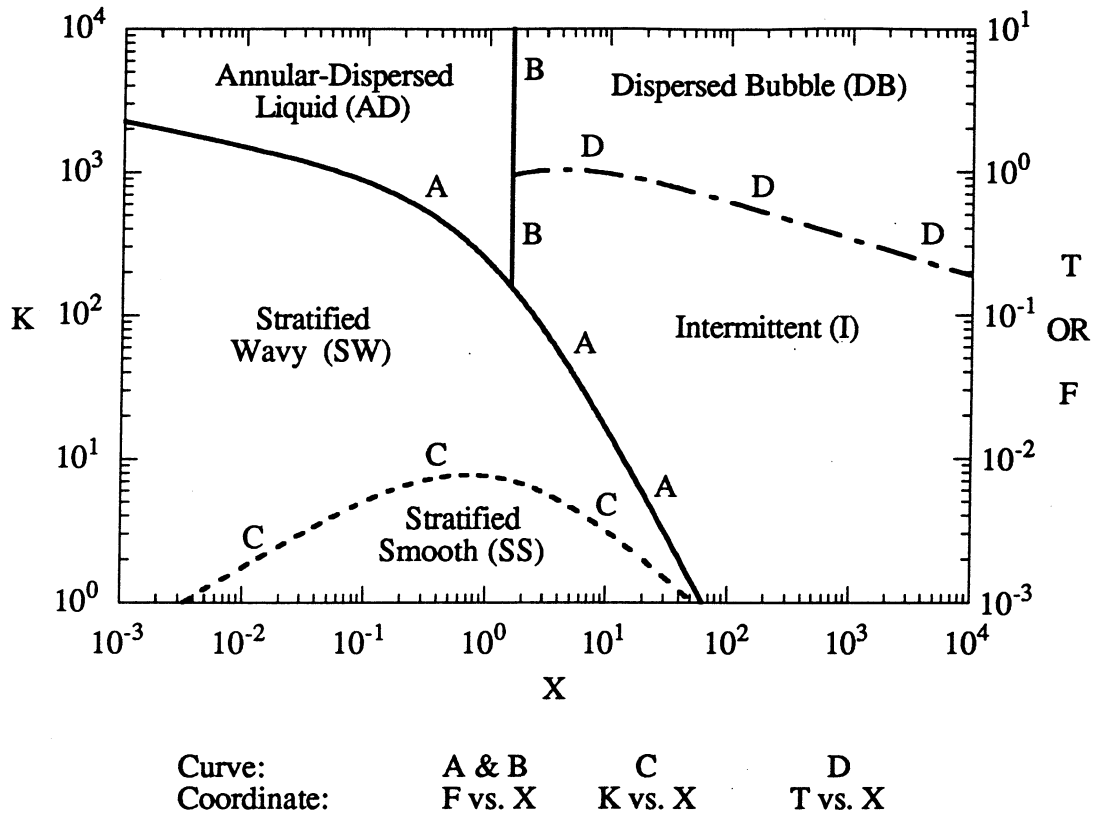

Figure 2.3. Plot of Taitel and Dukler (1976) flow regime map for horizontal flow.

wave growth. The criterion used by Taitel and Dukler for the occurrence of this transition is based on Kelvin-Helmholtz instabilities with wave stability determined by the Bernoulli equation. The criterion may be written as follows:

$$U_G \geq \left(1-\frac{h_L}{D}\right)\left[\frac{(\rho_L-\rho_G)\,g\cos\alpha\,A_G}{\rho_G\,(dA_L/dh_L)}\right]^{\frac{1}{2}} \tag{2.5}$$

In dimensionless form, this criterion becomes

$$F^2\left(\frac{1}{(1-h_L/D)^2}\frac{\tilde{U}_G^2\,d\tilde{A}_L/d\tilde{h}_L}{\tilde{A}_G}\right) \geq 1 \tag{2.6}$$

where ~ indicates a dimensionless quantity. The reference variables used to nondimensionalize equation 2.6 are D for length, D^2 for area, and U_{GS} and U_{LS} for the vapor and liquid velocities, respectively. This transition criterion is represented by curve A in Figure 2.3.

Transition from stratified-wavy flow can be to either the annular or slug flow regime. The regime that will occur therefore depends on the transition criterion between annular and slug flow. For slug flow to occur there must be sufficient liquid present to form a stable bridge across the conduit. Taitel and Dukler give this condition in nondimensional terms as h_L / D greater than 0.35 to 0.50, depending on the flow conditions. The criterion, plotted as line B in Figure 2.3, is considered to be 0.35 for this work since to predict all cases for which hydraulic shocks may occur it is necessary to account for the worst case scenario. It should be noted that, according to the Taitel and Dukler flow map, for a liquid inventory less than $h_L / D = 0.35$ slug flow can not occur, no matter what phase velocities or flow conditions are present.

Transition from stratified-smooth to stratified-wavy occurs when the velocity of the vapor phase is sufficient to cause wave growth but not large enough to create the rapid wave growth required for transition to slug or annular flow. The criterion given by Taitel and Dukler is that the pressure and shear forces on a wave must overcome the viscous dissipation in the wave. This criterion may be written as:

$$U_G \geq \left[\frac{4\,\upsilon_L(\rho_L-\rho_G)\,g\cos\alpha}{s\,\rho_G U_L}\right]^{\frac{1}{2}} \tag{2.7}$$

where s is a Jeffrey's sheltering coefficient and has been determined by theory and experiment to be 0.01 (Dukler and Taitel, 1986). In nondimensional form equation (2.7) may be written as:

$$K^2 = \left[\frac{\rho_G\,(U_{GS})^2}{(\rho_L-\rho_G)\,D\,g\cos\alpha}\right]\left(\frac{D\,U_{LS}}{\upsilon_L}\right) \tag{2.8}$$

where K is a nondimensional parameter defined as:

$$K = \sqrt{F^2\,Re_{LS}} \tag{2.9}$$

This transition criterion is plotted as line C in Figure 2.3.

The final transition occurs between intermittent and dispersed bubble flow. Taitel and Dukler propose that this transition takes place at high liquid velocities when the turbulent forces of the liquid phase are strong enough to overcome the buoyant forces that tend to keep the vapor

phase at the top of the conduit. Mathematically, this criterion is written as

$$U_L \geq \left[\frac{4A_G}{S_i} \frac{g \cos\alpha}{f_L} \left(1 - \frac{\rho_G}{\rho_L} \right) \right]^{\frac{1}{2}} \tag{2.10}$$

where f_L is the liquid friction factor. Expressing this equation in nondimensional form results in:

$$T^2 \geq \frac{8 \tilde{A}_G}{\tilde{S}_i \tilde{U}_L^2 \left(\tilde{U}_L \tilde{D}_L \right)^{-n}} \tag{2.11}$$

where n = 0.2 when the flow of the liquid is turbulent and n = 1.0 when the flow is laminar.

The dimensionless quantities used to express the transition criteria include pipe diameter, pipe inclination, phase densities, laminar and turbulent effects, phase viscosities, and phase velocities. It is therefore expected that the Taitel and Dukler's flow map is applicable to a larger range of fluids and flow conditions than most maps. The scope of this map is still limited, and it may not be valid for large changes from the parameters on which it is based.

2.2.2 Vertical Flow Maps

Flow regime maps for vertical fluid flows have the same format as those for horizontal fluid flows. There are significant differences, however, in the flow patterns and transition criteria due to the differing impact of gravity. The force of gravity is always normal to the flow direction for horizontal piping systems. For vertical fluid flows gravity acts tangentially and its effects depend on whether the fluid flow direction is upward or downward. As a result, flow transition criteria for vertical flow regimes are divided into upflow and downflow arrangements.

Like horizontal flow regime maps, most vertical flow regime maps are based on correlations of experimental results. Such maps are accurate only for the narrow range of parameters upon which they are based. It is desirable to have general transition criteria that are valid over a wide range of fluid and flow parameters. For this reason, and for the sake of consistency, the transition criteria of Dukler and Taitel (1986) are used to predict the regime transitions for concurrent vertical upflow and downflow. Plots of these criteria are given in Figures 2.4 and 2.5, respectively. Unlike the horizontal flow regime maps, the only set of coordinates used for these regime maps are superficial liquid and vapor velocities.

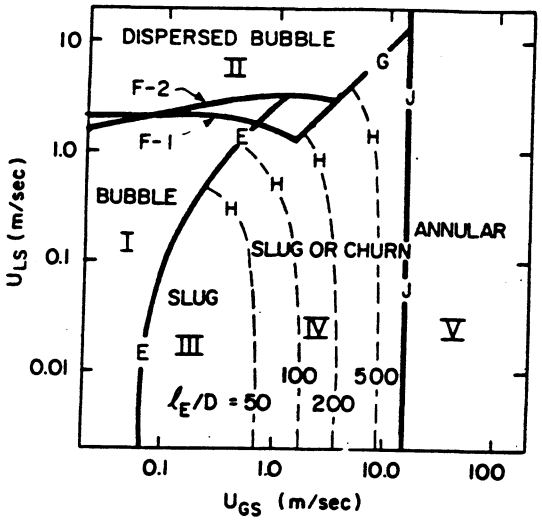

Figure 2.4. Plot of the Dukler and Taitel (1986) flow regime map for upward vertical flow.

For concurrent vertical upflow, bubble flow exists at low liquid and vapor velocities. This flow regime is shown as zone I in Figure 2.4. During bubble flow some of the bubbles in the vapor phase coalesce into larger bubbles. As the vapor velocity of the flow increases, the number density of the bubbles increases. Eventually the bubbles become so closely packed that the rate of coalescence is sufficient for a transition to slug flow. Since the rate of agglomeration is directly dependent upon the number density of the bubbles present, the criterion for transition from bubble flow to slug flow is based on the void fraction. Experiments and calculations have determined this void fraction to be in the range of 0.25 to 0.30. Dukler and Taitel have presented this criterion as the vapor flow rate necessary to produce a void fraction greater than 0.25 for a given liquid flow. It may be expressed as

$$U_{LS} = 3.0 U_{GS} - \left[\frac{g(\rho_L - \rho_G)\sigma}{\rho_L^2}\right]^{\frac{1}{4}} \qquad (2.12)$$

where σ is the interfacial tension. This transition criterion is represented by line E in Figure 2.4.

During bubble flow, increases in the liquid velocity magnify the turbulent effects of the liquid. These forces act to break up the bubbles in the vapor phase into smaller bubbles.

Eventually, the turbulent dispersive forces become sufficient to break up the vapor bubbles and to prevent transition to slug flow, even for void fractions above 0.25. This flow is called dispersed bubble flow. Although similar to bubble flow, dispersed bubble flow differs in that the larger bubbles no longer exist and the void fraction of the fluid is greater than 0.25. This flow regime is shown in Figure 2.4 as zone II. It should be noted, however, that turbulent forces can only delay transition to slug flow. If the size of the dispersed bubbles is so large that they begin to rapidly coalesce then transition to slug flow will occur. The criterion for transition to dispersed bubble flow is therefore a determination of the critical bubble diameter below which rapid bubble coalescence is avoided for void fractions above 0.25. This criterion is expressed as

$$\frac{\left[\rho_L/(\rho_L-\rho_G)g\right]^{0.50}\upsilon_L^{0.08}}{(\sigma/\rho_L)^{0.10}D^{0.48}}U_M^{1.12}=3.0 \tag{2.13}$$

where U_M is the velocity of the mixture of the phases and is defined as:

$$U_M = U_{LS} + U_{GS} \tag{2.14}$$

In Figure 2.4 this flow transition is shown as line F-1.

As previously stated, churn flow is an unstable entry length phenomenon of slug flow. Churn flow occurs at vapor velocities greater than those required for slug flow. This increased vapor flow rate increases the void fraction of the flow, causing the slugs to become aerated and unstable. Since churn flow is considered an entry length phenomenon, Dukler and Taitel developed an equation to determine the length of the entry section where churn flow exists. The equation is given as follows:

$$\frac{l_E}{D}=42.6\left(\frac{U_M}{\sqrt{gD}}+0.29\right) \tag{2.15}$$

The solution of this equation is plotted for several entry length values as line H in Figure 2.4. As demonstrated in the plot, when transition to slug flow occurs the superficial liquid and vapor velocities of the flow do not change. Therefore, unlike other zones the position along the pipe must be known for zone IV to accurately determine the flow regime present.

The final transition illustrated in Figure 2.4 is the transition to annular flow. During annular flow, shown as zone V in Figure 2.4, the liquid phase flows both as a thin film along the pipe circumference and as droplets entrained in the vapor phase. This upward flow is due to interfacial shear and drag forces produced by the vapor phase overcoming the force of gravity. Therefore, transition to annular flow can only occur when the vapor flow rate is sufficient to lift the liquid droplets. This criterion is represented by balancing the gravity and drag forces that occur on a single liquid droplet, and is given as:

$$\frac{U_{GS}\,\rho_G^{\frac{1}{2}}}{\left[\sigma\, g\,(\rho_L-\rho_G)\right]^{\frac{1}{4}}} = 3.1 \qquad (2.16)$$

This criterion, plotted as curve J in Figure 2.4, demonstrates that the transition to annular flow is not dependent on the liquid phase velocity or pipe diameter. This result is logical since only the vapor velocity and fluid properties significantly affect the magnitude of the gravity and drag forces on the liquid droplets.

Flow maps for concurrent vertical downflows use the same coordinate systems as the maps for concurrent vertical upflows, but the maps demonstrate that the transition sequence between the various flow regimes is in reverse order. At low superficial vapor and liquid velocities, the annular flow regime exists as opposed to the bubble flow regime. In this flow regime, the liquid

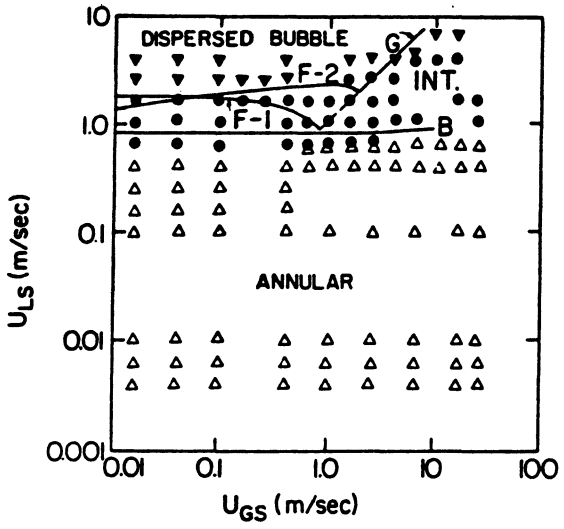

Figure 2.5. Plot of the Dukler and Taitel (1986) flow regime map flow downward vertical flow.

flows in a wavy film down the walls of the pipe. As the liquid flow rate is increased, the thickness of the film and the height of the waves increase until a slug of liquid is able to form a stable bridge across the conduit. When this occurs, the flow undergoes a transition from annular flow to either slug or dispersed bubble flow, depending on the vapor flow rate. The requirements for annular flow transition are thus the existence of waves on the vapor-liquid interface and a sufficient liquid supply to form a stable bridge. These are the same physical requirements for the transition from stratified to slug flow for horizontal flow configurations. Therefore, Dukler and Taitel use the same criterion for transition from annular flow. As previously stated, however, waves always exist on the liquid-vapor interface during annular flow. Thus the only condition that must be met is the requirement of sufficient liquid inventory. This condition is written as

$$\frac{A_L}{A} \geq 0.35 \tag{2.17}$$

where A_L is the area of the liquid falling film. This criterion is given as curve B in Figure 2.5.

As in vertical upflow, a combination of two mechanisms determines the flow regime after transition from annular flow. The first is that at higher vapor flow rates the bubble number density increases which promotes slug growth. The second mechanism, however, has an opposite effect in that at higher liquid velocities the turbulent forces of the liquid phase act to break apart the vapor bubbles causing transition to dispersed bubble flow. The balance of these two mechanisms is given by Dukler and Taitel as

$$U_{LS} = 3.0\, U_{GS} + \left[\frac{g(\rho_L - \rho_G)\sigma}{\rho_L^2}\right]^{\frac{1}{4}} \tag{2.18}$$

and is plotted as curve G in Figure 2.5. This equation predicts that when the superficial vapor velocity is large enough to make the right hand side of the equation greater than the superficial liquid velocity, the first mechanism is dominant and slug flow will occur. If the superficial liquid velocity is larger, then the second mechanism is the controlling factor, and the flow transition will be to dispersed bubble flow. Thus, it is the balance of these two mechanisms that determines the flow regime.

2.3 Countercurrent Flow Transitions

The flow regime maps previously presented are intended for the prediction of the flow regimes present in concurrent fluid flows. In some piping arrangements, however, it is possible for the vapor and liquid phases to flow in countercurrent directions, as shown in Figure 2.6. Like concurrent flow, the flow regimes in countercurrent flows are directly dependent on the effects of inertial, gravitational, and frictional forces (Wallis and Dobson, 1973). Due to the altered physical flow arrangements, however, the effects of these forces vary. It is thus necessary to determine whether current flow regime maps are accurate under these flow conditions.

Most studies of countercurrent flows are concerned with the transition from stratified to slug flow. This specific transition was analyzed by Wallis and Dobson (1973) for countercurrent flows of water and air in horizontal, rectangular ducts. They found that slug formation was more dependent on flow rates for countercurrent fluid flows. The reason is that there is a constant supply of liquid throughout the wave growth process. As the waves form on the liquid interface, the amplitudes of the waves vary randomly with time. Wallis and Dobson noted that groups of waves were continuously created and dispersed throughout the pipe. These wave groups shift up and down the pipe, but allow individual waves to propagate through them. Transition to slug flow was first noted by Wallis and Dobson at the downwind end of a wave packet. During this transition, a wave from the group grew, bridged the conduit, and was propelled down the channel by the vapor phase. The type of slug formed depends on the amount of liquid available. Wallis and Dobson observed that if the void fraction was less than 0.5 at transition conditions, then a long wave would grow until it could bridge the channel,

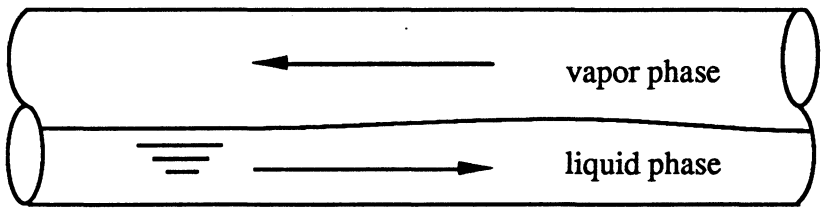

Figure 2.6. Stratified countercurrent two-phase flow.

resulting in the transition to plug flow. However, if the void fraction of the flow was greater than 0.5, the higher vapor flow rates created rough liquid interfaces until a turbulent wave grew, spanning the channel and rolling down the pipe, causing a transition to slug flow.

As part of their analysis of slug formation in countercurrent flows, Wallis and Dobson (1973) developed their own semi-theoretical criterion for transition from stratified to slug flow. The criterion was given as

$$U_G = 0.5\sqrt{\frac{g\,h_G(\rho_L - \rho_G)}{\rho_G}} \tag{2.19}$$

This equation provides the vapor velocity required to retain a slug of liquid as it is propelled along a pipe. Wallis and Dobson found that this equation accurately predicts slug transition for concurrent and countercurrent flows, as well as vapor flow over a stagnant liquid. This result is important because it suggests that flow maps already developed for concurrent fluid flows may also be accurate for countercurrent flows.

Bjorge (1982) also examined slug initiation in countercurrent flows using saturated steam and subcooled water as the working fluids. The effect of condensation was noted to be an important factor in determining the onset of liquid slugging. During the flows, as steam was condensed onto the liquid the height of the liquid phase increased. The corresponding decrease in the area of the vapor phase caused the steam to accelerate. Thus, the critical vapor velocity required for slug initiation was reached at lower inlet liquid flow rates. Bjorge also analyzed the relative effects which various piping and fluid flow properties have on the onset of slugging. The parameters that exhibited the most effect on slug transition are pipe length, pipe diameter, and the amount of inlet liquid subcooling. Changes in each of these variables significantly altered the amount of condensation that occured within the pipe and was thus directly related to the phase velocities required for slug initiation.

Bjorge compared slug transition data for steam-water flows to the maps of Taitel and Dukler (1976) and Mishima and Ishii (1980). Equation 2.5 gives the Taitel and Dukler criterion for slug formation. The criterion used by Mishima and Ishii is based on a theoretical analysis of wave

stability and is given by

$$U_G = 0.487 \sqrt{\frac{g\, h_G\, \rho_L}{\rho_G}} \qquad (2.20)$$

It is interesting that this equation is similar to equation 2.19, the transition criterion of Wallis and Dobson (1973), which was obtained from correlations of experimental data. The Taitel and Dukler criterion for transition from stratified to slug flow more accurately predicted slug initiation. Both criteria, however, were found to agree well with the experimental data. Thus, Bjorge (1982) has also shown that transition criteria developed for concurrent fluid flows may be used for countercurrent flow arrangements.

2.4 Applicability of Flow Maps

The purpose of flow regime maps is to allow the prediction of the flow regimes that exist for given fluid properties, flow characteristics, and piping geometries. To develop these maps, many authors have simply used correlations of empirical data from various flow regime experiments. The flow maps of Baker (1954) and Mandhane *et al.* (1974) were developed in this fashion. While these maps accurately predict the flow conditions upon which they were based, the effectiveness of each map is uncertain for fluid and flow parameters beyond the original parametric range (Dukler and Taitel, 1986). Other researchers have attempted to extend the range of accuracy of these maps by modifying the coordinate systems to be more responsive to changes in fluid properties. Often, these modifications only consist of changing the coordinate systems by a ratio of a specific fluid property such as the fluid densities or surface tensions. An example of this type of map is the Schicht (1969) map as modified by Hashizume (1983). These changes are usually effective in increasing the accuracy of the original map as well as increasing the range over which the map is applicable. The other method of developing flow pattern maps is based on theory. The flow map of Taitel and Dukler (1976) was developed in this manner. This method attempts to create flow maps applicable to all ranges of fluids, flow conditions, and piping geometries. The effectiveness of a theoretical map is dependent on the accuracy with

which the physical mechanisms of flow transitions are modeled.

Most flow regime maps have been developed with water as the working fluid. Transitions between flow patterns, however, occur under different flow conditions for other fluids due to differences in fluid properties. This raises a significant concern over the ability of the flow maps to predict regimes for refrigerant flows. Presently, all of the flow maps have problems predicting flow transitions for variable working fluids. Even the Taitel and Dukler map, considered by many to be the best theoretical analysis of two-phase flow, can be highly inaccurate for a variety of fluids and flow conditions (Manwell and Bergles, 1989). To demonstrate this problem, analyses of several flow maps are presented for various refrigerants.

Tandon *et al.* (1983) plotted over 350 flow regime observations for condensing R-12 and R-22 on the flow maps of Baker (1954), Soliman (1974), Breber *et al.* (1980), and Tandon *et al.* (1982). The slug, plug, wavy, annular, semi-annular, and spray flow regimes were observed. The wavy flow regime is a combination of the stratified-wavy and the wavy-annular flow regimes previously discussed. Spray flow consists mostly of vapor with the liquid phase dispersed as a mist throughout the vapor. The Baker (1954) map is seen to have predicted slug flow well and to have predicted annular and semi-annular flow with moderate success. There are large discrepancies, however, between the map and the data for the wavy and spray flow. The flow maps of Soliman (1974) and Breber *et al.* (1980) showed improved accuracy over the Baker map in predicting flow regimes. The map that demonstrated the most agreement with experimental observations, however, was that of Tandon *et al.* (1982). The Tandon map was able to accurately predict all of the flow regions for the R-12 and the R-22 data.

Weisman *et al.* (1979) used evaporating R-113 to examine the effectiveness of the Taitel and Dukler (1976) and Mandhane *et al.* (1974) flow regime maps as well as to create their own map. The flow patterns predicted by the Taitel and Dukler map agreed well with the experimental data except for the transition between slug and annular flows. According to Taitel and Dukler, transition between these two flow regimes occurs at a constant liquid depth. This criterion is represented by the authors' flow regime map as a constant Lockhart-Martinelli parameter, X.

Weisman *et al.*, however, found that transition followed a line more closely represented by a constant modified Froude number, F. The map developed by Mandhane *et al.* (1974) also predicted all of the flow patterns well, except at the annular-to-slug transition. This coincidence suggests that the experimental data used to generate the slug-to-annular transition of their map may be inaccurate. The flow map developed by Weisman *et al.* (1979) agreed with all of the flow regimes for the R-113 data. Since this map is based on specific data, however, the accuracy of the map is uncertain for fluids and flow conditions beyond the original parametric ranges.

Manwell and Bergles (1989) analyzed the effectiveness of the Schicht (1969) map as modified by Hashizume (1983) in predicting the experimental data of Tandon *et al.* (1982), Weisman *et al.* (1979), and various other authors. In the various experiments, R-12, R-22, and R-113 were tested in adiabatic flows and in flows where condensation and evaporation occurred at low heat fluxes. For the Tandon *et al.* (1982) data, the Schicht and Hashizume map was in agreement for the wavy and semi-slug flow regimes. Annular flow, however, consistently occurred at vapor mass fluxes lower than predicted. The Schicht and Hashizume map was more consistent for annular flow with the R-113 data of Weisman *et al.* (1979). Good agreement was also attained for the wavy, slug, and semi-slug regimes. Much of the wavy data, however, occurred at vapor mass fluxes well below the Hashizume transition line for stratified-wavy flow.

Another analysis of the Baker (1954) flow map was conducted by Shah (1975). This analysis is the only one found in the literature that used ammonia as the working fluid. The Baker map predicted most of the data correctly. However, the map was unable to predict points in the wavy flow regime. These data points were predicted to be either slug, stratified, or annular flow. It should be noted, however, that wavy flow occurs at the transitions between these three flow regimes so that this type of error is not unexpected.

The effectiveness of each flow regime map varies substantially for different fluids and flow conditions. Because of this, no one flow map has emerged as a universal standard. Therefore, the choice of flow regime map should depend on the type of fluid in a system and the flow conditions which occur in a system.

2.5 Oil Concentration Effects

All of the flow regime maps reviewed have been for two-phase flows of a one component fluid. In most vapor compression refrigeration systems, however, oil is present in the system. The presence of oil in a two-phase flow has been found to have significant effects on the patterns of the fluid flow. These changes in flow regimes can alter the heat transfer and pressure drop through the conduit. Thus, determining how oil affects flow regimes is an important issue for the refrigeration industry.

Worsoe-Schmidt (1960) conducted one of the first investigations involving the effects of oil on flow pattern transitions. For the experiments, a laboratory-made oil was used with R-12 in a horizontal, smooth tube evaporator. The result of adding the oil was that a liquid film was formed around the walls of the tubing. The upper part of this film had a high oil concentration and thus a high viscosity. The lower portion of the film had oil concentrations which were consistent with concentrations in the bulk liquid flow. Worsoe-Schmidt noted that the film had the effect of increasing the wetted perimeter of the tube wall as well as promoting the transition to annular flow. He also observed that at higher oil concentrations foaming occurs in the flow.

The results of Manwell and Bergles (1989) are similar to the those of Worsoe-Schmidt (1960). Manwell and Bergles examined flow regime transitions for R-12 with varying concentrations of a 300 SUS naphthenic mineral oil. The results were plotted on the Schicht flow regime map as modified by Hashizume (1983) along with data for pure R-12. A comparison showed that the presence of oil promoted transition to annular-wavy flow at significantly lower vapor flow rates than those required for pure R-12. A similar shift was observed in the transition from annular-wavy to semi-annular, especially at low qualities. Manwell and Bergles attributed these premature transitions to foam roll waves that swept along the walls of the piping. The physical explanation offered by Manwell and Bergles is that the mechanical mixing of the two phases traps vapor in the liquid lattice, producing foam. The foam travels along the walls of the pipe and not in the vapor core. Therefore, the amount of fluid capable of wetting the perimeter is significantly increased. Due to the relatively low density of

the foam, a lower vapor core velocity is required to sweep the foam along the side walls. Thus, annular-wavy flow is initiated at lower vapor flow rates. It should be noted that Manwell and Bergles did not observe the non-homogeneous oil film around the piping perimeter that Worsoe-Schmidt noted. Manwell and Bergles offer the explanation that the apparatus used by Worsoe-Schmidt might have caused an uneven distribution of oil to be injected into the piping.

The changes in flow regime transition when oil is added to a fluid are partially due to changes in the properties of the fluid. Flow transition is significantly affected by fluid properties such as density, viscosity, and surface tension, each of which is altered by the addition of oil to the fluid. Schlager (1988) found that common oils are 20% to 50% less dense than CFC refrigerants, 2 to 3 times more viscous than pure halocarbons, and have surface tensions 2 to 3 times greater than those of most refrigerants. Schlager also noted that although the concentration of oil in the refrigerant may be only 2% to 5%, the concentration of oil in the liquid phase may be much greater. The reason for this is that the vapor pressures of the oils are much lower than for the refrigerants. Thus there is virtually no oil in the vapor phase of two-phase flows. All of the oil is mixed in the liquid phase of the fluid. Therefore, at high qualities the oil concentration in the liquid phase may be as high as 90% even though the overall oil concentration is only 5%.

Shah (1975) also studied the effects of oil concentration on two-phase flows. The working fluid in Shah's research was ammonia. This is significant because the oils commonly used in ammonia systems are immiscible. Therefore two separate liquid phases exist in the flow. Shah did not quantitatively analyze the effects of oil concentration but rather reported visual observations of the flow of ammonia-oil mixtures through a horizontal evaporator. The magnitude of the effects of the oil differed for the boiling and non-boiling regions of the evaporator. In the non-boiling region, Shah observed a thick oil film around the circumference of the pipe wall for high mass flow rates and low temperatures. This film was observed to either remain stationary or to flow slowly down the pipe walls. At higher temperatures the oil film became thinner and less prominent. Shah proposed that at low temperatures the oil was highly viscous. When the temperature of the fluid was increased, however, the oil was less viscous and

thus unable to form the thick films. In the boiling region of the evaporator, the effects of oil are much less noticeable. At the onset of boiling a small amount of oil generally flows along the bottom of the pipe. As evaporation of the ammonia occurs, the refrigerant undergoes transition to annular flow. The oil tends to follow this pattern, forming a semi-annular flow along the pipe walls. An interesting result of Shah's observations is that there appears to be an unsteady hold up of the oil in the non-boiling region of the evaporator. This result could play a significant role in the determination of the overall efficiency of an ammonia evaporator.

Although the research presented documents the effects of oil on the transition from stratified to annular flows, no work in the literature was found which produced conclusive evidence of the effect of oil on slug formation. Manwell and Bergles (1989) suggest that oil may suppress the transition from stratified to semi-slug flow. There are not enough data concerning this transition, however, to substantiate this observation.

Chapter 3

Condensation-Induced Shock

Condensation-induced shock results when a vapor bubble collapses with sufficient speed so as to cause shock waves to propagate into the surrounding liquid. This type of hydraulic shock is initiated when large pressure or temperature differences occur between the vapor and liquid phases. Bjorge (1982) has shown that the initiation of condensation-induced shock corresponds with the transition to the intermittent flow regime. During this transition, vapor bubbles are suddenly entrapped by the liquid phase. Due to the speed of the bubble formation it is possible for pressure and temperature differentials to exist between the two phases. The magnitude of the shock produced by the bubble collapse is affected by many variables, such as the initial bubble size, the properties of the fluid, and the flow conditions. The effects of condensation-induced shock are limited in distance because the shock waves can only propagate through a pipe that is full of liquid. The strength of the shock, though, is sufficient to cause severe damage to metals or other solids (Hunter, 1960; Hickling and Plesset, 1964).

3.1 Liquid Inertia Limits

For a given pressure difference between the vapor and liquid phases, the strength of a condensation-induced shock depends on the time it takes the bubble to collapse. Many properties of the fluid and of the flow affect this collapse rate. The maximum shock occurs when the only restraint on the collapse is the inertial limit of the liquid. Under this condition, the rate of collapse becomes a function of the speed at which the liquid phase can reach the center of the bubble.

3.1.1 Incompressible Limit

The upper bound of the liquid inertial limit occurs when the liquid phase is able to instantaneously respond to flow changes and the bubble does not contain any vapor to resist the inflow of liquid. Rayleigh (1917) modeled this scenario as the adiabatic collapse of a spherical

void in an inviscid, incompressible liquid. At the beginning of the collapse, an instantaneous pressure difference is applied to the fluids. Analysis of this model shows that the minimum time for the collapse of a vapor bubble is given by

$$\tau = .91468\, R_o \left(\frac{\rho_L}{P_L}\right)^{\frac{1}{2}} \tag{3.1}$$

The maximum pressure at any point during the collapse is given by

$$\frac{P}{P_{Lo}} = \frac{R_o^3}{\left(4\frac{4}{3} R^3\right)} \tag{3.2}$$

and occurs at a radial distance of r = 1.587 R from the center of the bubble. These results show that the time of collapse and the pressures in the fluids are directly related to the initial bubble radius. Because of the assumption of an incompressible liquid, this model predicts that the pressure at the bubble center is infinite at the point of complete collapse. Therefore, this model only provides a theoretical upper bound on the bubble collapse rate and the resulting pressures.

3.1.2 Compressibility Effects

The compressibility of the vapor and liquid phases is an important factor in the physical description of the bubble collapse during condensation-induced shock. Although the theoretical inertial limits were determined using the assumption of an incompressible fluid, the actual inertial limits must account for compressibility effects. Thus, the previous model is altered by filling the void with a perfect, inviscid, compressible gas and making the liquid phase compressible. As in the previous model, at some instance a pressure difference is applied to the liquid and vapor phases to initiate the bubble collapse. As the liquid at the bubble wall instantaneously moves toward the bubble center, the sudden change in velocity causes a shock wave to propagate into the bubble and an expansion wave to radiate into the surrounding liquid. When the shock wave reaches the center of the bubble, it is reflected as another shock wave. The shock then propagates radially outward until it reaches the liquid-vapor interface at the collapsing bubble wall. At this point, the wave is partially reflected into the bubble as another shock wave and partially refracted into the liquid as a shock wave. The shock wave then repeats this process.

At the beginning of the collapse, the vapor phase condenses into liquid quickly enough to maintain a constant vapor pressure in the bubble and hence does not interfere with the collapse process (Hunter, 1960). As the collapse continues, the liquid-vapor interface accelerates towards the bubble center. Once the interface velocities are near the speed of sound in the vapor phase, the vapor does not have time to condense. The vapor inside the bubble the becomes compressed, resulting in an increase in the vapor pressure. Eventually, the vapor pressure in the bubble becomes large enough to overcome the momentum of the liquid and stops the collapse process. The bubble will then rebound to a fraction of its original size and the collapse process will be repeated (Trilling, 1952; Hunter, 1960).

A comparison between the incompressible and compressible flow models reveals substantial differences in the results. A significant difference is that the incompressible flow model does not account for the pressure pulses which propagate into the liquid during the collapse. This is important because these pressure pulses are the cause of condensation-induced shock. Another difference is that the pressures predicted by the compressible flow analysis are less than those obtained from the incompressible flow model (Biasi, *et al.*, 1972). This is especially noticeable at the end of the collapse when incompressible flow theory allows the vapor pressure to go to infinity (Rayleigh, 1917) but compressible flow theory gives a finite pressure in the bubble (Hickling and Plesset, 1964).

3.2 Heat Transfer Effects

Heat transfer is an important factor in determining the actual rate of bubble collapse. Physically, in order for a bubble to collapse the vapor in the bubble must be condensed into the liquid phase. During this process the heat of condensation is rejected at the liquid-vapor interface. The heat transfer rate thus becomes important to the rate of collapse of a vapor bubble. The relative importance of heat transfer effects can be determined by the Jakob number (Block, 1980). The Jakob number is defined as

$$Ja = \frac{\rho_L c_L (T_S - T_L)}{\rho_G h_{fg}} \tag{3.3}$$

and represents a ratio of the liquid's ability to absorb heat over the amount of heat transfer required for phase change to occur. As the Jakob number increases, larger condensation rates are possible and the rate of bubble collapse tends toward the inertial limits of the liquid. Decreases in the Jakob number reflect a reduced ability of the liquid to remove heat from the vapor phase; the collapse process is limited by the rate of heat transfer.

Physically, a high Jakob number corresponds to a large difference in temperature between the liquid and vapor phases. In this case, the liquid can absorb the heat required for condensation and the collapse is limited by the inertial effects of the liquid. At low temperature differentials between the liquid and vapor phases the collapse is represented by a low Jakob number. For this type of collapse, the amount of heat that the liquid can absorb is limited. This results in a decrease in the rate of condensation and thus a reduction in the rate at which the bubble collapses. Also, the increase in the amount of vapor left in the bubble causes a greater increase in the vapor pressure. Therefore, unlike the liquid inertia limited collapses where the collapse rates continue to increase, the collapse rates of heat transfer limited cases are relatively slow and decrease as the collapse progresses (Florschuetz and Chao, 1965).

During the collapse of a vapor bubble, heat is transferred from the vapor phase to the liquid immediately surrounding the bubble. As the bubble collapse progresses, the absorbed heat increases the temperature of the liquid near the bubble wall. This increased liquid temperature causes a decrease in the transient Jakob number associated with the collapse, thus reducing the condensation rate as well as the rate of the bubble collapse. If the liquid phase is moving past the bubble, this translatory motion allows heat from the condensation process to be advected* away by bulk fluid motion. This reduces the effect on the Jakob number due to local heating. Thus, translatory motion enhances heat transfer from the vapor phase and promotes higher collapse rates (Wittke and Chao, 1967).

---

* *Advection* of heat refers to energy carried with the flow; *convection* refers to energy transferred at a surface.

Chapter 4

Vapor-Propelled Liquid Slugging

As the name of the shock mechanism suggests, vapor-propelled liquid slugging is an expression for the hydraulic shocks that occur during two-phase slug flow. The momentum of a slug is much greater than that of other types of two-phase flow because the slug has the greater density of the liquid phase combined with the higher velocity of the vapor phase. This increased momentum can create impact forces as high as 3000 psi in end caps, tees, and piping bends (Loyko, 1992).

4.1 Influences on Vapor-Propelled Liquid Slug Initiation

The mechanisms that trigger transition to slug flow are influenced by many variables. The characteristics of the fluid flow, the properties of the working fluid, and the physical parameters of the piping system each have significant effects on the initiation of slug flow. Knowledge of these effects is needed to determine the susceptibility of a system to vapor-propelled liquid slugging.

4.1.1 Fluid Flow Effects

The characteristics of the fluid flow are an integral part of determining the transition to slug flow. For a prescribed fluid and piping system, properties such as phase velocity, turbulent or laminar effects, and liquid height determine when the transition to slug flow will occur. Two characteristics of fluid flows which are significant in determining the onset of vapor-propelled liquid slugging are heat transfer between the liquid and vapor phases and transient velocity changes. During some operating scenarios in ammonia systems, saturated vapor is admitted across subcooled liquid. As the vapor phase flows over the liquid some of the vapor condenses. The condensation increases the height of the liquid phase, resulting in a reduction of the vapor velocity required for the initiation of slug flow. Therefore, any flow parameter that promotes

heat transfer between the phases increases the susceptibility of a system to vapor-propelled liquid slugging.

Most theories predict slug flow transition based on quasi-steady, equilibrium changes of the phase velocities. Transition to slug flow may also result from the transient increase in phase velocities. This type of slug initiation differs physically. Under equilibrium conditions, as the vapor velocity increases the liquid height required for slug transition decreases. For fast transients, the liquid depth required for transition decreases until it reaches a critical limit where it is independent of the vapor velocity. This critical liquid height is based only on the viscosity of the liquid. For rapid vapor transients, the liquid-vapor interface is covered by large-amplitude, irregular waves. These waves do not grow, but rather coalesce along the liquid-vapor interface. Transition to slug flow occurs when enough of these interfacial waves have combined to bridge the pipe. Taitel *et al.* (1978) analyzed this mechanism of transition and argued that the same criteria for slug transition are still applicable. The dependence of the flow properties on time and position causes flow transition to occur at vapor and liquid velocities that vary greatly from those predicted by equilibrium conditions (Dukler and Taitel, 1986).

4.1.2 Fluid Property Effects

Establishing the effects of fluid properties on the transition to slug flow allows an evaluation of the relative susceptibility of various fluids to vapor-propelled liquid slugging. By understanding how fluid properties affect slug formation, a working fluid may be chosen that is not susceptible to slug flow for the given flow conditions. The important properties are vapor density, liquid density, liquid viscosity, and surface tension. However, the effects that these properties have on slug initiation are not completely understood.

Weisman *et al.* (1979) experimented with fluids of varying vapor density and reported no significant effects on the transition from stratified to slug flow. However, the analysis of Weisman *et al.* (1979) only involved the quasi-steady initiation of slug flow. Andritsos *et al.* (1992) found that vapor density mainly affects the transition to slug flow that occurs through wave coalescence. Andritsos *et al.* reported that as the density of the vapor phase was increased,

the vapor velocity required for the transition to slug flow decreased. Physically, the vapor phase affects the liquid phase through interfacial shearing forces. An expression for interfacial shear stress used by Taitel and Dukler (1976) is

$$\tau_i = f_i \frac{\rho_G (U_G - U_i)^2}{2} \tag{4.1}$$

where f_i is the interfacial friction factor. The equation indicates that the magnitude of the shearing forces between the phases is directly proportional to the density of the vapor phase. Thus increases in the vapor density magnify the influence of the vapor phase on the liquid phase, allowing for transition to slug flow at reduced vapor velocities.

Increases in the density of the liquid phase produce an opposite effect on slug transition. As the liquid density is increased, higher vapor or liquid velocities are required for transition to slug flow (Weisman *et al.*, 1979). Agreement with this conclusion can also be found in theory. Kelvin-Helmholtz theory (Milne-Thomson, 1960) states that a wave will grow on the liquid surface when

$$U_G > \left[\frac{g\, h_G (\rho_L - \rho_G)}{\rho_G} \right]^{\frac{1}{2}} \tag{4.2}$$

where h_G is the height of the vapor phase. The equation also shows that the velocity of the vapor phase required for wave formation is directly proportional to the density of the liquid phase. Thus, theory and experimental evidence agree on the effect of liquid density on the initiation of slug flow.

There is disagreement in the literature as to the effect that the viscosity of the liquid phase has on vapor-propelled liquid slugging in separated flows. Kordyban (1993) and Weisman *et al.* (1979) did not notice any changes in the formation of slugs due to changes in liquid viscosity. However, Barnea (1991), Dukler and Taitel (1986), and Andritsos *et al.* (1992) found a significant relationship between the viscosity of the liquid and the onset of liquid slugging. The experiments of these authors demonstrate that at higher liquid viscosities, the height of the liquid phase is increased and thus the liquid velocities required for slug initiation are greatly reduced.

Barnea (1991) also noted that at constant liquid height, increases in the liquid viscosity have a stabilizing effect on the system and larger vapor velocities are required for transition to slug flow. According to Dukler and Taitel (1986), the reason for the difference in results is the length of the test section used by Weisman *et al.* (1979). As liquid viscosity is increased slugs take longer to form. Therefore, if the pipe length is too short, transition to slug flow will not occur.

The effect that surface tension has on slug formation is even less clear than that of liquid viscosity. Weisman *et al.* (1979) state that the surface tension of a fluid does not affect the transition to slug flow. Kordyban and Okleh (1992), however, conclude that decreases in surface tension significantly reduce wave growth and hence delay slug formation. This conclusion is contrary to the results of Barnea *et al.* (1983), where the authors state that in small diameter pipes surface tension causes the premature transition from stratified to slug flow. Experimental data concerning surface tension do not consistently support any of the arguments. Therefore, Andritsos *et al.* (1992) simply conclude that there is not substantial evidence at present to determine the effects of surface tension on slug initiation.

4.1.3 Piping Configuration Effects

Various characteristics of a piping system affect the transition to slug flow. Wallis and Dobson (1973) found that any sizable mechanical excitation of the liquid phase resulted in premature slug initiation. Within a piping system, there exist many opportunities for such a disturbance. In a study of flow through an evaporator, Barnhart and Peters (1992) found that the return bends triggered the formation of slugs at velocities much lower than predicted by theory. Taitel (1977) found that rough piping creates disturbances at the vapor-liquid interface, causing the premature transition to slug flow. In general, any nonideality in the piping system will promote the onset of vapor-propelled liquid slugging.

The diameter of the pipe can effect the transition to slug flow in several different ways. For saturated fluid flows, Andritsos *et al.* (1992) show that as the diameter of the pipe is decreased, lower liquid velocities are required for slug initiation. This effect is reinforced if the liquid phase is subcooled. Bjorge (1982) demonstrates that decreasing the pipe diameter increases the effect

of condensation on the flow, causing slugs to form at even lower liquid velocities. Finally, for small diameter tubing, Barnea *et al.* (1983) found that surface tension effects become enhanced, causing the liquid phase to climb the piping walls and to prematurely initiate slug flow. The combination of these three effects makes the diameter of a pipe a potentially important parameter in determining the initiation of vapor-propelled liquid slugging.

In adiabatic two-phase fluid flows, the only effect which pipe length has is to limit the amount of space which slugs have to form. Thus a short pipe can prevent the formation of slugs under normal flow conditions. In this case, to initiate slug flow requires higher than predicted liquid velocities so that the slugs may form earlier (Andritsos, *et al.*, 1992). When condensation occurs in the flow, the length of the pipe is a significant parameter in determining the onset of liquid slugging. Bjorge (1982) has shown that increases in pipe length increase the amount of condensation in the pipe. Thus, the height of the liquid phase is increased and the corresponding vapor velocity required for slug formation is decreased.

The largest effect which piping has on slug transition, however, is the angle of inclination of the piping system. In piping systems with concurrent flow and small inclination angles (up-hill) the stratified flow regime is greatly reduced and the transition to slug flow is almost immediate. When the angle is adjusted to a small decline (down-hill), however, the liquid velocity for the transition to slug flow is greatly increased (Dukler and Taitel, 1986; Barnea, *et al.*, 1980). Therefore, the incorrect installation of horizontal pipes greatly increases the risk of vapor-propelled liquid slugging.

4.2 Pressure Calculations

Current practice in the refrigeration industry is to design systems that avoid hydraulic shocks. These systems are only designed for normal operating conditions. Therefore, the sudden pressures surges associated with hydraulic shocks are a serious danger to the system. It is important to know the magnitude of the pressures that may occur in a system so that operating

procedures and system designs may be altered to account for these shocks.

To this point, condensation-induced shock and vapor-propelled liquid slugging have been discussed separately. In ammonia systems, the hydraulic shocks that occur are often a combination of these two shock mechanisms (Loyko, 1992). A common scenario is for transition to slug flow to occur, causing the onset of vapor-propelled liquid slugging. These slugs of liquid are propelled down the pipe, pushing a region of vapor ahead of them. Once the slug enters an end cap or other entrapping section of piping, the vapor region is compressed between the slug and the piping wall. The momentum of the slug provides the pressure differential required for bubble collapse. Thus, the resulting shock is a combination of vapor-propelled liquid slugging and condensation-induced shock.

Loyko (1992) presented a sample calculation of the pressures that can occur when these two hydraulic shocks combine. This example is a representation of a possible shock scenario that may occur at the termination of hot gas defrost. The scenario involves a piping configuration where the suction stop valve is located below the suction line, as shown in Figure 4.1, so that condensate from the suction accumulates at the valve. The suction branch is a 6 in. schedule 40 steel pipe and the suction main is a 12 in. standard weight pipe that is 30% full of condensate.

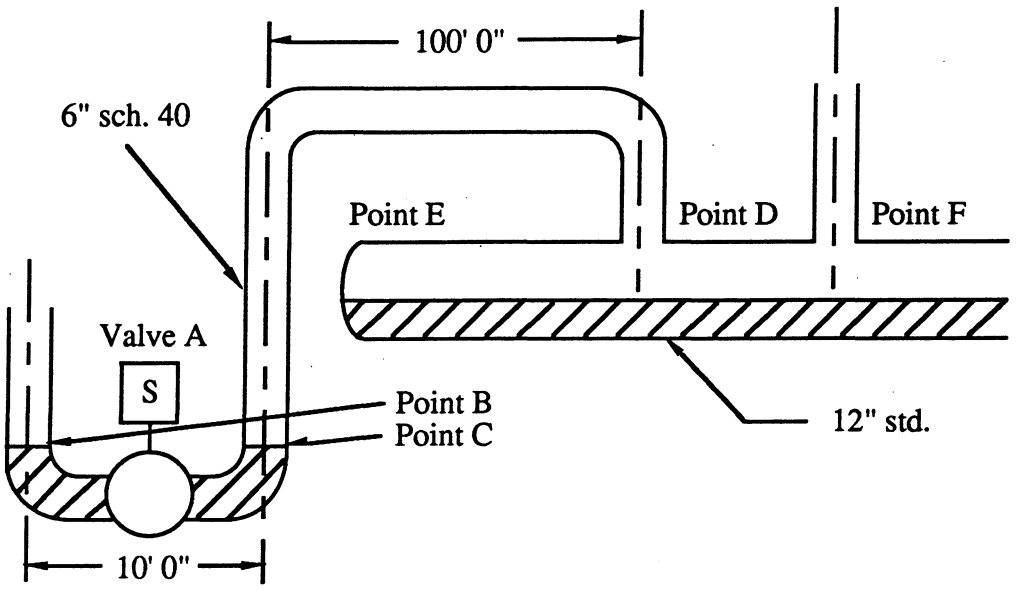

Figure 4.1. Diagram of the piping arrangement for the pressure analysis (Loyko, 1992).

The defrost pressure is set at 70 psig and the suction pressure at 0 psig. At the instant the valve is opened, a 10 ft slug of liquid is propelled down the suction line. The acceleration of the slug is found from a simple momentum balance on the slug, written as

$$F = \left(\frac{144\,in^2}{ft^2}\right)\Delta P\,A \tag{4.3}$$

Loyko used Newton's second law,

$$F = \left(\frac{lbf \cdot s^2}{32.2\,lbm \cdot ft}\right)m\,a \tag{4.5}$$

and equations of linear motion,

$$a = \frac{dU}{dt} \tag{4.6}$$

$$U = \frac{dx}{dt} \tag{4.7}$$

to derive the resulting velocity of the liquid slug after it has been propelled 100 ft down the pipe. The velocity at this point was determined to be 390 ft/s.

When the slug reaches the suction main at point D, it is modeled as dividing into two halves. One half travels down the pipe toward point F. The other half traps a vapor bubble in the end cap, compressing the vapor and causing the onset of condensation-induced shock. The increased pressure in the vapor caused a corresponding increase in the saturation temperature so that a temperature differential existed between the liquid and vapor phases. By assuming a heat transfer coefficient representative of turbulent flow, Loyko calculated the rate of condensation as

$$Q = \frac{h\,A\,\Delta T}{h_{LG}} \tag{4.8}$$

where Q = 7.66 lbm/s for this scenario. For a 10 ft^3 vapor bubble, the collapse time is 0.25 sec. and the fluid velocity is approximately 70 ft/s. Although the collapse velocity is much less than the initial velocity of the liquid slug, it is capable of producing a significant shock. This is because once the collapse is complete, the flow of liquid is immediately stopped by the pipe

wall. The Joukowski equation is used to determine the magnitude of the pressures produced by the shock. This equation is given as

$$-\Delta P = \rho_o a \Delta U \tag{4.9}$$

where a is the speed of sound in liquid ammonia. For the example analyzed by Loyko, the pressure surge created by the shock was 3149 psi. Loyko determined that this pressure transient causes an axial stress in the suction main of approximately 26,000 psi. While this shock may not seriously damage the piping system, repeatedly exposing the piping system to sudden large stresses can cause the premature destruction of the piping components.

Chapter 5

Critical Flow Regimes in Refrigerant Piping

Several two-phase flow patterns may exist in industrial refrigeration systems. The only flow regimes that are critical to this study, however, are those regimes that may initiate either vapor-propelled liquid slugging or condensation-induced shock. As shown in the previous chapters, the occurrence of both types of hydraulic shocks corresponds to the transition to intermittent flow. Therefore, establishing the parts of the refrigeration system that are susceptible to condensation-induced shock and vapor-propelled liquid slugging involves determining which parts of the system are able to cause the transition to intermittent flow.

5.1 Hot Gas Defrost

The only documented occurrences of hydraulic shock in refrigeration systems are associated with the initiation and termination of hot gas defrost in low-temperature ammonia evaporators (Loyko, 1989). A sample schematic for a low-temperature evaporator during the hot gas defrost process is given in Figure 5.1. At the initiation of hot gas defrost, the liquid line solenoid valve (J) and the gas-powered suction stop (C) are each closed. The gas-powered suction stop valve is closed in either of two manners, depending on whether the valve is normally open or closed. If the valve is normally open, then high pressure gas from the hot gas line is used to close the valve by shutting the suction pilot (A) and opening the hot gas pilot (B). If the valve is normally closed, then the high pressure gas that holds the valve open during normal operating conditions is removed by closing the hot gas pilot (B) and allowing the gas to bleed off. This arrangement is commonly used in ammonia systems (Cole, 1994) because it avoids the inherent ΔP associated with conventional solenoid valves.

Hot gas flow is initiated by the opening of the hot gas solenoid valve (I). The hot gas hand expansion valve (K) shown in Figure 5.1 is typically used only to control the distribution of the

hot gas from the condenser to the various evaporators. The hot gas first enters the drain pan (M) at the bottom of the evaporator. Then the hot gas check valve (E) opens to allow the hot gas to flow into the suction header (F). Since the suction stop (C) has been closed the hot gas flows through the evaporator (L) in a path that is opposite the ammonia flow during normal evaporator use. The hot gas then exits through the liquid header (G) and into a hot gas drainage line. A hot gas relief regulator (D) on this line acts as a pressure relief valve that maintains a minimum pressure in the evaporator during hot gas defrost. The purpose of maintaining a minimum pressure in the evaporator is to ensure that the saturated ammonia in the evaporator remains at a temperature sufficient for defrost.

In general, temperature or pressure sensors are not used to determine the end of the hot gas defrost cycle. This is because the conditioned room air is so cold that the ammonia typically leaves the evaporator as a saturated fluid instead of a superheated vapor. Therefore, the pressure and temperature of the ammonia will be almost constant. Thus, the hot gas defrost process is

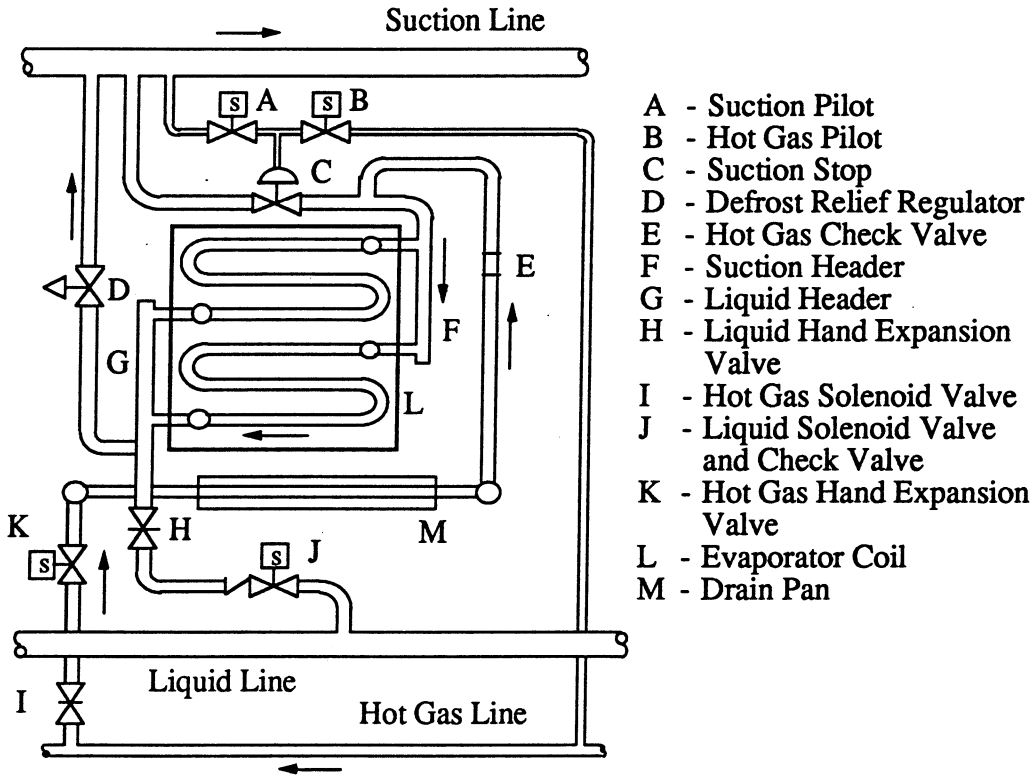

Figure 5.1. Schematic of low-temperature evaporator during hot gas defrost

controlled by timers that are preset by the system operator. When hot gas defrost is complete, the hot gas solenoid valve (I) closes. In some systems, there is a delay before the liquid line solenoid (J) and the gas-powered suction stop (C) valves reopen. During this time a bleed valve can reduce the pressure of the hot gas to decrease the pressure difference at the liquid solenoid and the gas-powered suction stop valves. The extent of this delay is also set by the system operator. After this time, the liquid line solenoid and suction stop valves are opened and normal operating conditions are reestablished (Cole, 1994).

5.2 Hydraulic Shock During Hot Gas Defrost

At the beginning of the hot gas defrost cycle, hydraulic shock is associated with the opening of the hot gas defrost valve. At this time, hydraulic shock may be initiated in two areas. First, if there is enough condensate in the hot gas line, then the sudden flow of hot gas may cause a transition to slug flow. The liquid slugs that are formed are propelled through the hot gas valve and into the pan of the evaporator. This may lead to hydraulic shock in pipe caps and coil headers with pressures exceeding 2000 psig (IIAR, 1992). The second manner in which hydraulic shock may be initiated is due to condensate remaining in the pan coil or the evaporator coil. This condensate may be the result of either a leaking check valve between the pan and the suction header or an improperly drained evaporator. Similar to the previous incident, the sudden flow of hot gas through the coil can cause the formation of liquid slugs resulting in hydraulic shocks in the pan coil header or an evaporator header. The magnitude of these shocks may range from 1000 to 2000 psig (IIAR, 1992).

At the termination of hot gas defrost, hydraulic shock corresponds with the opening of the gas-powered suction stop. The manner in which hydraulic shock is initiated depends on piping configuration. If the gas-powered suction stop is located below the level of the suction header, condensate from the suction header will drain and collect at the suction stop valve. Therefore, when the gas-powered suction stop is opened, the liquid slug has already formed and the occurrence of hydraulic shock is a function of the amount of condensate collected and the speed

to which the vapor can accelerate the slug (Loyko, 1992). This scenario also occurs if the suction line is allowed to slope down toward the suction stop. It is now recommended that the suction stop be installed above the suction header to prevent the collection of liquid at the suction stop valve (Loyko, 1992). For this recommended piping arrangement the transition to slug flow results from hot gas flowing over condensate that has collected in the suction line during the hot gas defrost cycle. Since the piping arrangement with the suction stop lower than the suction header has already been analyzed (Loyko, 1992) and does not involve transition to slug flow based on vapor flow over a liquid, this work will focus on the system with the suction stop elevated above the suction header.

Although the large pressure differentials associated with hot gas defrost are usually the focus of hydraulic shock discussions, the temperatures associated with the hot gas defrost process are also important. First, the large temperature differential between the hot gas and the subcooled condensate enhances heat transfer between the vapor and liquid phases. Thus, when a vapor bubble becomes trapped by the liquid, the rate of bubble collapse becomes limited by liquid inertia effects and the magnitude of the shock is increased. This analysis indicates that a shock incident is not just vapor-propelled liquid slugging or condensation-induced shock, but rather a combination of both types of shock acting together. The second manner in which temperature promotes hydraulic shock concerns the piping system. Incidents of hydraulic shock in ammonia systems have all been for systems with refrigerant temperatures below -20 F (Loyko, 1989). At these temperatures, steel is below its nil ductility limit and becomes brittle (Loyko, 1989). Therefore, not only does temperature increase the magnitude of hydraulic shocks, it also decreases the ability of the piping system to handle shocks.

Chapter 6

Flow Analysis

Hydraulic shock in refrigeration systems is complicated by the number of scenarios through which a shock may occur and by the wide range of pipes, valves, and system designs in use. An analysis that covers every eventuality is impossible. The scenarios previously discussed involve some speculation, but because the hydraulic shock initiation mechanisms are essentially the same, a generalized analysis is developed for these situations. In each case, vapor-propelled liquid slugging or condensation-induced shock occurred after a valve was rapidly opened and vapor at a high pressure was emitted into a pipe partially filled with quiescent condensate at low side pressure. It is this manifestation of a hydraulic shock that is under study. The analysis consists of modeling the gas flow through the valve for a prescribed pressure difference to determine the vapor velocity over the liquid, and then to use transition criteria from the literature to determine whether a slug could form. This approach is consistent with the operation of the system.

An instant after a valve is opened, the flow conditions are transient and the fluid is in a state of nonequilibrium. It is during this time that, if the flow conditions are sufficient, a hydraulic shock is initiated. The purpose of the model is to gain insight into the physics of the flow through the valve. This allows comparison of the existing flow conditions to the initiating mechanisms of hydraulic shocks to determine the susceptibility of the system to shock.

6.1 Flow Model

For the initial pressure differences across a typical hot-gas or suction-stop valve in a liquid overfeed ammonia system, it is readily found that the flow through the valve is choked at the throat when the valve opens. Limited empirical data may be used to predict the gas flow through a specific valve under certain flow conditions. This situation is made more complicated by the

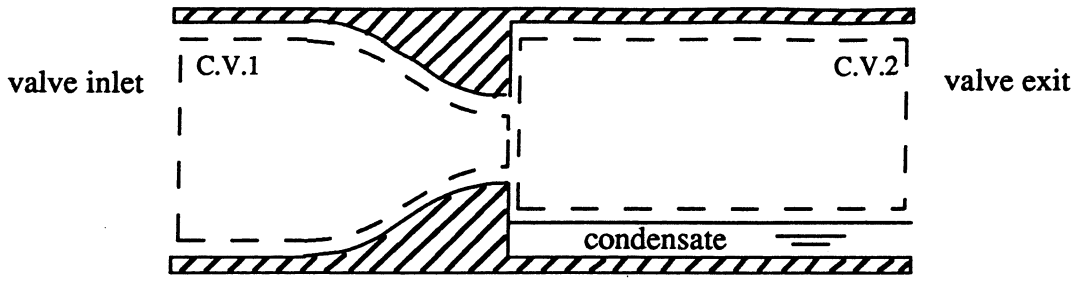

Figure 6.1. Diagram of the orifice representation of a valve.

presence of liquid downstream of the valve. The generalized approach of the flow model is to assume a simplified valve geometry, and that the liquid is initially unaffected by the sudden flow of vapor through the valve.

The valve is assumed to consist of a smooth contraction with a sudden expansion at its discharge, as shown in Figure 6.1. Only the flow conditions that occur immediately after the valve is opened are analyzed. This is because the driving pressure differential and thus the phase velocities immediately decrease as the flow continues. Thus, the flow conditions and fluid properties immediately before the valve is opened are used to model the flow before any changes can occur in the flow parameters. This allows the assumptions of adiabatic and steady flow.

For the flow upstream of the valve, the additional assumption of frictionless flow is made. For the sake of developing a conservative estimate and because the event of interest has a short time duration, the vapor pressure at the valve inlet is assumed to remain constant. The flow in the control volume upstream of the valve throat can then be analyzed using well-known equations for isentropic flow in a variable area duct (e.g., see Zucker, 1977). For the flow model, the upstream pressure of the saturated vapor, the inner diameter of the pipe and the diameter of the throat of the valve are prescribed. Imposing the choked flow condition at the valve throat, which depends on operating conditions, all other flow properties in the control volume are then determined.

The second control volume is analyzed to determine the flow conditions downstream of the valve. Within this control volume, an aerodynamic boundary separates at the throat and attaches

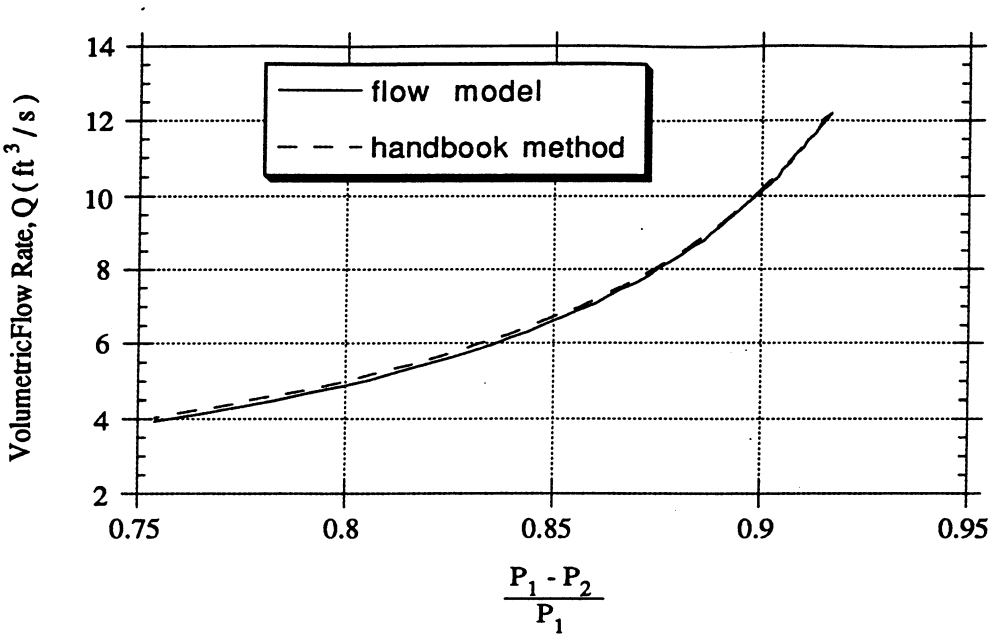

Figure 6.2. Plot of the flow model results for $D_{throat} / D_{pipe} = 0.614$ versus the handbook method results for $C_v / D^2 = 11$ for schedule 80 steel pipe of 0.75 in. nominal diameter.

to the pipe walls and liquid pool. Although there is friction along this aerodynamic boundary, the control volume has been selected so that friction and heat transfer are negligible at its boundaries. Assuming the compressible, one-dimensional flow of an ideal gas, the model determines the downstream volumetric flow rate for a prescribed downstream pressure and known flow properties at the valve throat.

The results of the flow model for the flow of ammonia with realistic pipe and valve throat diameters are plotted in Figure 6.2. The flow equations used for this model, given in Appendix A, are based on the general flow of a compressible vapor through a valve. By altering the diameter of the valve throat, the equations are made to represent the flow through a specific valve. Therefore, for the flow model to be an applicable tool, a representative throat diameter would have to be known for each type of valve.

The flow immediately downstream of the valve is supersonic. This is possible because of the sudden area expansion. Eventually, a normal shock will form in the flow to balance the system

pressures. The model, however, considers slug formation to occur before the normal shock can be established. Unfortunately, the validity of the model becomes dubious in the supersonic cases due to the breakdown of the one-dimensional flow assumption and the neglect of other potentially important flow features. For example, because the flow at the throat is underexpanded, expansion and compression waves will propagate down the pipe affecting the vapor velocities as well as the vapor-liquid interface. The vapor at the throat is also subcooled, causing the assumption of a perfect gas to be questionable. Furthermore, the asymmetrical compliant boundary provided by the liquid pool will certainly have an effect on the flow. Lastly, the gas flow has been assumed to be quasi-steady; the liquid depth and pressures are assumed constant. An increase in the complexity of the flow model is not warranted until experimental data exist to evaluate the accuracy of the current model.

6.2 Handbook Method

The effectiveness of a method of flow analysis is partially determined by the ease with which it may be used. Although the flow model allows for the exploration of the physical phenomena that occur in the flow, this type of analysis is not commonly used in design and would be of limited practical value. Current industry practice for analyzing the flow through valves consists of using a handbook method where the flow is evaluated with a single flow equation. While this analysis does not offer the physical insight of the flow model, the handbook method provides a quick, simple tool for evaluating flow through valves.

The equation used by handbooks to determine the volumetric flow rate through a valve is based on a general analysis of the head loss through a valve but is modified by flow factors to account for various flow and piping conditions. The flow equation, which is derived in Appendix B, is given as

$$Q = 1360\, C_V\, P_1\, (F_P Y)\sqrt{\frac{x}{G\, T_1\, Z}} \tag{6.1}$$

where C_V is the flow coefficient, F_P is the piping geometry factor, x is the pressure drop ratio, Y

is the expansion factor, G is the gas specific gravity at standard conditions, and Z is the compressibility factor. The flow coefficient is heavily dependent on the geometry of the valve and is representative of a specific valve. The value of this coefficient is determined experimentally for each valve and may be obtained from any valve sizing handbook. Other geometrical characteristics are represented by the piping geometry factor, which is used to account for any variations in the flow due to the addition of fittings and other physical attachments to the valve. While formulas exist to approximate this factor, accurate values are determined experimentally and listed in handbooks.

Other factors account for variations in the flow properties through the valve. The pressure drop ratio, x, is a nondimensional expression of the pressure drop across the valve. This ratio is defined by equation B.23 in Appendix B. Variables also account for compressibility effects within the flow. The expansion factor, Y, is used to represent the changes in the fluid density and the area of the vena contracta created by the pressure variations. This factor may be calculated from equations B.22 through B.24 in Appendix B.

The purpose of the remaining factors is to alter the general flow equation to represent the working fluid. The gas specific gravity, G, specifies which fluid is being used. This factor is defined as the ratio of the molecular weight of the gas over the weight of air at standard conditions. Finally, the compressibility factor is a correction for the departure of the fluid from the perfect gas state. The procedure for calculating this factor is to determine the reduced pressure and temperature of the gas, using equations B.25 and B.26. These values are then used to find Z from a compressibility chart. Once all of these flow factors are calculated, the general flow equation then becomes specific for a particular fluid through a given valve.

The results of the handbook method for the flow of ammonia through a valve are plotted in Figure 6.2 and in Appendix C. The coordinates of this plot are the pressure drop ratio, x, versus the volumetric flow rate, Q, and were chosen to correspond to the input and output of the general flow equation. Figure 6.2 shows good agreement between the results of the handbook method and the flow model. This indicates that the simpler handbook method may be substituted for the

flow model as part of the method for determining the susceptibility of a system to hydraulic shock.

The handbook method has many of the same inaccuracies as the flow model. The general flow equation is derived for the steady, incompressible flow of a perfect gas through a valve. Although flow factors have been introduced into the equation to account for specific flow and piping conditions, the handbook method still has the same difficulties as the flow model in analyzing transient conditions and pressure waves. It is possible, however, that some of these inaccuracies are accounted for by the modifications to the general flow equation.

6.3 Shock Maps

Flow regime maps provide excellent tools for predicting the possibility of a hydraulic shock. A careful review of the literature, however, located no flow criteria directly applicable to the situation under study. Most flow correlations are based on the steady, incompressible flow of vapor over a moving liquid. The flow downstream of the valve, though, consists of the transient, compressible, non-equilibrium flow of vapor over a stagnant liquid. Present flow maps are sensitive to changes in system and fluid properties. Therefore, selection of an appropriate transition criterion is challenging.

The flow transition criterion of Taitel, *et al.* (1978) was selected as the most suitable for the existing flow conditions. This theory was chosen for several reasons. First, the transition criteria is an extension of the original Taitel and Dukler flow regime map (Taitel and Dukler, 1976). This map was derived from a theoretical analysis of slug formation rather than a correlation to experimental data. Therefore, the transition requirements are less sensitive to changes in fluid and system properties. Another reason for choosing this criterion is that it is the only analysis found in the literature to address transient flow conditions. Taitel, *et al.* demonstrated that under transient conditions the initiation of slug flow occurred at phase velocities different from those predicted for normal flow conditions. The Taitel, *et al.* theory, though, was still able to successfully predict the conditions for transition to slug flow. A third reason for selecting the

Taitel, *et al.* (1978) transition criteria is its ability to handle viscous effects. The original theory was derived on the assumption of inviscid flow but was modified to include a viscous correction factor. Barnea (1991) and Choe *et al.* (1978) found that, due to this correction factor, the Taitel and Dukler (1976) transition theory worked well at low viscosities. The final reason for the selection of the Taitel, *et al.* (1978) criterion is because of condensation effects. Although the theory was derived for no mass transfer between the two phases, Bjorge (1982) found that the Taitel and Dukler (1976) transition criterion was able to successfully predict slug initiation for a system containing condensing steam flowing over water. In ammonia systems, the vapor upstream of the valve may be saturated. Therefore, the ability of a transition criterion to account for condensation effects is a significant advantage.

The first part of the Taitel, *et al.* (1978) criterion for slug initiation is given in equation 2.5 as

$$U_G \geq \left(1-\frac{h_L}{D}\right)\left\{\frac{(\rho_L-\rho_G)\,g\,A_G}{\rho_G\,(dA_L/dh_L)}\right\}^{\frac{1}{2}} \tag{6.2}$$

where α is zero for horizontal fluid flows, the area of the vapor phase is

$$A_G = .25\,D^2\left\{\cos^{-1}\left(\frac{2h_L}{D}-1\right)-\left(\frac{2h_L}{D}-1\right)\sqrt{1-\left(\frac{2h_L}{D}-1\right)^2}\right\} \tag{6.3}$$

and the rate of change of the area of the liquid with respect to liquid depth is

$$dA_L/dh_L = D\sqrt{1-\left(\frac{2h_L}{D}-1\right)^2} \tag{6.4}$$

Besides the vapor velocity criterion given in equation 6.2, there must also be enough liquid available to bridge the pipe and form a stable slug. This condition is represented by the requirement that $h_L / D \geq .5\Phi$, where Φ is the volume fraction of liquid in a slug. The volume fraction varies from 0.7 to 1.0 due to the differences in the liquid requirements of the flow regimes within the intermittent flow regime. No correlations have been found for determining Φ, so the worst case scenario of $\Phi = .7$ is used. At liquid depths near the worst case scenario the flow regime may only be pseudo-slug (Andritsos, *et al.*, 1992).

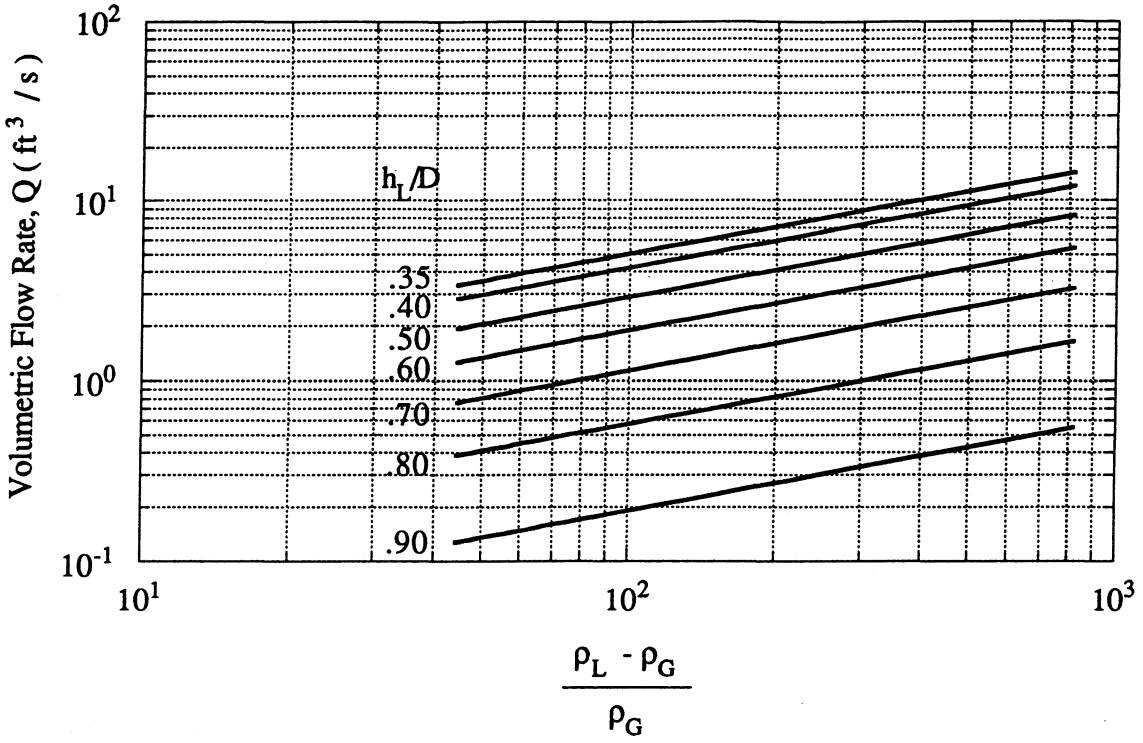

Figure 6.3. Graph of the criterion for transition to intermittent flow for schedule 80 steel and a nominal diameter of 0.75 in.

6.4 Use of the Shock Maps

The equations used to develop the shock maps have been given in this chapter and the appendices. It is convenient to present the transition criterion graphically for a particular pipe diameter as shown in Figure 6.3. Such a representation allows the following graphical procedure: for a given design, the volumetric flow rate is determined for a known defrost pressure difference using a plot similar to Figure 6.2; this flow rate is then used to determine the critical liquid depth using a plot like that of Figure 6.3. Condensate should not be allowed to collect beyond this depth if hydraulic shock is to be avoided. Example plots of volumetric flow rate versus pressure drop are given for several valves in appendix C. Plots of the Taitel, *et al.* (1978) transition are given in Appendix D for various nominal pipe diameters commonly used in ammonia refrigeration systems. Using these two appendices, the susceptibility to slug formation and, therefore, hydraulic shock may be evaluated. For cases not given in the appendices, plots similar to Figures 6.2 and 6.3 may be developed using the given equations.

Chapter 7

Conclusions and Recommendations

The focus of this work has been to develop a rational means to prevent the occurrence of condensation-induced shock and vapor-propelled liquid slugging. This was accomplished in the previous chapters by reviewing two-phase flow, analyzing the initiating mechanisms of hydraulic shocks, and determining the critical flow regimes that occur in industrial refrigeration systems. In Chapter 2, the characteristics of two-phase flow were explored. This study analyzed the basic flow regimes that occur in two-phase flow and established the effects which variations in flow configuration, refrigerant, and oil concentration have on flow patterns. An important outcome of this examination was that the flow maps were demonstrated to be an effective tool for predicting flow regimes.

The properties of hydraulic shocks were presented in Chapters 3 and 4. Condensation-induced shock was analyzed in Chapter 3 by establishing the liquid inertial limits of the shock and determining the effects that heat transfer has on the final pressure surge. A similar review of vapor-propelled liquid slugging was presented Chapter 4. This chapter examined the effects which fluid properties, flow conditions, and piping geometry have on the initiation mechanisms of this hydraulic shock. Also, a practical example of a hydraulic shock scenario was analyzed to demonstrate the pressure surges that may occur.

The occurrence of these shocks in industrial refrigeration systems was studied in Chapter 5. The parts of refrigeration systems that were susceptible to vapor-propelled liquid slugging and condensation-induced shock were documented and descriptions of possible shock scenarios were presented. A theoretical model of the initiation of these shocks was developed in Chapter 6. From this model, flow maps were developed to provide a graphical tool for determining the flow conditions present in a system. To make this tool more applicable, maps were also created using a handbook method that is currently used in industry. Shock maps were developed to establish

the flow conditions necessary for shock initiation. These shock maps were designed to be used with the flow maps to provide a graphical technique for analyzing the susceptibility of a refrigeration system to hydraulic shock.

Several changes in system designs and operating procedures are recommended to reduce the susceptibility of a system to hydraulic shocks. As described previously, hydraulic shock occurs during the hot gas defrost cycle when hot vapor from a region of high pressure is admitted into a pipe containing condensate at low pressure. Therefore, to avoid occurrences of hydraulic shocks in a system, the pressure differential and the amount of condensate in the pipes must be minimized. Several system changes have been recommended by the International Institute of Ammonia Refrigeration, Bulletin 116 (1992), and by L. Loyko (1989, 1992) and are summarized as follows:

- Install valves or valve combinations that allow for the gradual release of pressure into a low pressure pipe. An example of this is the use of a small and a large hot gas solenoid valve in parallel (Loyko, 1992). With this configuration, the small solenoid valve opens fully at the initiation of hot gas defrost while the large solenoid valve remains closed until the pressure differential across the valve has been sufficiently reduced. An arrangement similar to this is the installing of a small bleed solenoid that bypasses the gas-powered suction stop (IIAR, 1992). For this arrangement, the solenoid is opened first at the termination of hot gas defrost so that the pressure in the evaporator may be bled down. Pressures should be bled down such that the formation of a slug (per the shock maps) will not occur .

- Do not depend on pressure relief valves for the prevention of hydraulic shock. During most shock incidents, the shock wave is reflected off the relief valve too fast to trigger the opening of the valve. Therefore during most pressure transient incidents pressure relief valves will never open (Loyko, 1989).

- Avoid the use of liquid traps in hot gas lines and suction lines (Loyko, 1989). The trapped liquid becomes a triggering mechanism for the initiation of liquid slugs and thus enhances the occurrences of hydraulic shock in a system. Liquid drains, however, may be installed in the hot gas main at any low points that can not be avoided (IIAR, 1992).

- Evaporators should be pumped-out before the initiation of hot gas defrost. The pipes in the liquid-overfeed evaporators used in low-temperature ammonia systems are usually filled with liquid, especially during low-load periods. This allows any compression waves created by hydraulic shocks to propagate through the pipes with pressures up to 2000 psig (IIAR, 1992)

- Minimize the condensation of hot gas in the hot gas main. To do this requires the reduction of heat transfer from the hot gas main to the environment. This can be accomplished in several ways. The hot gas main should be routed outside the conditioned room when possible (Loyko, 1989). Insulation should be added to the hot gas main (IIAR, 1992). Also, the minimum size hot gas pipe that is required for defrost should be used (IIAR, 1992).

- Examine the positioning of check valves throughout the hot gas defrost system. Check valves should be on the downstream side of any device that can be completely closed. This is so that liquid does not become trapped between the device and the check valve (IIAR, 1992). Also, a check valve should be placed between the evaporator and the pan coil so that flow from the evaporator does not enter the pan coil and become an instrument for slug initiation (Loyko, 1989).

- Ensure that welds are complete penetration (Loyko, 1992). Any notches, grooves, or discontinuities that occur in a piping system magnify the effects of

hydraulic shock thereby increasing the chances of pipe damage or breaks. Also, end caps should be used instead of fillet-welded flat plates whenever possible (Loyko, 1989).

The purpose of this research has been to develop a rational means with which to prevent or at least decrease the occurrence of vapor-propelled liquid slugging and condensation-induced shock in industrial refrigeration systems. Several changes in system designs and operating procedures have been recommended which reduce the pressure and temperature discontinuities that cause hydraulic shocks. Two techniques have been presented to determine the susceptibility of a refrigeration system to hydraulic shocks under specific flow conditions. While these methods should be verified with experimental data, the combination of these tools provides an effective means with which to avoid hydraulic shocks in refrigeration systems.

References

Andritsos, N., Bontozoglou, V. and Hanratty, T.J., 1992, "Transition to Slug Flow in Horizontal Pipes," *Chemical Engineering Communications*, Vol. 118, pp. 361-385.

Baker, O., 1954, "Simultaneous Flow of Oil and Gas," *The Oil and Gas Journal,* July 26, pp. 185-195.

Barnea, D., 1991, "On the Effect of Viscosity on Stability of Stratified Gas-Liquid Flow -- Application to Flow Pattern Transition at Various Pipe Inclinations," *Chemical Engineering Science*, Vol. 46 (8), pp. 2123-2131.

Barnea, D., Luninski, Y. and Taitel, Y., 1983, "Flow Pattern in Horizontal and Vertical Two Phase Flow in Small Diameter Pipes," *Canadian Journal of Chemical Engineering*, Vol. 61, pp. 617-620.

Barnea, D., Shoham, O., Taitel, Y. and Dukler, A.E., 1980, "Flow Pattern Transition for Gas-Liquid Flow in Horizontal and Inclined Pipes," *International Journal of Multiphase Flow,* Vol. 6, pp. 217-226.

Barnhart, J.S. and Peters, J.E., 1992, "An Experimental Investigation of Flow Patterns and Liquid Entrainment in a Horizontal-Tube Evaporator," ACRC TR-28, University of Illinois at Champaign-Urbana, Urbana, IL.

Biasi, L., Prosperetti, A. and Tozzi, A., 1972, "Collapse of a Condensing Bubble in Compressible Liquids," *Chemical Engineering Science*, Vol. 27, pp. 815-822.

Bjorge, R.W., 1982, "Initiation of Water Hammer in Horizontal or Nearly-Horizontal Pipes Containing Steam and Subcooled Water," PhD Thesis, Massachusetts Institute of Technology, Cambridge, MA.

Breber, G., Palen, J.W. and Taborek, J., 1980, "Prediction of Horizontal Tubeside Condensation of Pure Components Using Flow Regime Criteria," *Journal of Heat Transfer*, Vol. 102, pp. 471-476.

Choe, W.G., Weinberg, L. and Weisman, J., 1978, "Observation and Correlation of Flow Pattern Transition in Horizontal, Co-Current Gas-Liquid Flow," In *Two-Phase Transport and Reactor Safety*, ed. by T.N. Veziroglu and S. Kakac, Hemisphere Publ. Co., Washington.

Cole, R.A., 1994, Cole R.A. & Associates, Personal communication.

Dukler, A.E. and Taitel, Y., 1986, "Flow Pattern Transitions in Gas-Liquid Systems: Measurement and Modeling," *Multiphase Science and Technology*, Vol. 2, ed. by G.F. Hewitt, J.M. Delhaye, and N. Zuber, Hemisphere Publ. Co., Washington, pp. 1-94.

Florschuetz, L.W. and Chao, B.T., 1965, "On the Mechanics of Vapor Bubble Collapse," *Journal of Heat Transfer*, Vol. 87 (2), pp. 209-220.

Hashizume, K., 1983, "Flow Pattern and Void Fraction of Refrigerant Two-Phase Flow in a Horizontal Pipe," *Bulletin of the JSME*, Vol. 26 (219), pp. 1597-1602.

Hickling, R. and Plesset, M.S., 1964, "Collapse and Rebound of a Spherical Bubble in Water," *Physics of Fluids*, Vol. 7 (1), pp. 7-14.

Hunter, C., 1960, "On the Collapse of an Empty Cavity in Water," *Journal of Fluid Mechanics*, Vol. 8, pp. 241-262.

International Institute of Ammonia Refrigeration, 1992, "Guidelines for Avoiding Component Failure in Industrial Refrigeration Systems Caused by Abnormal Pressure or Shock," BULLETIN 116.

Instrument Society of America, 1985, "Flow Equations for Sizing Control Valves," ANSI / ISA-S75.01.

Kordyban, E., 1990, "Horizontal Slug Flow: A Comparison of Existing Theories," *Journal of Fluids Engineering*, Vol. 112, pp. 74-83.

Kordyban, E. and Okleh, A.H., 1993, "The Effect of Surfactants on Wave Growth in the Transition to Slug Flow," *Instability in Two-Phase Flow Systems*, HTD-Vol. 260 / FED-Vol. 169, ASME, pp. 73-84.

Kordyban, E. and Okleh, A.H., 1992, "Growth of Interfacial Waves and the Transition to Slug Flow: Effect of Liquid Properties," *Cavitation and Multiphase Flow Forum*, FED-Vol. 135, ASME, pp. 17-21.

Loyko, L., 1992, "Condensation-Induced Hydraulic Shock," Presented at IIAR 14th Annual Meeting, March 22-25.

Loyko, L., 1989, "Hydraulic Shock in Ammonia Systems," Presented at IIAR 11th Annual Meeting, March 12-15.

Mandhane, J.M., Gregory, G.A. and Aziz, K., 1974, "A Flow Pattern Map for Gas-Liquid Flow in Horizontal Pipes," *International Journal of Multiphase Flow*, Vol. 1, pp. 537-553.

Manwell, S.P. and Bergles, A.E., 1989, "Gas-Liquid Flow Patterns in Refrigerant-Oil Mixtures," Heat Transfer Laboratory Report #HTL-3, Rensselaer Polytechnic Institute, Troy, NY.

Milne-Thomson, L.M., 1960, Theoretical Hydrodynamics, MacMillan, New York, NY.

Mishima, K. and Ishii, M., 1980, "Theoretical Prediction of Onset of Horizontal Slug Flow", *Journal of Fluid Engineering*, Vol., 102, pp. 441-445.

Moalem, D. and Sideman, S., 1973, "The Effect of Motion on Bubble Collapse," *International Journal of Heat and Mass Transfer*, Vol. 16, pp. 2321-2329.

Rayleigh, Lord, 1917, "On the Pressure Developed in a Liquid During the Collapse of a Spherical Cavity," *Philosophical Magazine*, Vol. 34, pp. 94-98.

Schict, H.H., 1969, "Flow Patterns for an Adiabatic Two-Phase Flow of Water and Air Within a Horizontal Tube," *Verfahrenstechnik*, Vol. 3, pp. 153-161.

Schlager, L.M., 1988, "The Effect of Oil on Heat Transfer and Pressure Drop During Evaporation and Condensation of Refrigerant Inside Augmented Tubes," PhD Thesis, Iowa State University, Ames, IA.

Shah, M.M., 1975, "Visual Observations in an Ammonia Evaporator," *ASHRAE Transactions*, Vol. 81, pp. 295-301.

Soliman, H.M., 1974, "Analytical and Experimental Studies of Flow Patterns During Condensation Inside Horizontal Tubes," PhD Thesis, Kansas State University, Manhattan, KS.

Taitel, Y., 1977, "Flow Pattern Transition in Rough Pipes," *International Journal of Multiphase Flow*, Vol. 3, pp. 597-601.

Taitel, Y., Barnea, D. and Dukler, A.E., 1980, "Modelling Flow Pattern Transitions for Steady Upward Gas-Liquid Flow in Vertical Tubes," *AIChE Journal*, Vol. 26 (3), pp. 345-354.

Taitel, Y. and Dukler, A.E., 1976, "A Model for Predicting Flow Regime Transitions in Horizontal and Near Horizontal Gas-Liquid Flow," *AIChE Journal*, Vol. 22 (1), pp. 47-55.

Taitel, Y., Lee, N. and Dukler, A.E., 1978, "Transient Gas-Liquid Flow in Horizontal Pipes: Modeling the Flow Pattern Transitions," *AIChE Journal*, Vol. 24 (5), pp. 920-934.

Tandon, T.N., Varma, H.K. and Gupta, C.P., 1983, "An Experimental Study of Flow Patterns During Condensation Inside a Horizontal Tube," *ASHRAE Transactions*, Vol. 89 (2A), pp. 471-482.

Trilling, L., 1952, "The Collapse and Rebound of a Gas Bubble," *Journal of Applied Physics*, Vol. 23 (1), pp. 14-17.

Wallis, G.B. and Dobson, J.E., 1973, "The Onset of Slugging in Horizontal Stratified Air-Water Flow," *International Journal of Multiphase Flow*, Vol. 1, pp. 173-193.

Weisman, J., Duncan, D., Gibson, J. and Crawford, T., 1979, "Effects of Fluid Properties and Pipe Diameter on Two-Phase Flow Patterns in Horizontal Lines," *International Journal of Multiphase Flow*, Vol. 5, pp. 437-462.

Wittke, D.D. and Chao, B.T., 1967, "Collapse of Vapor Bubbles with Translatory Motion," *Journal of Heat Transfer*, Vol. 89 (1), pp. 17-24.

Worsoe-Schmidt, P., 1960, "Some Characteristics of Flow Pattern and Heat Transfer of Freon-12 Evaporationg in Horizontal Tubes," *The Journal of Refrigeration*, Vol. 3, pp. 40-44.

Zucker, R., 1977, Fundamentals of Gas Dynamics, Matrix Publishers Inc., Chesterland, OH.

Appendix A

Flow Model Derivation

To analyze the physics of the fluid flow, the valve opening process is modeled as a diaphragm bursting in an orifice. As shown in Figure A.1, the flow in the model is separated into two regions. The first control volume, located upstream of the orifice, consists of a converging nozzle which represents the region of from the valve inlet to the valve port. The flow conditions in this region are modeled with general one-dimensional compressible flow equations assuming quasi-steady, adiabatic, calorically perfect, isentropic flow.

Flow through the valve is choked for pressure differences representative of the hot gas defrost process. Therefore, basic one-dimensional compressible flow property ratios are used to relate the flow properties at the orifice to the inlet conditions. With knowledge of the diameters of the orifice and the pipe, the Mach number at the valve inlet is obtained by

$$\frac{A_1}{A_{orf}} = \frac{1}{M_1}\left[\frac{1+\left(\frac{\gamma-1}{2}\right)M_1^2}{\left(\frac{\gamma+1}{2}\right)}\right]^{\frac{\gamma+1}{2(\gamma-1)}} \tag{A.1}$$

where the subscripts 1 and orf indicate the inlet and orifice locations respectively. Once the Mach number at the inlet is found and the inlet flow properties are specified, the stagnation

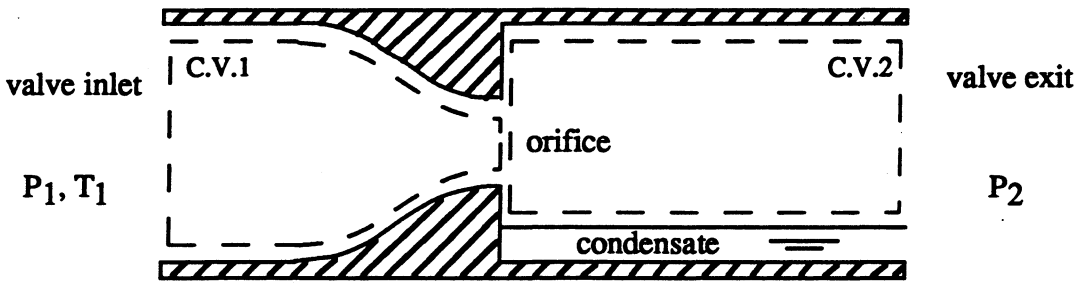

Figure A.1. Schematic of orifice with control volumes used to simulate valve.

properties may be determined using the following static-to-stagnation relationships:

$$P_t = P_1\left(1+\frac{\gamma-1}{2}M_1^2\right)^{\frac{\gamma}{\gamma-1}} \tag{A.2}$$

$$T_t = T_1\left(1+\frac{\gamma-1}{2}M_1^2\right) \tag{A.3}$$

$$\rho_t = \rho_1\left(1+\frac{\gamma-1}{2}M_1^2\right)^{\frac{1}{\gamma-1}} \tag{A.4}$$

Based on the assumption of a calorically perfect gas in an isentropic flow, the stagnation properties of the flow are constant throughout the control volume. Thus the same static-to-stagnation equations are rearranged as

$$P_{orf} = P_t\left(1+\frac{\gamma-1}{2}M_{orf}^2\right)^{\frac{\gamma}{1-\gamma}} \tag{A.5}$$

$$T_{orf} = T_t\left(1+\frac{\gamma-1}{2}M_{orf}^2\right)^{-1} \tag{A.6}$$

$$\rho_{orf} = \rho_t\left(1+\frac{\gamma-1}{2}M_{orf}^2\right)^{\frac{1}{1-\gamma}} \tag{A.7}$$

where the static properties are now those at the orifice.

The final flow property desired from the analysis of the first control volume is the mass flow rate of the fluid. Mass flow rate is defined as

$$\dot{m} = \rho A U \tag{A.8}$$

The previous equations, however, express the flow properties in terms of Mach number. In order to relate the mass flow through the valve to the Mach values of the flow, the Mach number is related to the velocity of the flow through the definition of Mach number, given as

$$M = \frac{U}{a} \tag{A.9}$$

where a is the speed of sound in the medium. For a perfect gas undergoing an isentropic process,

the speed of sound may be expressed as

$$a = \sqrt{\gamma R T} \tag{A.10}$$

where γ is the ratio of specific heats for the fluid. Combining equations A.8 through A.10 allows the mass flow rate to be written as

$$\dot{m} = \rho A M \sqrt{\gamma R T} \tag{A.11}$$

Substituting in the equation of state for a perfect gas, equation A.11 becomes

$$\dot{m} = P A M \left(\frac{\gamma}{R T} \right)^{\frac{1}{2}} \tag{A.12}$$

Converting to units consistent with the established nomenclature, the final expression for the mass flow rate through the orifice is

$$\dot{m} = \left(144 \frac{in^2}{ft^2} \right) P_{orf} \, A_{orf} \, M_{orf} \left(\frac{\left(32.174 \frac{lbm \cdot ft}{lbf \cdot s^2} \right) \gamma}{R \, T_{orf}} \right)^{\frac{1}{2}} \tag{A.13}$$

The second control volume, shown in Figure A.2, consists a sudden enlargement into a pipe partially filled with condensate. This region was modeled as adiabatic, steady, one-dimensional flow. An aerodynamic boundary exists within the flow but it is within the control volume so that is is assumed that there is no friction at any of the boundaries of the

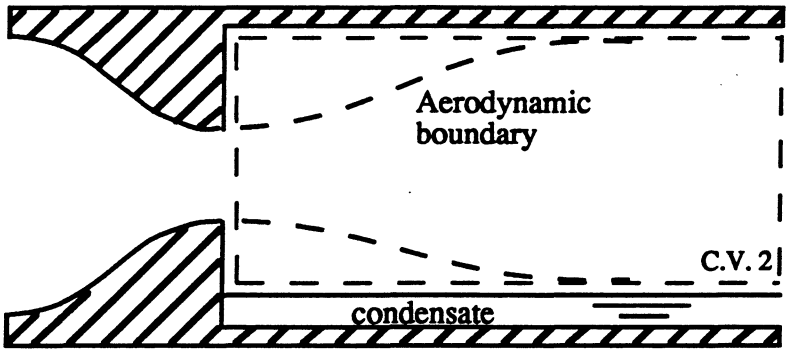

Figure A.2. Control volume for analysis downstream of orifice.

control volume. The flow conditions at the orifice obtained from the upstream analysis are used as the input conditions for the downstream control volume.

The purpose of the analysis of the second control volume is to determine the volumetric flow rate downstream of the orifice where the hydrodynamic boundary reattaches. For the previously stated assumptions, the continuity and energy equations are

$$\dot{m} = \rho_{orf} A_{orf} U_{orf} = \rho_2 A_2 U_2 = \text{constant} \tag{A.14}$$

$$i + \frac{U^2}{2} = i_t = \text{constant} \tag{A.15}$$

Again assuming a calorically perfect gas such that c_p is constant, the energy equation is further reduced to T_t = constant. For the fluid flow, a mass flow rate function is defined at each point in the flow as

$$\text{mass flow function} = \frac{\dot{m}\sqrt{R T_t}}{P A} \tag{A.16}$$

Assuming a perfect gas, equations A.3, A.9, and A.10 are substituted into equation A.16, which gives the expression

$$\frac{\dot{m}\sqrt{R T_t}}{P A} = M\left[\gamma\left(1+\frac{\gamma-1}{2}M^2\right)\right]^{\frac{1}{2}} \tag{A.17}$$

where the mass flow function is now a function of Mach number, M, and the ratio of specific heats of the vapor, γ. Fom the continuity and energy equations, the mass flow rate, $\dot{m}$, and the stagnation temperature, T_t, are constant. Therefore, the mass flow equation becomes a constant with stream location when multiplied by pressure, P, and area, A. This may be written for the control volume as

$$P_{orf} A_{orf}\left(\frac{\dot{m}\sqrt{R T_t}}{P_{orf} A_{orf}}\right) = P_2 A_2\left(\frac{\dot{m}\sqrt{R T_t}}{P_2 A_2}\right) \tag{A.18}$$

Substituting in equation A.17, equation A.18 is rewritten as

$$P_{orf}\, A_{orf}\, M_{orf}\left[\gamma\left(1+\frac{\gamma-1}{2}M_{orf}{}^{2}\right)\right]^{\frac{1}{2}} = P_2\, A_2\, M_2\left[\gamma\left(1+\frac{\gamma-1}{2}M_2{}^{2}\right)\right]^{\frac{1}{2}} \qquad \text{(A.19)}$$

With all of the other variables either specified or determined from the first control volume analysis, equation A.19 is solved for the Mach number downstream of the orifice at the valve exit. Once the Mach number at the exit is determined, equation A.12 is rewritten as

$$T_2 = \frac{\gamma}{R}\left(\frac{P_2\, A_2\, M_2}{\dot{m}}\right)^2 \qquad \text{(A.20)}$$

Finally, with knowledge of the downstream temperature the volumetric flow rate at the valve exit is solved by

$$Q_2 = A_2\, U_2 = A_2\, M_2\sqrt{\gamma R T_2} \qquad \text{(A.21)}$$

In terms of the established nomenclature, this equation becomes

$$Q_2 = A_2\, M_2\sqrt{\left(\frac{32.174\ \text{lbm}\cdot\text{ft}}{\text{lbf}\cdot\text{s}^2}\right)\gamma R T_2} \qquad \text{(A.22)}$$

Appendix B

Handbook Method for Flow Calculations

The handbook method used by engineers to determine the volumetric flow rate through a valve is based on the head loss through the valve and the definition of a flow coefficient, C_v. The governing equations for incompressible flow through a valve are Bernoulli's equation,

$$h_l = \frac{\Delta P}{\rho} + \frac{\Delta(U^2)}{2} = k\frac{U^2}{2} \tag{B.1}$$

and the continuity equation,

$$\dot{m} = \rho A_1 U_1 = \rho A_2 U_2 = \text{constant} \tag{B.2}$$

For the refrigeration systems analyzed, the nominal pipe sizes upstream and downstream of the valve are equal. Since the flow is incompressible, the continuity equation thus indicates that the fluid velocity upstream and downstream of the valve must be equal (i.e. $\Delta U = 0$) and equation B.1 reduces to

$$h_l = \frac{\Delta P}{\rho} = k\frac{U^2}{2} \tag{B.3}$$

Converting to units consistent with the established nomenclature and defining the head loss at upstream flow conditions, equation B.3 becomes

$$\left(144\frac{in^2}{ft^2}\right)\left(32.174\frac{lbm\cdot ft}{lbf\cdot s^2}\right)\frac{(P_1 - P_2)}{\rho} = k\frac{U_1^2}{2}. \tag{B.4}$$

The equation is then solved for U_1, such that

$$U_1 = \left[\frac{2\left(32.174\frac{lbm\cdot ft}{lbf\cdot s^2}\right)\left(144\frac{in^2}{ft^2}\right)(P_1 - P_2)}{k\rho}\right]^{\frac{1}{2}} \tag{B.5}$$

Substituting this expression for U_1 into equation B.2, the continuity equation becomes

$$\dot{m} = \rho A_1 \left[\frac{2\left(32.174 \frac{lbm \cdot ft}{lbf \cdot s^2}\right)\left(144 \frac{in^2}{ft^2}\right)(P_1 - P_2)}{k\rho} \right]^{\frac{1}{2}} \tag{B.6}$$

The vapor flowing through the valve is assumed to be a perfect gas, following the equation of state of

$$P = \rho R T \tag{B.7}$$

Equation B.7 is solved for ρ at the upstream conditions and put in terms of units consistent with nomenclature, such that

$$\rho = \frac{\left(144 \frac{in^2}{ft^2}\right) P_1}{R T_1} \tag{B.8}$$

After defining the fluid density through the valve, equation B.8 is substituted into B.6 so that the mass flow rate is written as

$$\dot{m} = \left[\frac{2\left(144 \frac{in^2}{ft^2}\right)^2 \left(32.174 \frac{lbm \cdot ft}{lbf \cdot s^2}\right) A_1^2 (P_1 - P_2) P_1}{k R T_1} \right]^{\frac{1}{2}} \tag{B.9}$$

Equation B.9 determines the mass flow rate through the valve using k, a loss coeficient. In order to obtain an expression for the volumetric flow rate in terms of the flow coefficient, C_v, a relationship must be derived between C_v and k. Since C_v is defined for a liquid, Bernoulli's equation is applied to the flow of a liquid with the head loss defined at upstream conditions, giving the expression

$$\frac{\left(144 \frac{in^2}{ft^2}\right)\left(32.174 \frac{lbm \cdot ft}{lbf \cdot s^2}\right)(P_1 - P_2)}{\rho_w} = k \frac{U_1^2}{2} \tag{B.10}$$

Solving equation B.10 for k,

$$k = \frac{2\left(144\frac{in^2}{ft^2}\frac{ft^2}{ft^2}\right)\left(32.174\frac{lbm \cdot ft}{lbf \cdot s^2}\right)(P_1 - P_2)}{\rho_w U_1^2} \tag{B.11}$$

The flow coefficient, C_v, is defined as the number of gallons per minute of liquid that will flow through a valve for a given one p.s.i. pressure drop. This may be written as

$$gpm = C_v\sqrt{\frac{\Delta P}{G}} \tag{B.12}$$

Converting the flow rate to units consistent with the presented nomenclature,

$$\left(7.48\frac{gal}{ft^3}\right)\left(60\frac{s}{min}\right)U_1 A_1 = C_v\sqrt{\frac{P_1 - P_2}{G}} \tag{B.13}$$

This expression is then rearranged to solve for the pressure difference, such that

$$\left(7.48\frac{gal}{ft^3}\right)^2\left(60\frac{s}{min}\right)^2 U_1^2 A_1^2 = C_v^2\left(\frac{P_1 - P_2}{G}\right) \tag{B.14}$$

$$(P_1 - P_2) = \frac{\left(7.48\frac{gal}{ft^3}\right)^2\left(60\frac{s}{min}\right)^2 U_1^2 A_1^2 G}{C_v^2} \tag{B.15}$$

Substituting B.15 into equation B.11, the relationship between C_v and k is then established as

$$k = \frac{2\left(144\frac{in^2}{ft^2}\right)\left(32.174\frac{lbm \cdot ft}{lbf \cdot s^2}\right)\left(7.48\frac{gal}{ft^3}\right)^2\left(60\frac{s}{min}\right)^2 A_1^2 G}{\rho_w C_v^2} \tag{B.16}$$

Combining this equation with equation B.9, the mass flow rate through the valve is now expressed in terms of C_v as

$$\dot{m} = \left[\frac{\left(144\frac{in^2}{ft^2}\right)(P_1 - P_2)P_1\rho_w C_v^2}{\left(7.48\frac{gal}{ft^3}\right)^2\left(60\frac{s}{min}\right)^2 GRT_1}\right]^{\frac{1}{2}} \tag{B.17}$$

The volumetric flow rate of air through the valve at standard temperature and pressure is

$$Q = \frac{\dot{m}}{\rho_a} \tag{B.18}$$

where the units of Q for this derivation are scfh (standard cubic feet per hour). Equation B.18 is combined with the expression developed for mass flow rate, such that

$$Q = \left[\frac{\left(144\frac{in^2}{ft^2}\right)(P_1 - P_2)P_1 \rho_w C_v^2 \left(3600\frac{s}{hr}\right)^2}{\left(7.48\frac{gal}{ft^3}\right)^2 \left(60\frac{s}{min}\right)^2 \rho_a^2 G R T_1} \right]^{\frac{1}{2}} \tag{B.19}$$

Substituting in the various properties for air and water, this expression is reduced to:

$$Q = \left[\frac{\left(144\frac{in^2}{ft^2}\right)(P_1 - P_2)P_1 \left(62.4\frac{lbm}{ft^3}\right) C_v^2 \left(3600\frac{s}{hr}\right)^2}{\left(7.48\frac{gal}{ft^3}\right)^2 \left(60\frac{s}{min}\right)^2 \left(0.0762\frac{lbm}{ft^3}\right)^2 G \left(53.3\frac{ft \cdot lbf}{lbm \cdot °R}\right) T_1} \right]^{\frac{1}{2}} \tag{B.20}$$

$$Q = \left(1360\frac{in^2 \cdot ft^6 \cdot min \cdot °R}{gal^2 \cdot lbf \cdot hr^2}\right) P_1 C_v \sqrt{\frac{(P_1 - P_2)}{P_1 G T_1}} \tag{B.21}$$

The volumetric flow equation is altered to account for additional flow losses through the valve. To account for the density changes in the fluid and the changes in the area of the vena contracta with pressure variations, equation B.21 is multiplied by an expansion factor,

$$Y = 1 - \frac{x}{3F_K x_T} \tag{B.22}$$

where x is the pressure drop ratio,

$$x = \frac{(P_1 - P_2)}{P_1} \tag{B.23}$$

F_K is the ratio of specific heats factor,

$$F_K = \frac{\gamma}{1.40} \tag{B.24}$$

and x_T is the pressure drop ratio factor which is listed in valve sizing handbooks. The volumetric flow equation is also modified by a general compressibility factor, Z. This factor accounts for the nonidealities in the fluid properties that exist in the compressible flow of gases. The compressibility factor is a function of both the reduced pressure and the reduced temperature of the fluid,

$$P_r = \frac{P}{P_c} \tag{B.25}$$

$$T_r = \frac{T}{T_c} \tag{B.26}$$

Finally, a piping geometry factor, F_P, is introduced to adjust the volumetric flow rate for the effects of fittings that are attached to the valve. F_P is a ratio of C_V with pipe fittings to C_V without fittings for a particular valve and may be found in valve sizing handbooks.

Combining each of the factors into equation B.21, the equation for the volumetric flow rate through the valve becomes

$$Q = 1360\, C_V P_1 (F_P Y) \sqrt{\frac{x}{G T_1 Z}} \tag{B.27}$$

which is the official formula by the American National Standards Insitute and the Instrument Society of America (ISA, 1985).

Appendix C

Handbook Maps

The results of the handbook method are plotted for three different types of valves. The procedure for using the maps is as follows:

I. Determine the ratio of upstream and downstream flow pressures present in the system before the valve opens.

II. For a given ratio, read the volumetric flow rate from the flow map.

Descriptions of the three valves analyzed were obtained from the ISA Standard S75.01 (ISA, 1985) and are given in Table C.1.

Table C.1. Representative Values of Valve Capacity Factors

Valve Type	Trim Type	Flow Direction	x_T	C_V / D^2
Globe: single port	Ported Plug	Either	0.75	9.5
	Contoured Plug	Open	0.72	11
	Characterized Cage	Close	0.70	16

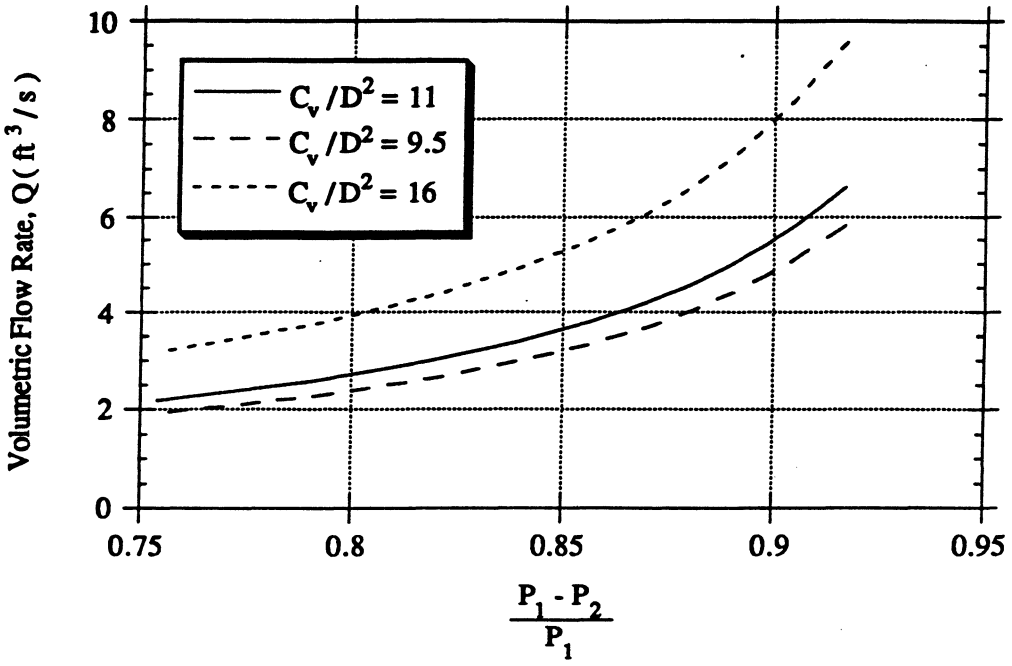

Figure C.1. Plot of the handbook results for flow through a valve with schedule 80 steel pipe of 0.5 in. nominal diameter.

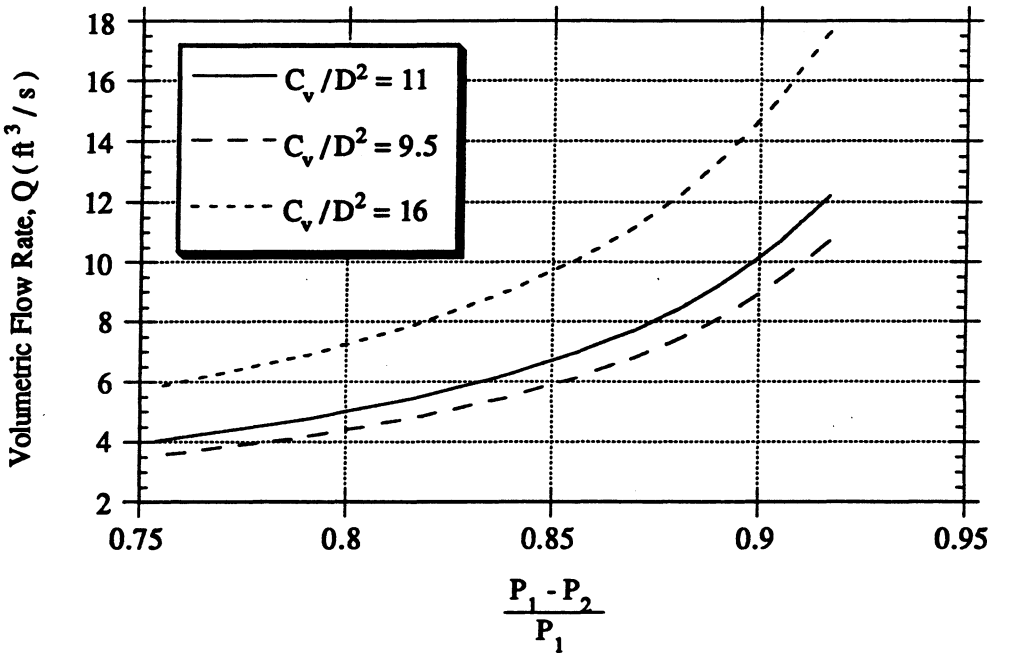

Figure C.2. Plot of the handbook results for flow through a valve with schedule 80 steel pipe of 0.75 in. nominal diameter.

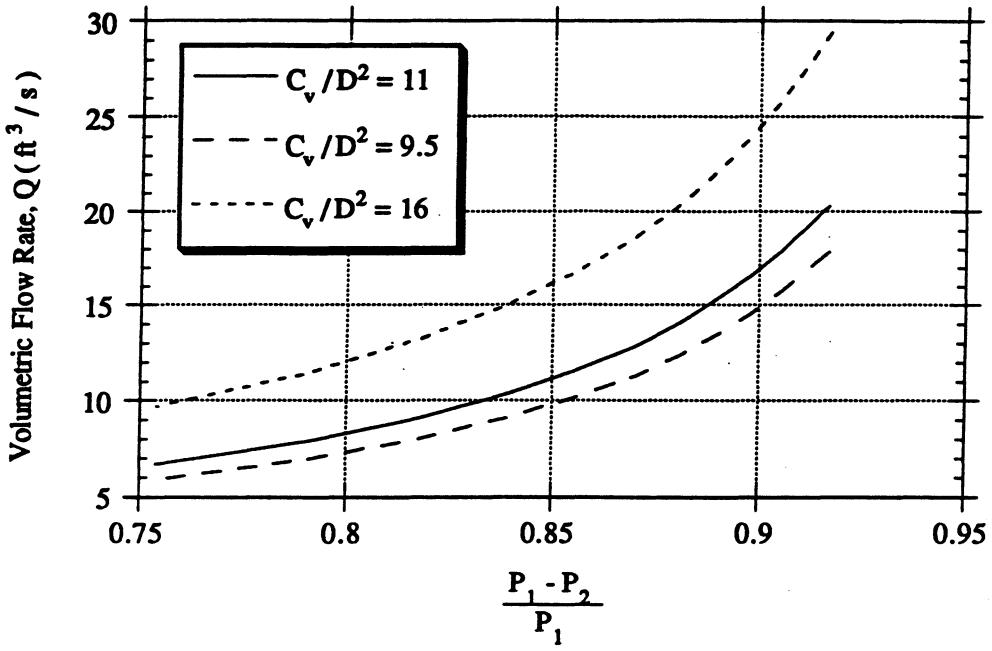

Figure C.3. Plot of the handbook results for flow through a valve with schedule 80 steel pipe of 1.0 in. nominal diameter.

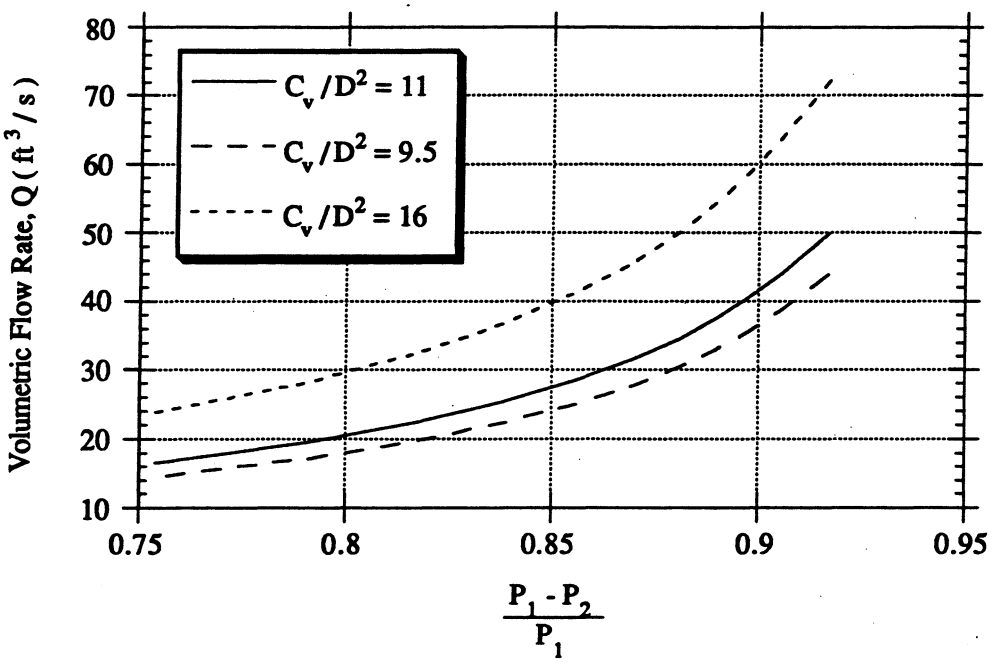

Figure C.4. Plot of the handbook results for flow through a valve with schedule 80 steel pipe of 1.5 in. nominal diameter.

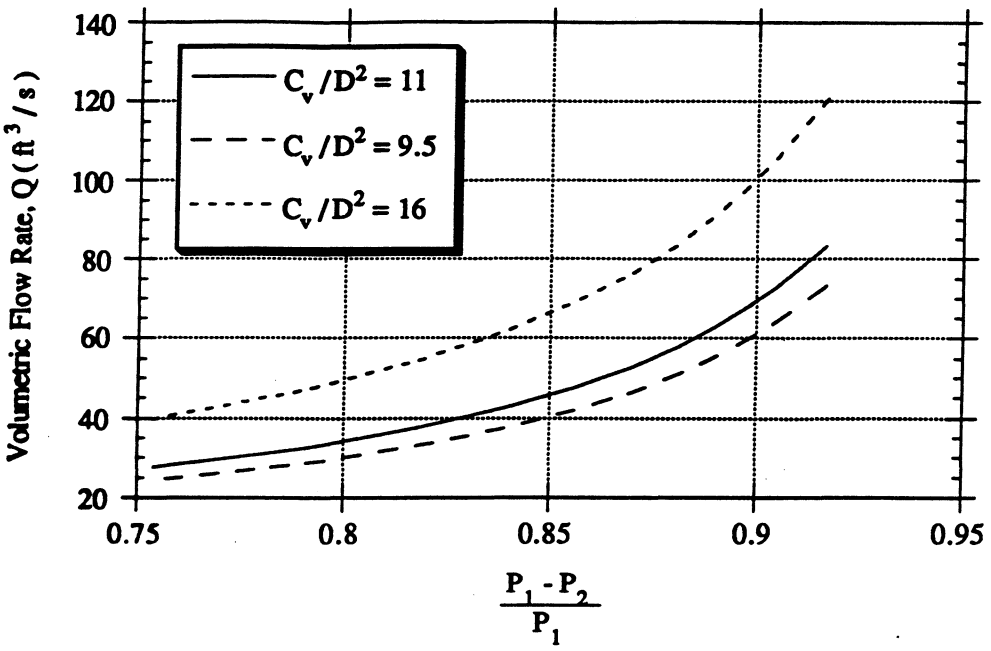

Figure C.5. Plot of the handbook results for flow through a valve with schedule 80 steel pipe of 2.0 in. nominal diameter.

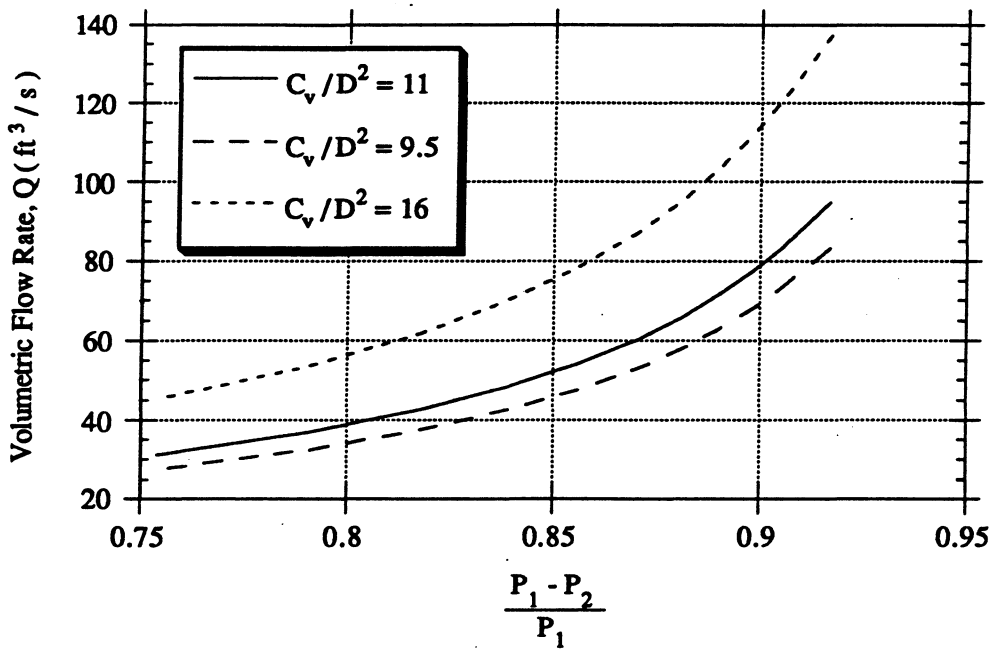

Figure C.6. Plot of the handbook results for flow through a valve with schedule 40 steel pipe of 2.0 in. nominal diameter.

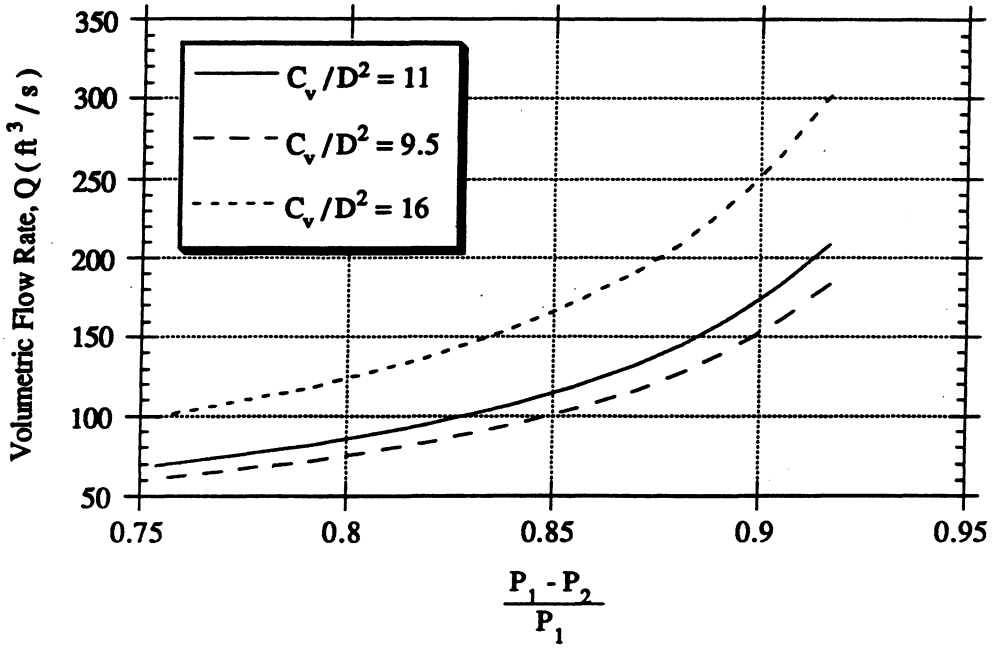

Figure C.7. Plot of the handbook results for flow through a valve with schedule 40 steel pipe of 3.0 in. nominal diameter.

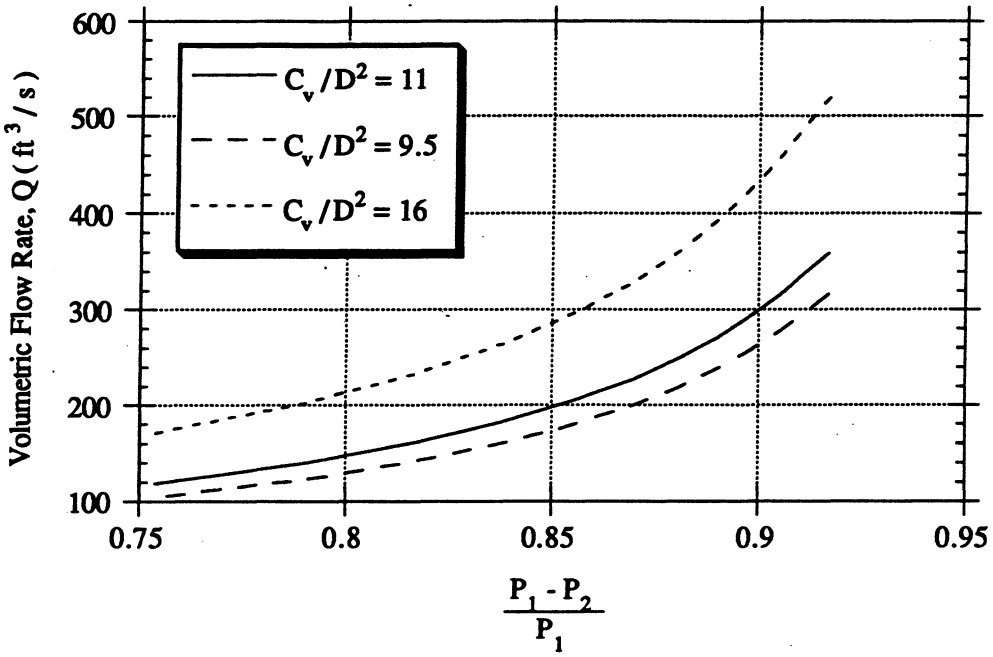

Figure C.8. Plot of the handbook results for flow through a valve with schedule 40 steel pipe of 4.0 in. nominal diameter.

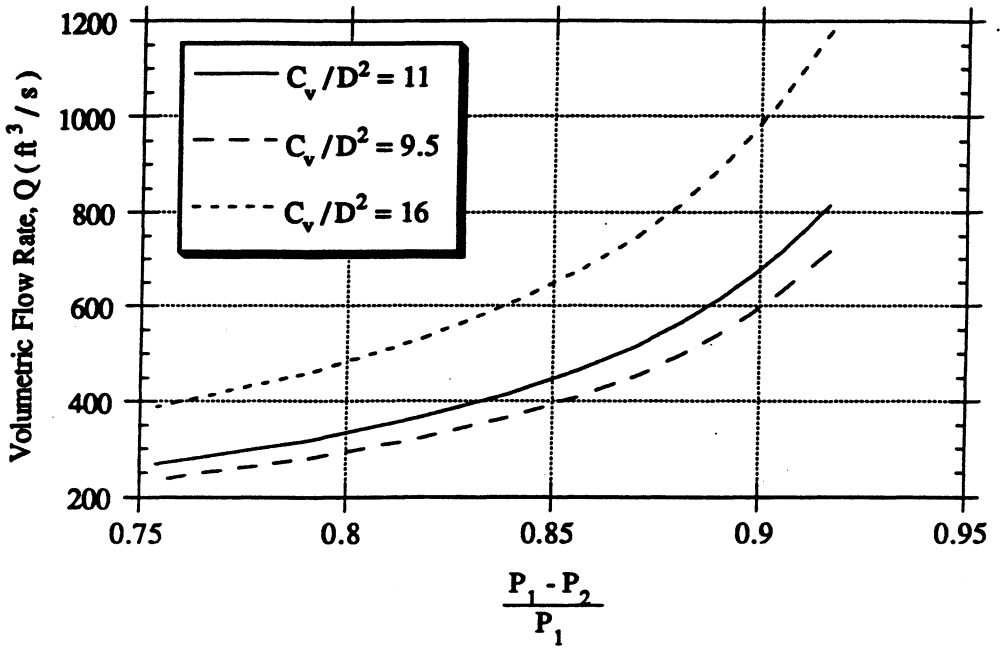

Figure C.9. Plot of the handbook results for flow through a valve with schedule 40 (standard weight) steel pipe of 6.0 in. nominal diameter.

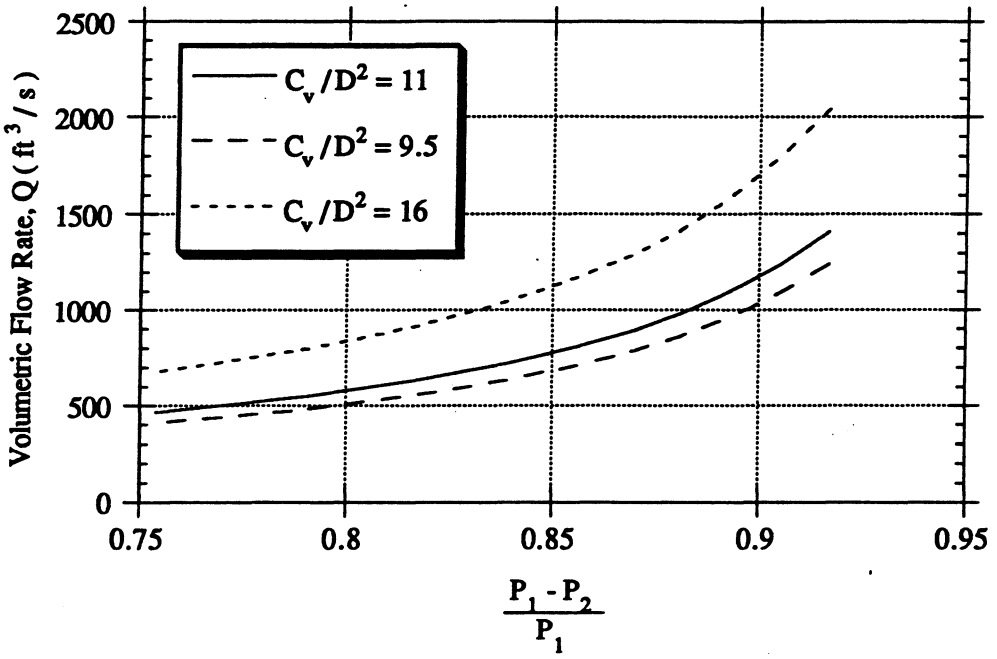

Figure C.10. Plot of the handbook results for flow through a valve with standard weight steel pipe of 8.0 in. nominal diameter.

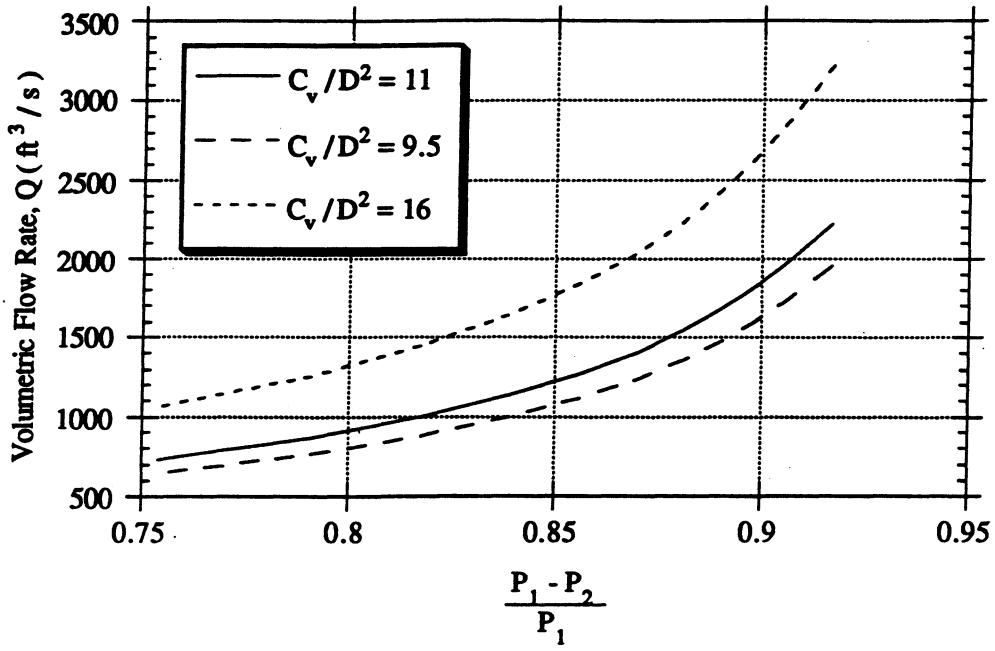

Figure C.11. Plot of the handbook results for flow through a valve with standard weight steel pipe of 10.0 in. nominal diameter.

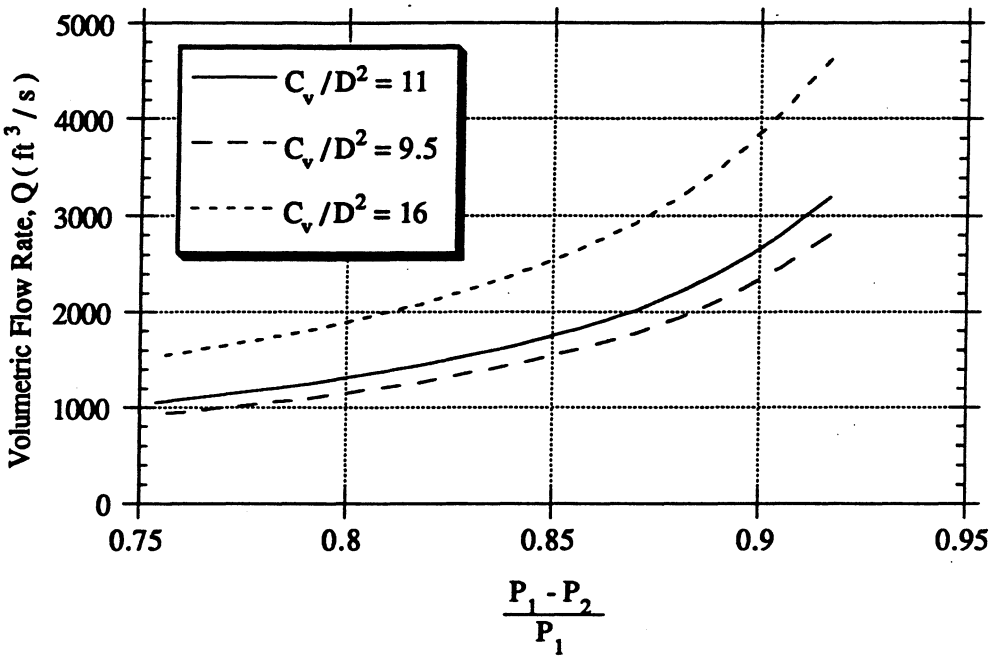

Figure C.12. Plot of the handbook results for flow through a valve with standard weight steel pipe of 12.0 in. nominal diameter.

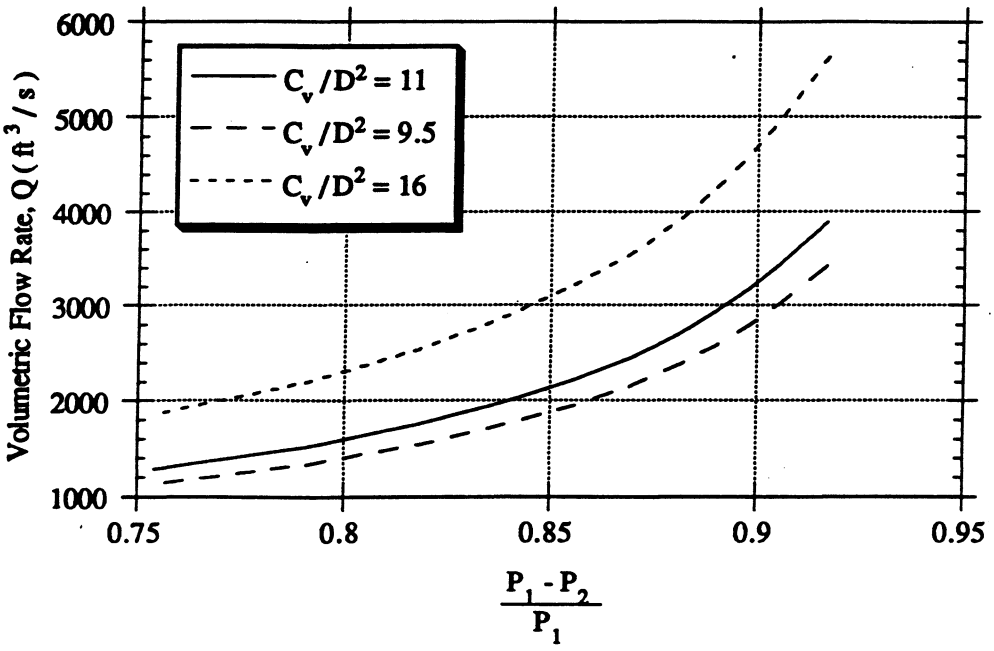

Figure C.13. Plot of the handbook results for flow through a valve with standard weight steel pipe of 14.0 in. nominal diameter.

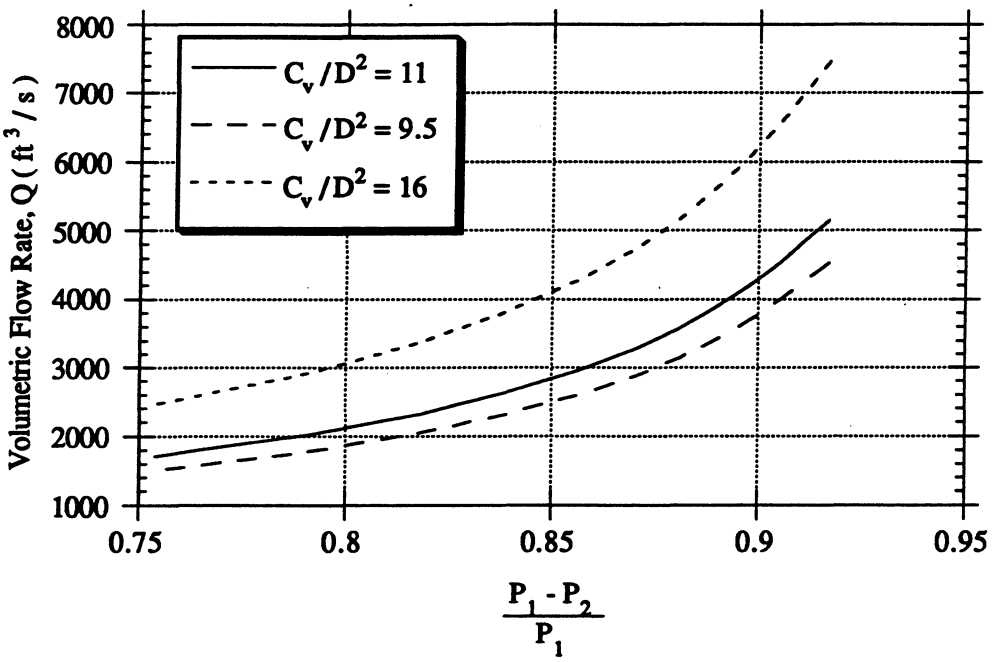

Figure C.14. Plot of the handbook results for flow through a valve with standard weight steel pipe of 16.0 in. nominal diameter.

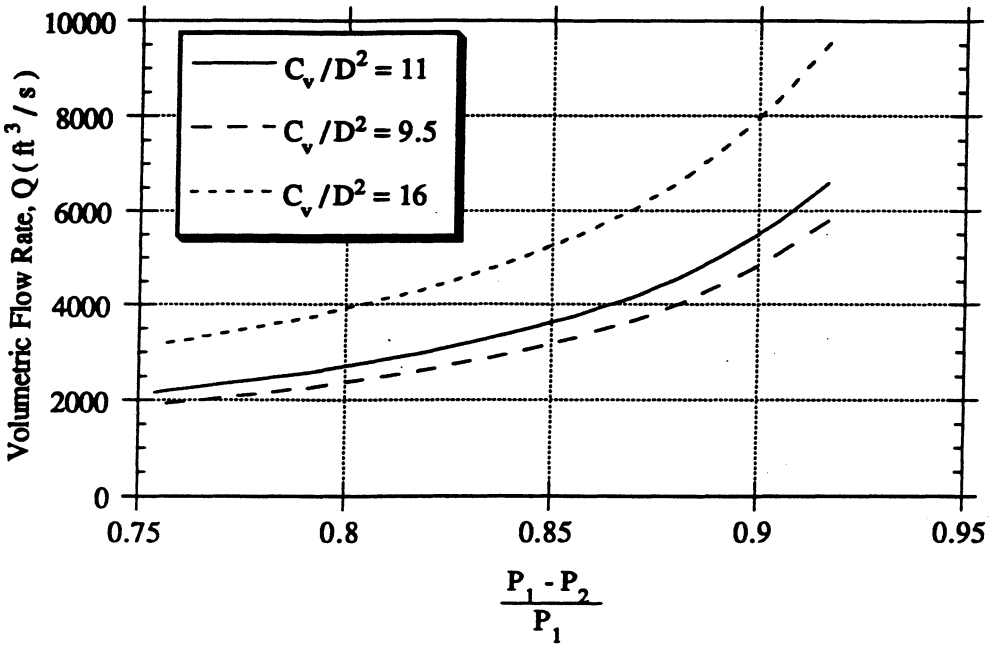

Figure C.15. Plot of the handbook results for flow through a valve with standard weight steel pipe of 18.0 in. nominal diameter.

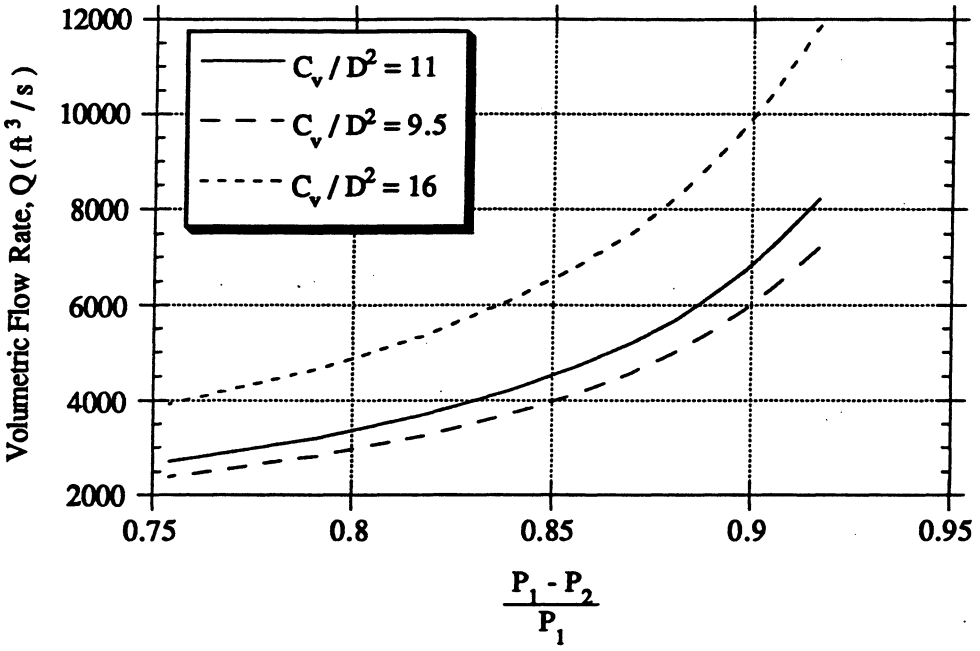

Figure C.16. Plot of the handbook results for flow through a valve with standard weight steel pipe of 20.0 in. nominal diameter.

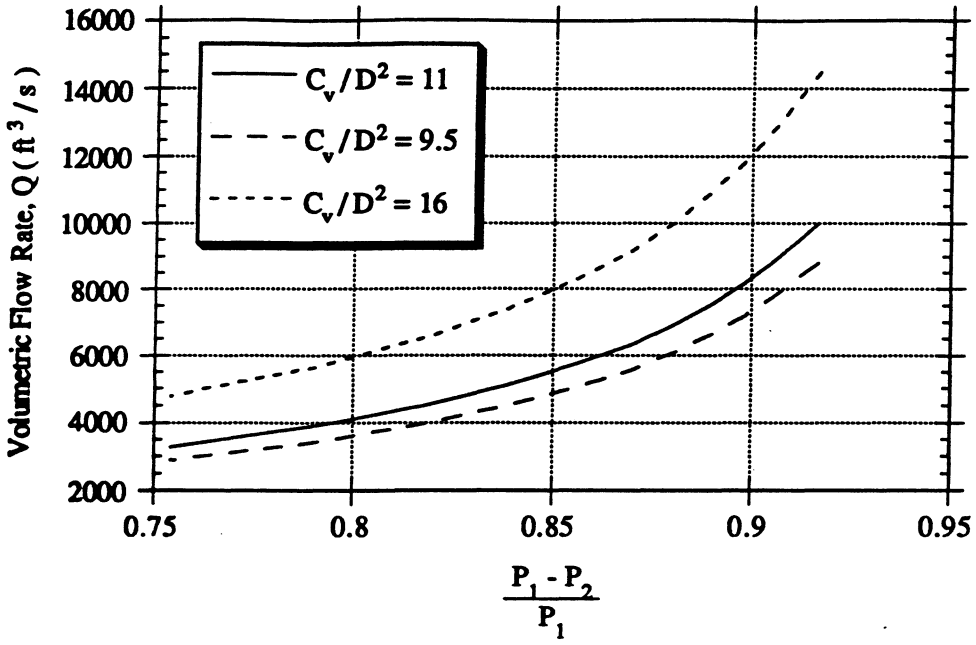

Figure C.17. Plot of the handbook results for flow through a valve with standard weight steel pipe of 22.0 in. nominal diameter.

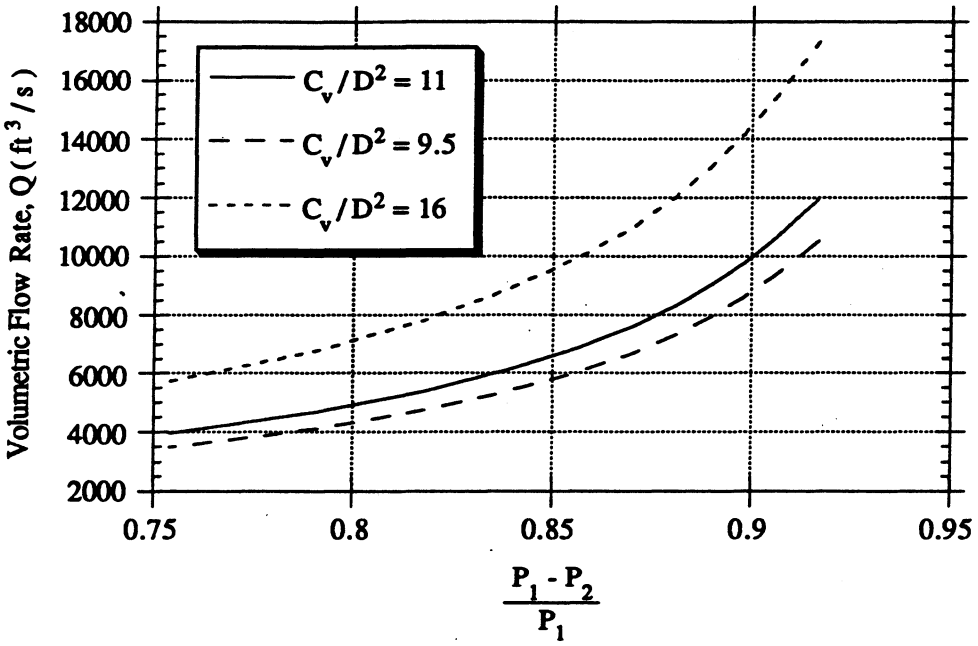

Figure C.18. Plot of the handbook results for flow through a valve with standard weight steel pipe of 24.0 in. nominal diameter.

Appendix D

Shock Maps

The shock maps indicate when a system is susceptible to vapor-propelled liquid slugging and condensation-induced shock. For each map, the criterion for shock occurrence is plotted for various liquid depths. The ordinate is given as a ratio of the phase densities at the downstream conditions. For a given amount of condensate in a pipe, if the volumetric flow rate determined from the flow map is above the transition line on the corresponding shock map then hydraulic shocks may occur.

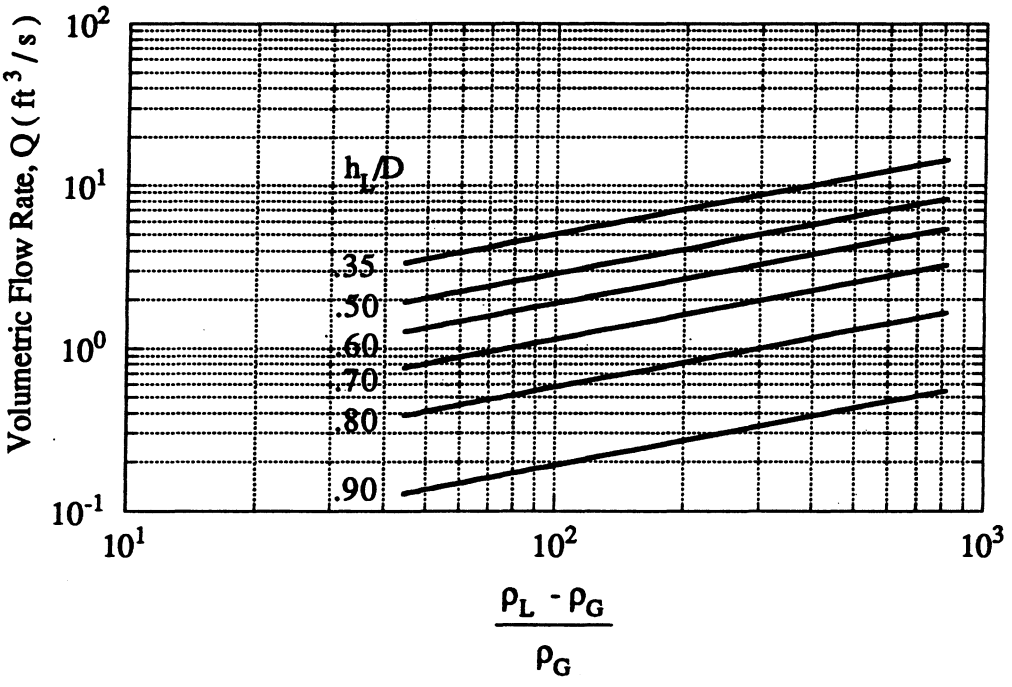

Figure D.1. Plot of transition criterion at constant liquid depths for schedule 80 steel pipe 0.75 in. nominal diameter.

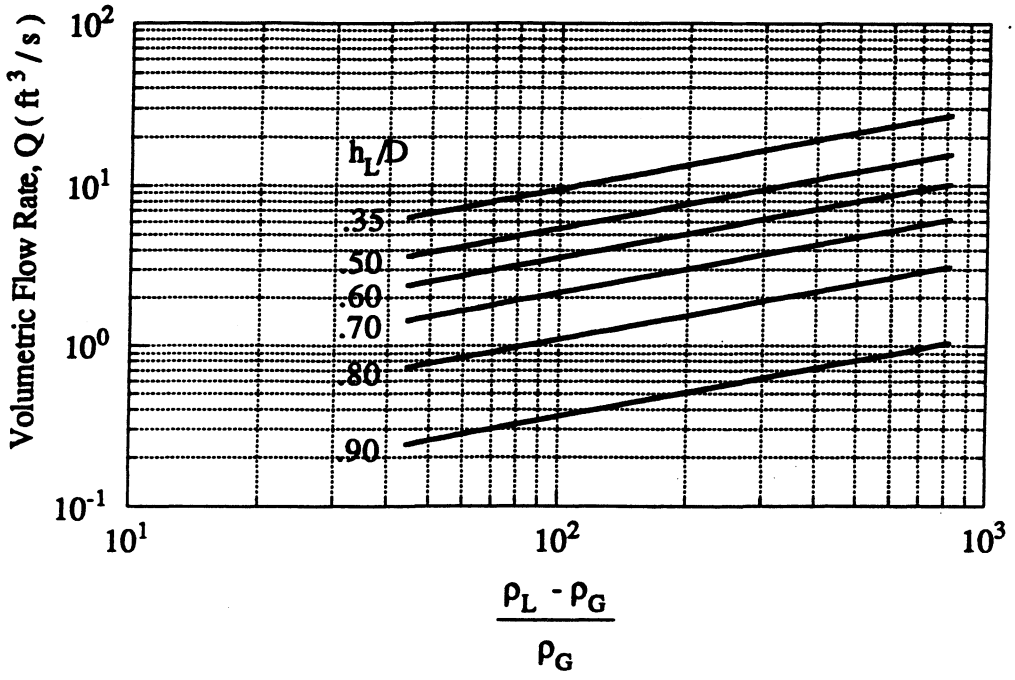

Figure D.2. Plot of transition criterion at constant liquid depths for schedule 80 steel pipe of 1.0 in. nominal diameter.

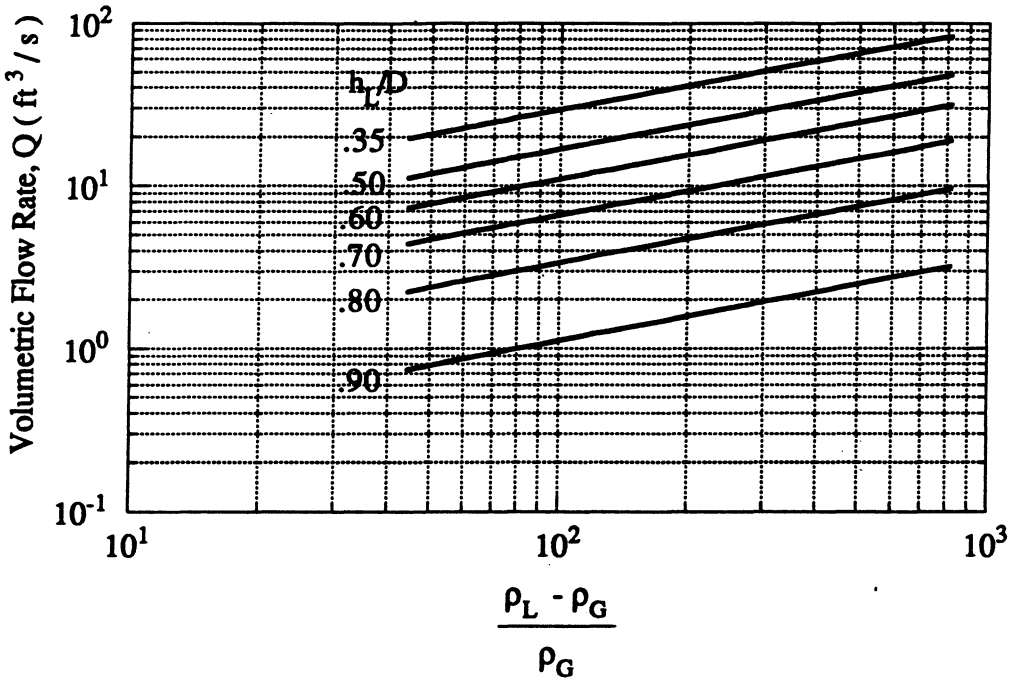

Figure D.3. Plot of transition criterion at constant liquid depths for schedule 80 steel pipe of 1.5 in. nominal diameter.

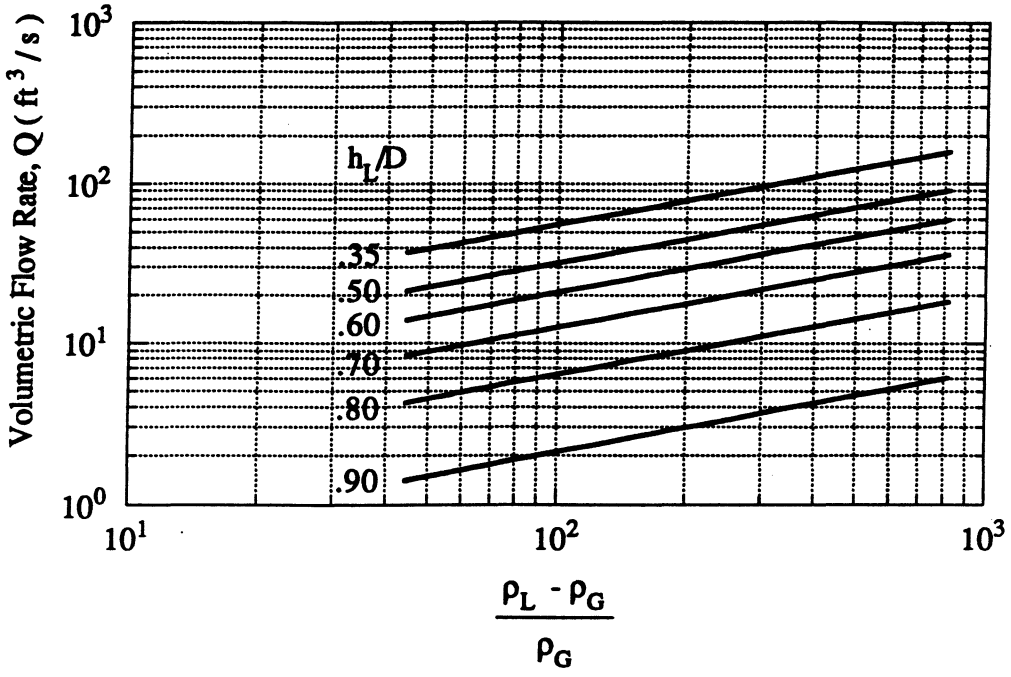

Figure D.4. Plot of transition criterion at constant liquid depths for schedule 80 steel pipe of 2.0 in. nominal diameter.

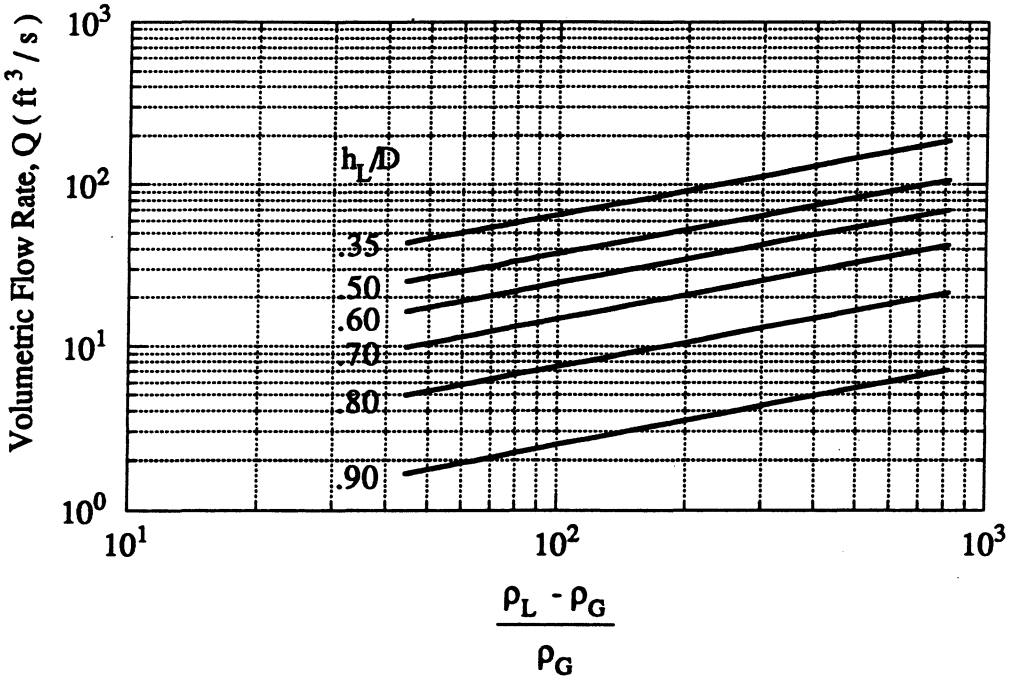

Figure D.5. Plot of transition criterion at constant liquid depths for schedule 40 steel pipe of 2.0 in. nominal diameter.

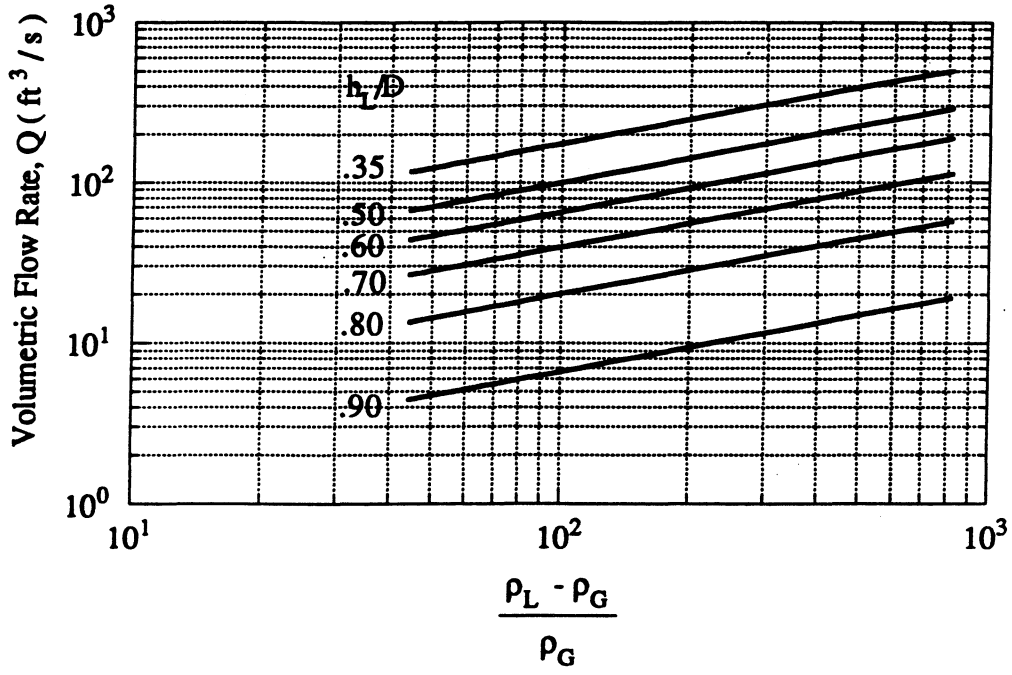

Figure D.6. Plot of transition criterion at constant liquid depths for schedule 40 steel pipe of 3.0 in. nominal diameter.

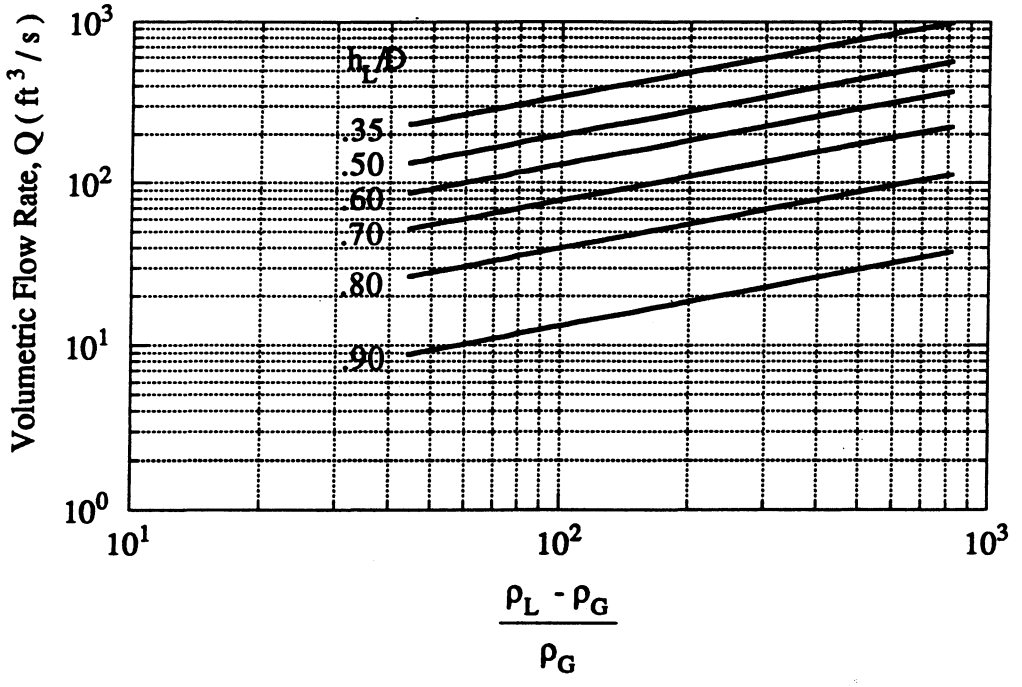

Figure D.7. Plot of transition criterion at constant liquid depths for schedule 40 steel pipe of 4.0 in. nominal diameter.

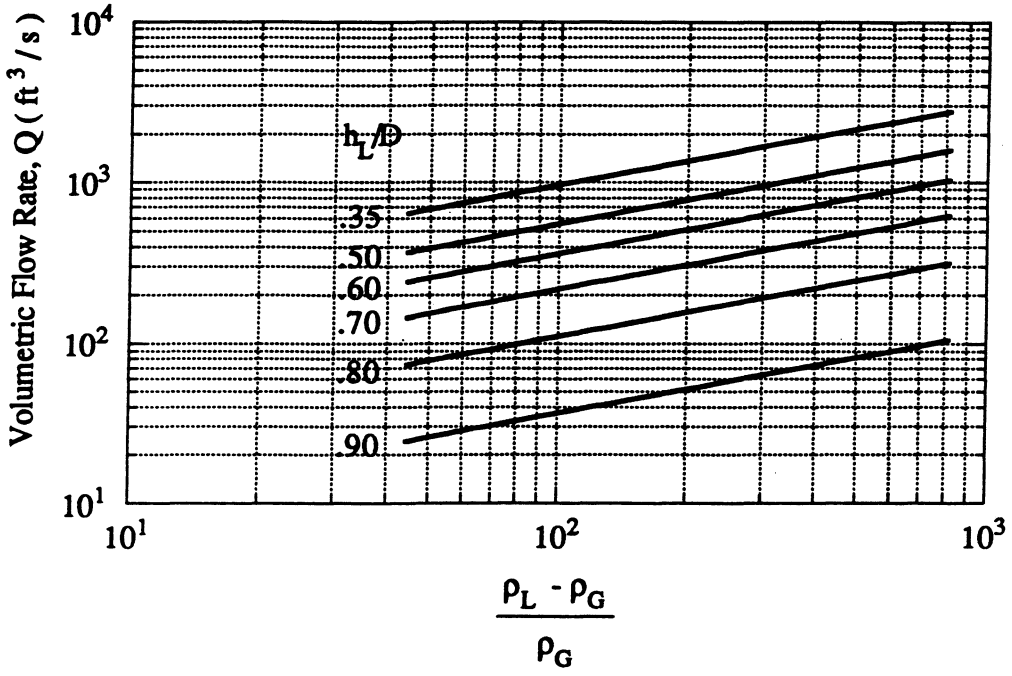

Figure D.8. Plot of transition criterion at constant liquid depths for schedule 40 (standard weight) steel pipe of 6.0 in. nominal diameter.

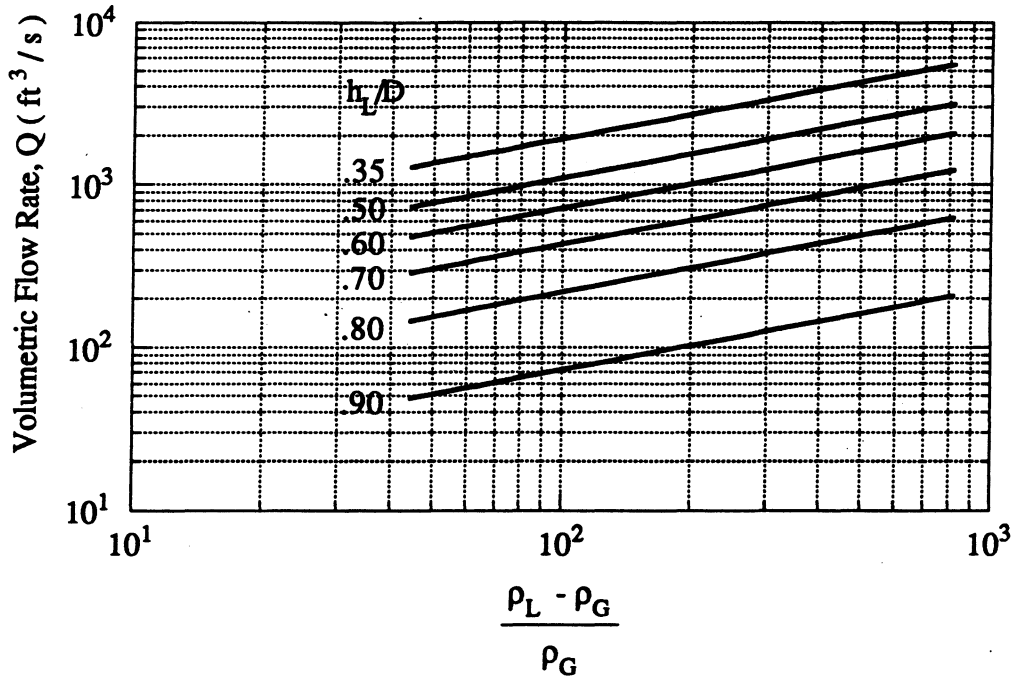

Figure D.9. Plot of transition criterion at constant liquid depths for standard weight steel pipe of 8.0 in. nominal diameter.

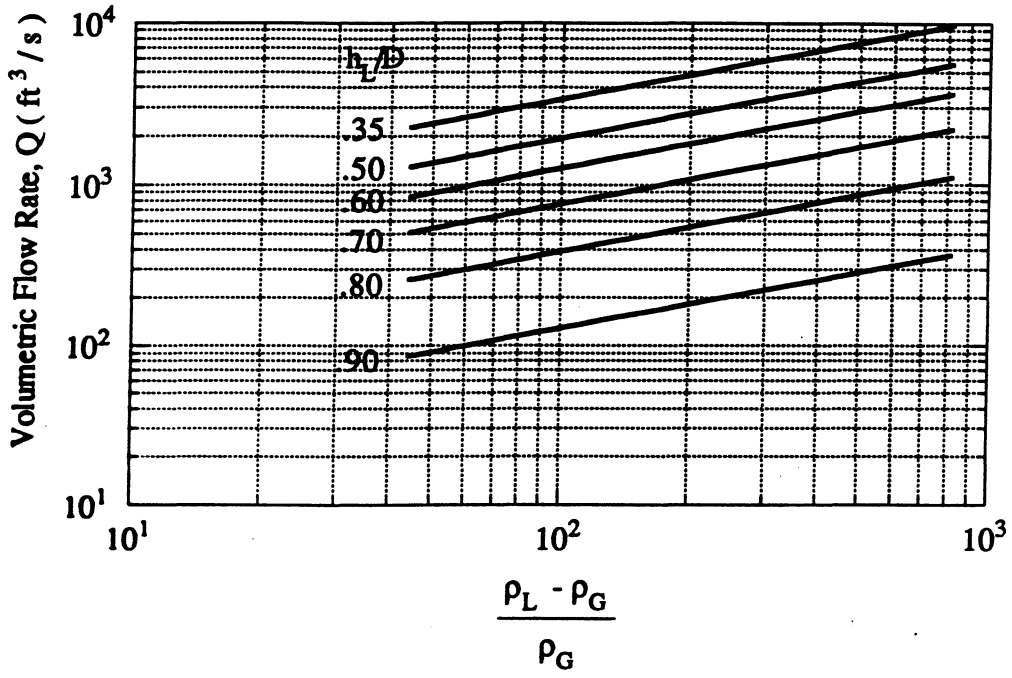

Figure D.10. Plot of transition criterion at constant liquid depths for standard weight steel pipe of 10.0 in. nominal diameter.

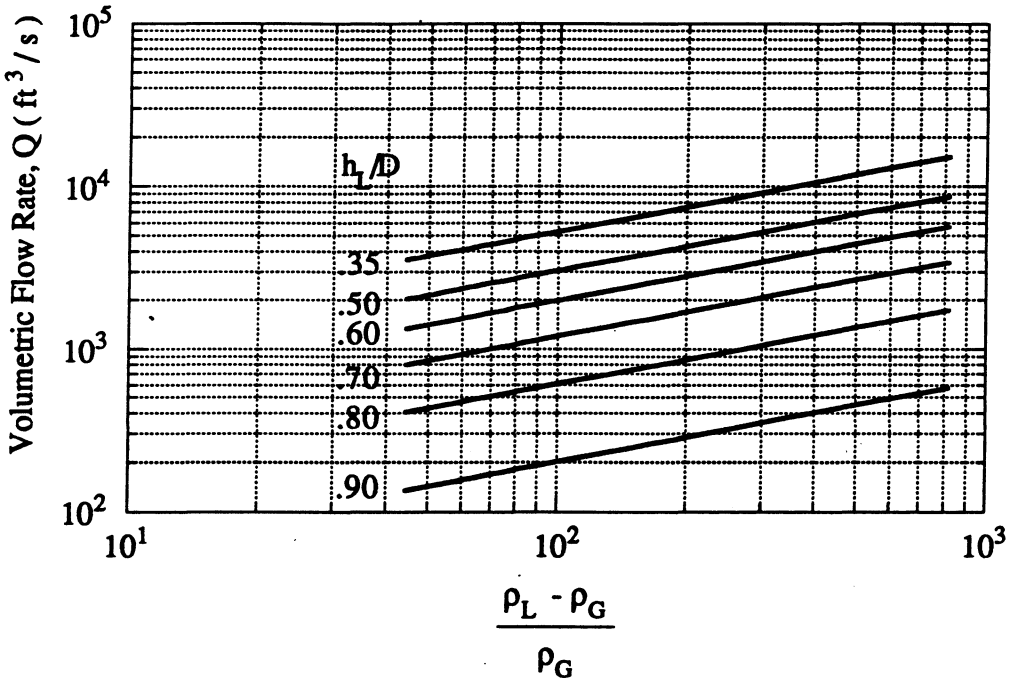

Figure D.11. Plot of transition criterion at constant liquid depths for standard weight steel pipe of 12.0 in. nominal diameter.

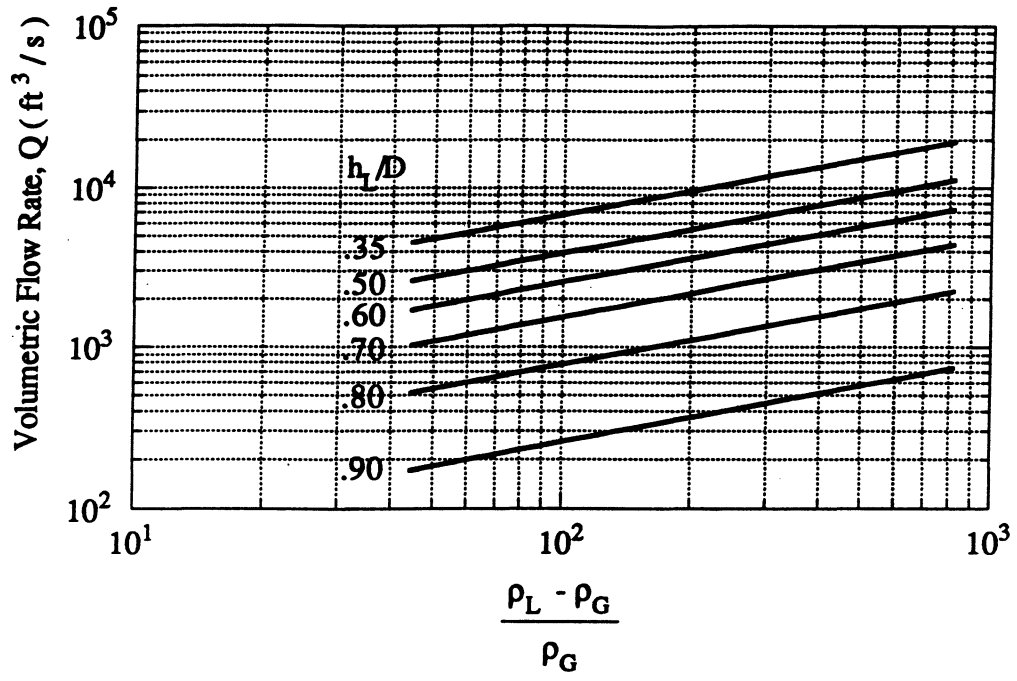

Figure D.12. Plot of transition criterion at constant liquid depths for standard weight steel pipe of 14.0 in. nominal diameter.

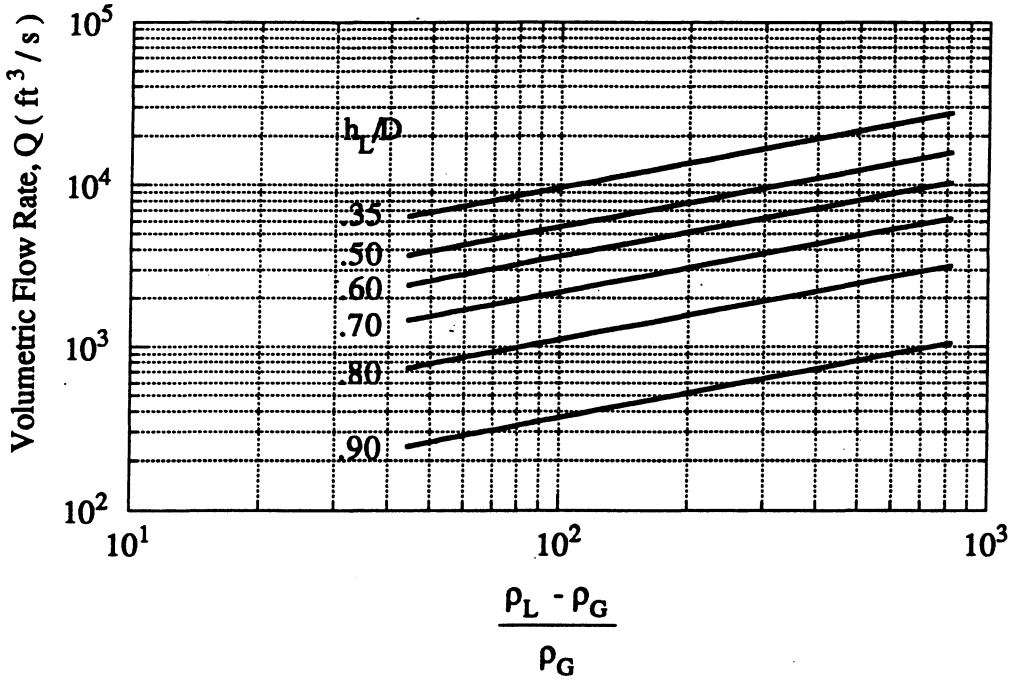

Figure D.13. Plot of transition criterion at constant liquid depths for standard weight steel pipe of 16.0 in. nominal diameter.

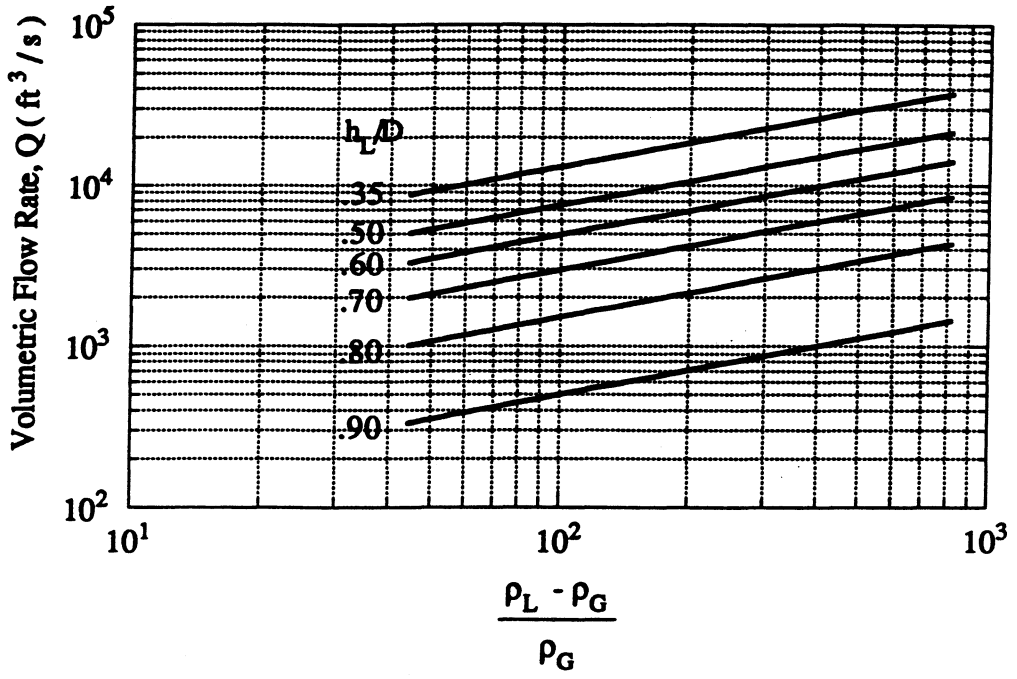

Figure D.14. Plot of transition criterion at constant liquid depths for standard weight steel pipe of 18.0 in. nominal diameter.

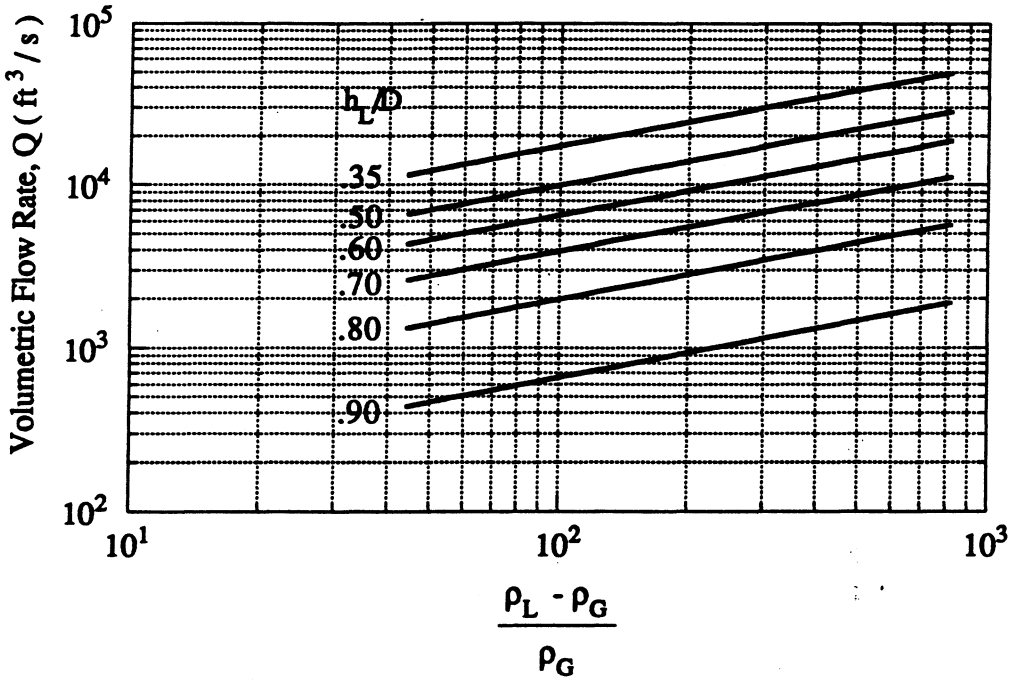

Figure D.15. Plot of transition criterion at constant liquid depths for standard weight steel pipe of 20.0 in. nominal diameter.

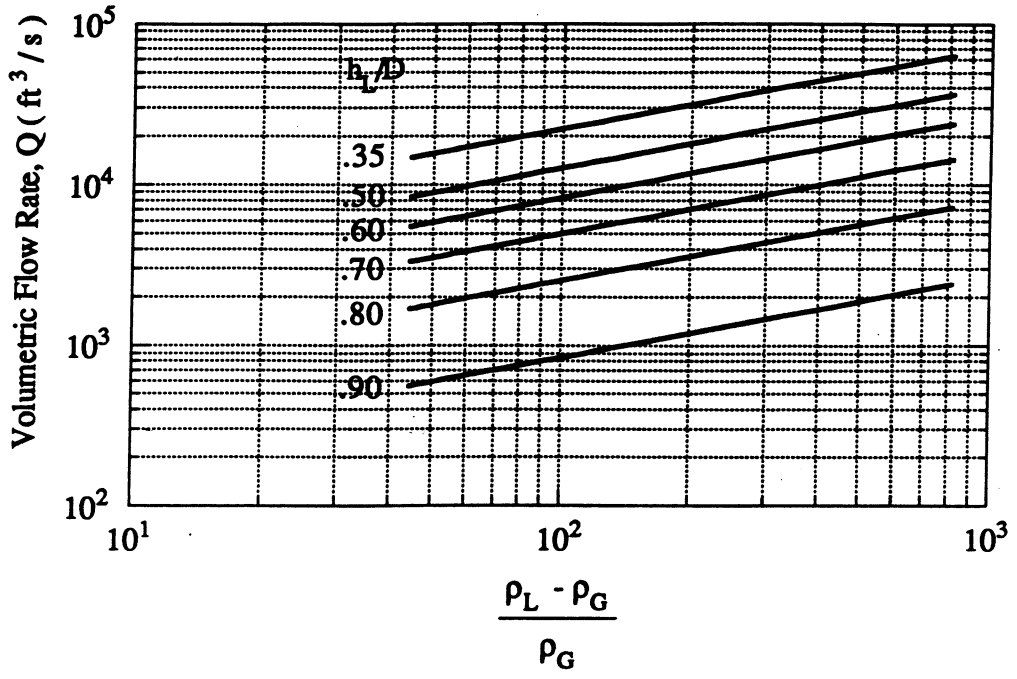

Figure D.16. Plot of transition criterion at constant liquid depths for standard weight steel pipe of 22.0 in. nominal diameter.

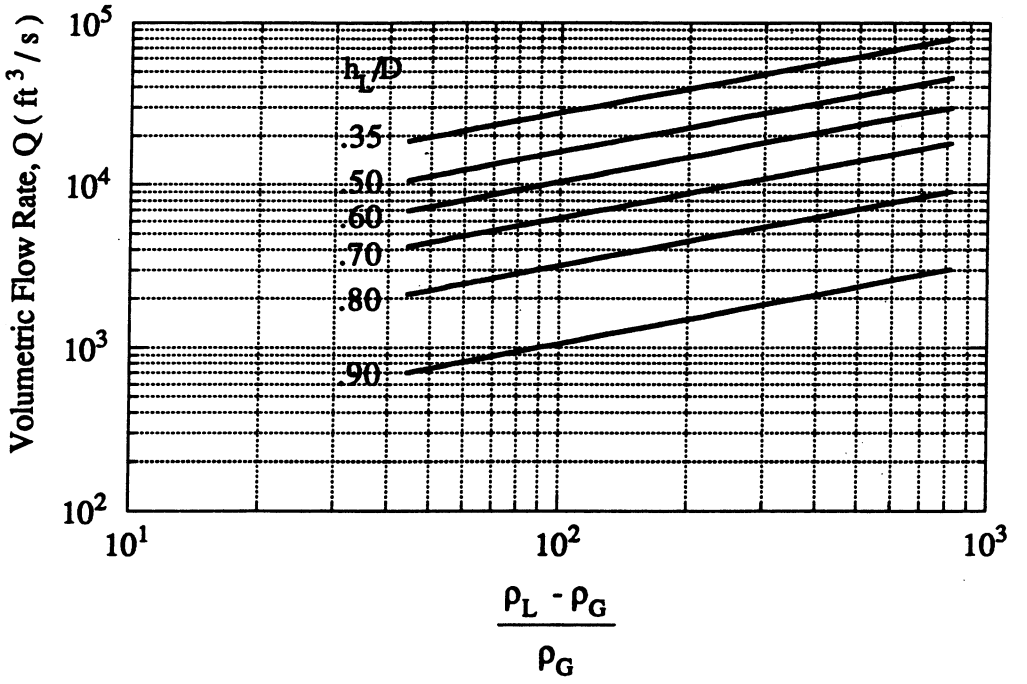

Figure D.17. Plot of transition criterion at constant liquid depths for standard weight steel pipe of 24.0 in. nominal diameter.

Appendix E

Experimental Design for the Study of Hydraulic Shocks

There are many variables significantly affecting the initiation of hydraulic shock in refrigeration equipment, including effects due to the physical design of the piping system, the properties of the working fluid, and the characteristics of the fluid flow. Although the theoretical work we have reported provides a deeper understanding of these effects and recommendations for avoiding hydraulic shock, experiments are needed to validate this work and to determine the actual pressure excursions during these events. In this appendix, these experiments are described in a form that may help extend this work.

E.1 TITLE

An experimental study of refrigerant line transients: condensation-induced shock and vapor-propelled liquid slugging.

E.2 BACKGROUND

On November 13, 1973, a reactor trip occurred at the Indian Point nuclear reactor station, and a steam generator feedwater line was damaged by an accompanying water hammer event. The water hammer event was subsequently attributed to condensation-induced shock (Bjorge, 1983). In the years following this incident, the NRC initiated a series of water hammer research programs, and designated water hammer *Unresolved Safety Issue A-1*. Condensation-induced shock and vapor-propelled liquid slugging emerged as the two most serious water-hammer initiating mechanisms in the nuclear power industry. Chou (1988) classified 281 water hammer events reported to the NRC over a nineteen-year period beginning in 1967 and found that these two mechanisms account for the majority of all water hammer events reported in that industry.

The refrigeration industry faces similar difficulties with condensation-induced shock and vapor-propelled liquid slugging. These mechanisms for hydraulic shock have reportedly contributed to incidents and failures in refrigeration systems (Loyko, 1989, 1992), but they are not well understood. As ozone depletion and global warming issues force the industry's move to alternative refrigerants, including ammonia, and as the shift to centralized system designs continues, the implications on public safety, system down-time, repair costs, and product loss make hydraulic shock in refrigeration lines a crucial issue.

ASHRAE sponsored a literature review and theoretical study of shock initiating mechanisms in refrigerant lines (736-RP); that study provided convincing evidence that condensation-induced shock and vapor-propelled liquid slugging can be important in refrigeration systems. Preliminary recommendations for design and operating procedures to reduce the frequency of hydraulic shock in refrigerant lines were also provided.

E.3 JUSTIFICATION OF NEED

The earlier ASHRAE-sponsored project significantly advanced our understanding of two-phase transients in refrigerant lines. The results provide engineers and designers with preliminary recommendations for how to avoid the dangerous risks associated with condensation-induced shock and vapor-propelled liquid slugging. Unfortunately, a theoretical study is necessarily based on a number of simplifying assumptions, and some of these assumptions may have important impacts on the model accuracy. An experimental study is needed to assess the validity of the existing theoretical model of shock initiation. The results of this project will validate (or correct) the earlier study, and they will make a significant contribution to Chapter 4, "System Practices for Ammonia," of the Refrigeration Handbook.

E.4 SCOPE

1) Measure the flow rate downstream of a fast-opening valve for conditions representative of typical valves, piping arrangements, and operating conditions associated with the initiation

and termination of hot-gas defrost in ammonia systems. These experiments are to include situations in which the pipe downstream of the valve is partially filled with a standing liquid (of varying depths). Realistic operating conditions must include cases for which the flow is choked at the throat of the valve upon opening. It is expected that these experiments will be conducted for several downstream piping arrangements (with elbows, tees, and end-caps) and for representative thermal conditions. The experiments should include observations in horizontal and vertical pipes. The maximum flow rate and time-dependent behavior should be characterized and compared to analytical and/or handbook flow predictions.

2) Determine the two-phase flow regimes associated with the conditions described in part (1). Of particular interest is transition to intermittent flow during the rapid opening of a valve. Pipe lengths must allow the development of slug flow. The results will be compared to existing flow regime maps and dynamic (time dependent) criteria for the transition from wavy-stratified to slug flow.

3) Measure the pressure excursions and retaining forces exerted on the piping system during the flow transients described in part (1). These measurements should be compared to existing models (e.g., the Joukowski equation) for pressure shocks associated with slug impact.

4) The results of this study must be used to validate the models developed through 736-RP or to recommend alternative methods for characterizing the occurrence and outcome of condensation-induced shock and vapor-propelled liquid slugging during the initiation or termination of hot-gas defrost.

E.5 AN EXAMPLE EXPERIMENT DESIGN

Many approaches to experiment design can satisfy the scope defined in the previous section. A simplified candidate design is shown schematically in Figure E.1

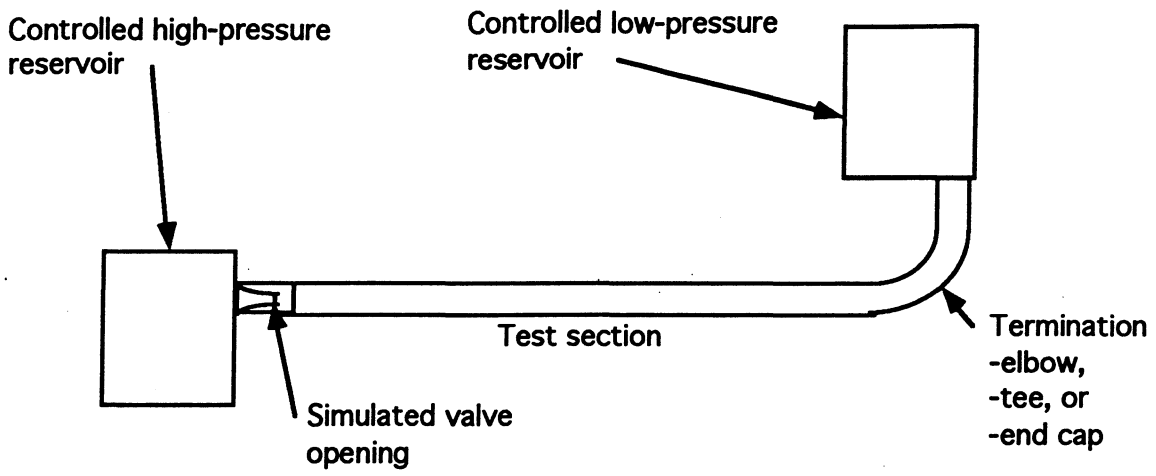

Figure E.1. A representative experiment schematic

Experiments would be conducted for the conditions discussed above by setting the controlled reservoirs to the desired states and simulating a valve opening by bursting a diaphragm located at the throat of the simulated valve. Experiments with a few commercial valves would be undertaken first to allow sizing of the simulated valve. Subsequent experiments would be conducted with the simulated valve, as it will provide better repeatability. The test section would be of variable length, diameter and orientation. It could be equipped with an elbow (as shown), a tee (with one branch terminated by an end cap, and the other feeding the low-p reservoir), or an end-cap. All of the measurements discussed above would be conducted in the test section.

Appendix F

Annotated Bibliography

The initial analysis of two-phase flow regimes, condensation-induced shock, vapor-propelled liquid slugging, and ammonia refrigeration systems was accomplished through a review of the extant literature concerning these topics. In order to complete the review, over 240 articles related to the subjects of this research were obtained. Each article was then reviewed and compiled into an extensive annotated bibliography. Due to its size, the annotated bibliography has been divided into four subject areas: two-phase flow, vapor bubble collapse, slug flow transition, and hydraulic shock analysis.

Two-Phase Flow Regimes

Author	Title	Source	Comments
Akagawa, K. Hamaguchi, H. Sakaguchi, T. Ikari, T.	Studies on the Fluctuation of Pressure Drop in Two Phase Slug Flow (1st Report)	*Bulletin of the Japan Society of Mechanical Engineers*, Vol. 14 (71), 1971, Pp. 447-454	Experimental study of the variance of pressure drop with time in a two-phase slug flow
Akagawa, K. Hamaguchi, H. Sakaguchi, T. Ikari, T.	Studies on the Fluctuation of Pressure Drop in Two Phase Slug Flow (2nd Report)	*Bulletin of the Japan Society of Mechanical Engineers*, Vol. 14 (71), 1971, Pp.455-461	Theoretical analysis of the fluctuation of pressure drop in two-phase slug flow
Akagawa, K. Sakaguchi, T.	Fluctuation of Void Ratio in Two Phase Flow	*Bulletin of the Japan Society of Mechanical Engineers*, Vol. 9 (33), 1966, Pp.111-120	A study of the velocities associated with gas and liquid slugs
Akai, M. Inoue, A. Aoki, S. Endo, K.	A Co-Current Stratified Air-Mercury Flow with Wavy Interface	*International Journal of Multiphase Flow*, Vol. 6 (3), 1980, Pp. 173-190.	Analytical and experimental study of a concurrent, stratified, air-mercury flow in a horizontal channel
Andritsos, N. Hanratty, T.J.	Influence of Interfacial Waves in Stratified Gas-Liquid Flows	*AIChE Journal*, Vol. 33 (3), 1987, Pp. 444-454.	An improved method for predicting frictional pressure drop and liquid height in a horizontal, stratified flow
Ardron, K.H.	One Dimensional Two Fluid Equations for Horizontal Stratified Two Phase Flow	*International Journal of Multiphase Flow*, Vol. 6 (4), 1980, Pp. 295-304.	Comparison of calculated wave propagation speeds and stability limits for horizontal stratified two phase flow with an exact solution

Azzopardi, B.J. Whalley, P.B.	The Effect of Flow Patterns on Two Phase Flow in a T Junction	*International Journal of Multiphase Flow*, Vol. 8 (5), 1982, Pp. 491-507.	Study of the effect of upstream flow patterns on two phase flow in sharp edged T junctions
Baker, O.	Simultaneous Flow of Oil and Gas	Thge Oil and Gas Journal, July, 26, 1954 Pp. 185-195.	Develops a flow map for horizontal flow regimes
Banerjee, S. Rhodes, E. Scott, D.S.	Film Inversion of Cocurrent Two Phase Flow in Helical Coils	*AIChE Journal*, Vol. 13 (1), 1967, Pp. 189-191.	Experimental results concerning the occurance of film inversion in cocurrent two phase flow in helical coils
Bankoff, S.G.	Some Condensation Studies Pertinent to LWR Safety	*International Journal of Multiphase Flow*, Vol. 6 (1-2), 1980, Pp. 51-67.	Discussion of steady-state turbulent stratified flows and of bubble studies as applied to reactor safety.
Bell, M.K. Howell, R.H. Sauer, Jr., H.J. Bosch, J.J.	Two-Phase flow in Sloped Gravity-Driven Condensate Return Lines of Steam Systems	*ASHRAE Transactions*, Vol.87 (2), 1981, Pp. 61-78.	Study of bubble flow, plug flow, stratified flow, and slug flow in condensate return lines of steam systems.
Boure, J.A.	On the Form of the Pressure Terms in the Momentum and Energy Equations of Two Phase Flow Models	*International Journal of Multiphase Flow*, Vol. 5 (2), 1979, Pp. 159-164.	Discussion of the proper form of the pressure terms in the momentum and energy equations of two phase flow models.
Butterworth, D.	An Analysis of film Flow and Its Application to Condensation in a Horizontal Tube	*International Journal of Multiphase Flow*, Vol. 1 (5), 1974, Pp. 671-682.	Analysis of turbulent flow in a liquid film with motion due to axial shear in a horizontal tube.

Caetano, E.F. Shoham, O. Brill, J.P.	Upward Vertical Two Phase Flow Through an Annulus -- Part I: Single Phase Friction Factor, Taylor Bubble Rise Velocity, and Flow Pattern Prediction	*Journal of Energy Resources Technology*, Vol. 114 (1), 1992, Pp. 1-13.	Analysis of upward two phase flows in vertical concentric and eccentric annuli. Also the study includes the development of flow pattern maps
Caetano, E.F. Shoham, O. Brill, J.P.	Upward Vertical Two Phase Flow Through an Annulus -- Part II: Modeling Bubble, Slug, and Annular Flow	*Journal of Energy Resources Technology*, Vol. 114 (1), 1992, Pp. 14-30.	Develops models for two phase flow in an annulus for bubble flow, slug flow, and annular flow
Cardle, J.A. Song, C.C.S. Yuan, M.	Measurements of Mixed Transients Flows	*Journal of Hydraulic Engineering*, Vol. 115 (2), 1989, Pp. 169-182.	Investigation of the transition between free-surface flow and pressurized flow in pipes and of the transition between positive and negative surges
Chang, H.C.	Nonlinear Waves on Liquid Film Surfaces--I: Flooding in a Vertical Tube	*Chemical Engineering Science*, Vol. 41 (10), 1986, Pp. 2463-2476.	An examination of flooding in two phase annular flow in vertical tubes including the interfacial stress created by the gas phase
Chen, S.S.	Flow Induced Vibrations in Two Phase Flow	*Journal of Pressure Vessel Technology*, Vol. 113 (2), 1991, Pp. 234-241.	Review of the vibration of circular cylinders in quiescent fluid, cross-flow, and axial flow. Also presents a model to describe cylinder oscillations for different flow conditions
Chrisholm, D.	Pressure Gradients Due to Friction During the Flow of Evaporating Two Phase Mixtures in Smooth Tubes and Channels	*International Journal of Heat and Mass Transfer*, Vol. 16 (2), 1973, Pp. 347-358.	Develops equations for predicting local pressure gradients in evaporating flow for two phase mixtures

Coad, W.J.	A Re-Evaluation of Two Phase Technology in Thermal Fluid Systems	*ASHRAE Transactions*, Vol. 87 (1), 1981, Pp. 943-953.	Discussion of the characteristics of steam systems and their use
Cohen, L.S. Hanratty, T.J.	Effect of Waves at a Gas Liquid Interface on a Turbulent Air Flow	*Journal of Fluid Mechanics*, Vol. 31 (3), 1968, Pp. 467-479.	Study of the resistance experienced by air flowing co-currently over a liquid surface in a closed channel.
Dukler, A.E. Smith, L. Chopra, A.	Flooding and Upward Film Flow in Tubes--I: Experimental Studies	*International Journal of Multiphase Flow*, Vol. 10 (5), 1984, Pp. 585-597.	Experimental study of flooding and upward film flow, including film and entrainment flow rates and pressure drop.
Dukler, E.D. Hubbard, M.G.	A Model for Gas-Liquid Slug Flow in Horizontal and Near Horizontal Tubes	*Industrial and Engineering Chemistry Fundamentals*, Vol. 14 (4), 1975, Pp. 337-347.	Presentation of a model to predict the hydrodynamic behavior of gas-liquid slug flow.
Fabre, J. Liné, A.	Modeling of Two Phase Slug Flow	*Annual Review of Fluid Mechanics*, Vol. 24, 1992, Pp. 21-46.	Theoretical model and analysis of gas-liquid slug flow.
Fan, Z. Jepson, W.P. Hanratty, T.J.	A Model for Stationary Slugs	*International Journal of Multiphase Flow*, Vol. 18 (4), 1992, Pp. 477-494.	Development of a model for stationary slugs.
Fan, Z. Ruder, Z. Hanratty, T.J.	Pressure Profiles for Slugs in Horizontal Pipelines	*International Journal of Multiphase Flow*, Vol. 19 (3), 1993, Pp. 421-437.	Experimental measurement of the variation of pressure caused by stable and unstable slugs in horizontal two phase flows.
Fleschner, R.A. Howell, R.H. Sauer, Jr., H.J.	Two-Phase Flow in Horizontal Condensate Return Lines of Steam Thermal Systems	*ASHRAE Transactions*, Vol. 86 (1), 1980, Pp. 440-459.	Comparison of different methods for calculating pressure drop in two phase flows.

Forster, K.E.	Growth of a Vapor Filled Cavity Near a Heating Surface and Some Related Questions	*Physics of Fluids*, Vol. 4 (4), 1961, Pp. 448-455.	Analysis of the conditions that exist in in the local vicinity of a heating element in a boiling liquid.
Fowler, A.C. Lisseter, P.E.	Flooding and Flow Reversal in Annular Two Phase Flows	*SIAM Journal of Applied Mathematics*, Vol. 52 (1), 1992, Pp. 15-33.	Presentation of a two-fluid model to predict flooding and flow reversal in annular flows.
Geraets, J.J.M. Borst, J.C.	A Capacitance Sensor for Two Phase Void Fraction Measurement and Flow Pattern Identification	*International Journal of Multiphase Flow*, Vol. 14 (3), 1988, Pp. 305-320.	Development of a capacitance sensor with which to measure time-averaged void fractions in two phase flow.
Gould, T.L. Tek, M.R. Katz, D.L.	Two Phase Flow Through Vertical, Inclined, or Curved Pipes	*Journal of Petroleum Technology*, Vol. 26, August 1974, Pp. 915-926.	Presentation of a computerized method designed to determine the flow regime and its properties for a given section of pipe.
Grace, J.R. Clift, R.	Dependence of Slug Rise Velocity on Tube Reynolds Number in Vertical Gas-Liquid Flow	*Chemical Engineering Science*, Vol. 34 (11), 1979, Pp. 1348-1350.	Development of an equation for the velocity of gas slugs rising in a vertical column.
Gregory, G.A. Nicholson, M.K. Aziz, K.	Correlation of the Liquid Volume Fraction in the Slug for Horizontal Gas Liquid Slug Flow	*International Journal of Multiphase Flow*, Vol. 4 (1), 1978, Pp. 33-39.	Development of an empirical correlation for gas holdup in liquid slugs for two phase horizontal slug flow.
Griffith, P.	The Prediction of Low Quality Boiling Voids	*Journal of Heat Transfer*, Vol. 86 (2), 1964, Pp. 327-333.	Experimental measurements of bubble rise velocity and the use of slug flow theory to predict fluid density in heated channels.

Griffith, P.	Multiphase Flow in Pipes	*Journal of Petroleum Technology*, March 1984, Pp. 361-367.	Review of two phase flow and related issues and problems.
Griffith, P. Wallis, G.B.	Two-Phase Slug Flow	*Journal of Heat Transfer*, Vol. 83 (3), 1961, Pp. 307-320.	Comparison of an expression developed for the mean density and a method for predicting pressure drop in slug flows with experimental data.
Gudushauri, E.G. Medvedev, A.E. Selifanov, I.V.	Interrelation Between Pressure Oscillations and Flow Rate of Liquid in the Film for an Oscillating Air-Water Dispersed-Annular Flow	*Thermal Engineering*, Vol. 38 (4), 1991, Pp. 216-218.	Experimental study of the relationship between pressure oscillations and liquid film flow rates for an oscillating dispersed-annular flow
Hand, N.P. Spedding, P.L. Ralph, S.J.	The Effect of Surface Tension on Flow Pattern, Holdup and Pressure Drop During Horizontal Air-Water Pipe Flow at Atmospheric Conditions	*Chemical Engineering Journal*, Vol. 48, 1992, Pp. 197-210.	Experimental study of the effects of surface tension on flow pattern, holdup,and pressure drop in cocurrent two-phase flows.
Hashizume, K.	Flow Pattern, Void Fraction and Pressure Drop of Refrigerant Two Phase Flow in a Horizontal Pipe -- I : Experimental Data	*International Journal of Multiphase Flow*, Vol. 9 (4), 1983, Pp. 399-410.	Presentation of experimental data on flow pattern, void fraction, and pressure drop in two phase flows of refrigerants R12 and R22.
Hashizume, K. Hiroyasu, O. Taniguchi, H.	Flow Pattern, Void Fraction and Pressure Drop of Refrigerant Two Phase Flow in a Horizontal Pipe -- II: Analysis of Frictional Pressure Drop	*International Journal of Multiphase Flow*, Vol. 11 (5), 1983, Pp. 643-658.	Analysis of annular and stratified two phase horizontal flows and calculation of the frictional pressure drop.

Hatfield, F.J. Wiggert, D.C. Otwell, R.S.	Fluid Structure Interaction in Piping by Component Synthesis	*Journal of Fluids Engineering*, Vol. 104, 1982, Pp. 318-325.	Modeling of the interaction of the liquid and piping during a pressure transient by analyzing the liquid and solid component separately and then combining the solutions.
Hewitt, G.F. Jayanto, S.	Prediction of Film Inversion in Two Phase Flow in Coiled Tubes	*Journal of Fluid Mechanics*, Vol. 236, 1992, Pp. 497-511.	Analytical study of film inversion and presentation of a new criterion to predict its occurrence.
Hooper, A.P. Grimshaw, R.	Nonlinear Instability at the Interface Between Two Viscous Fluids	*Physics of Fluids*, Vol. 28 (1), 1985, Pp. 37-45.	Examination of the nonlinear instability of cocurrent superposed viscous fluids.
Howell, R.H.	Evaluation of Sizing Methods for Steam Condensate Systems	*ASHRAE Transactions*, Vol. 91 (1A), 1985, Pp. 370-390.	Review of present techniques used to size condensate return lines and development of a procedure for pipe sizing based on the review.
Howell, R.H. Sauer, Jr., H.J. Bell, M.K. Bosch, J.J. Fleschner, R.A.	Validation of Steam Condensate System Flow Theories	*ASHRAE Transactions*, Vol. 87 (1), 1981, Pp. 963-982.	Experimental examination of two phase flow in condensate flow lines and development of a model of the condensate carrying capacity of the return lines.
Imura, H. Kusuda, H. Funatsu, S.	Flooding Velocity in a Counter-Current Annular Two-Phase Flow	*Chemical Engineering Science*, Vol. 32 1977, Pp. 79-87.	Derivation of a theoretical equation to describe the velocity of a falling liquid film relative to a counter-current gas at which flooding occurs.
Isbin, H.S.	Some Observations on the Status of Two Phase Critical Flow Models	*International Journal of Multiphase Flow*, Vol. 6 (1-2), 1980, Pp. 131-137.	A critique of different models for critical two phase flows.

Jelev, I.	The Damping of Flow and Pressure Oscillations in Water Hammer Analysis	*Journal of Hydraulic Research*, Vol. 27 (1), 1989, Pp. 91-114.	Mathematical analysis of flow and pressure oscillation damping based on structural friction forces.
Jepson, W.P. Taylor, R.E.	Slug Flow and Its Transitions in Large Diameter Horizontal Pipes	*International Journal of Multiphase Flow*, Vol. 19 (3), 1993, Pp. 411-420.	Compilation of a flow regime map for two phase horizontal flow in large diameter pipes and analysis of the effect of pipe diameter.
Jones, A.V. Properetti, A.	On the Suitability of First Order Differential Models for Two Phase Flow Prediction	*International Journal of Multiphase Flow*, Vol. 11 (2). 1985, Pp. 133-148.	Analysis of the stability features of one-dimensional first-order flow models.
Jones, Jr., O.C. Zuber, N.	The Interrelation Between Void Fraction Fluctuations and Flow Patterns in Two Phase Flow	*International Journal of Multiphase Flow*, Vol. 2 (3), 1975, Pp. 273-306.	Study of the use of the probability density function of void fraction fluctuations to determine flow regime.
Karney, B.W.	Energy Relations in Transient Closed-Conduit Flow	*Journal of Hydraulic Engineering*, Vol. 116 (10), 1990, Pp. 1180-1196.	Development of an alternative mathematical representation of transient conditions based on integrated energy relations.
Klausner, J.F. Chao, B.T. Soo, S.L.	An Improved Correlation for Two Phase Frictional Pressure Drop in Boiling and Adiabatic Downflow in the Annular Flow Regime	*Proceedings, Institution of Mechanical Engineers*, Vol. 205 (C5), 1991, Pp. 317-328.	Development of a correlation for determining the frictional pressure drop in annular, two phase, vertical downflow.
Kokal, S.L. Stanslav, J.F.	An Experimental Study of Two Phase Flow in Slightly Inclined Pipes--II. Liquid Holdup and Pressure Drop	*Chemical Engineering Sciences*, Vol. 44, 1989, Pp. 681-693.	Development of models for stratified, dispersed bubble, and annular flows to predict the pressure drop and liquid holdup in inclined pipes.

Kordyban, E.S.	Some Characteristics of High Waves in Closed Channels Approaching Kelvin-Helmholtz Instability	*Journal of Fluid Mechanics*, Vol. 99, 1977, Pp. 339-346.	Analysis of the characteristics of water waves produced at the gas-liquid interface to determine the effects of surface variation.
Kvernold, O. Vindoy, V. Sontvedt, T. Saasen, A. Selmer-Olsen, S.	Velocity Distribution in Horizontal Slug Flow	*International Journal of Multiphase Flow*, Vol. 10 (4), 1984, Pp. 441-457.	Development of a device to measure the velocity distribution in a two phase slug. Velocity profiles of the film and the liquid slug are given.
Laurinat, J.E. Hanratty, T.J. Dallman, J.C.	Pressure Drop and Film Height Measurements for Annular Gas-Liquid Flow	*International Journal of Multiphase Flow*, Vol. 10 (3), 1984, Pp. 341-356.	Experimental measurement of the film height and pressure drop for horizontal two phase annular flow.
Lesmez, M.W. Wiggert, D.C. Hatfield, F.J.	Modal Analysis of Vibrations in Liquid Filled Piping Systems	*Journal of Fluids Engineering*, Vol. 112, 1990, Pp. 311-318.	Comparison of a modal analysis method for predicting piping and liquid motion and the related forces with experimental results.
Liu, T.J.	Bubble Size and Entrance Length Effects on Void Development in a Vertical Channel	*International Journal of Multiphase Flow*, Vol. 19 (1), 1993, Pp. 99-113.	Experimental study of the effects of bubble size and entrance length have on the void distribution in a vertical upward cocurrent two phase flow.
Liu, T.J. Bankoff, S.G.	Structure of Air-Water Bubble Flow in a Vertical Pipe--I. Liquid Mean Velocity and Turbulence Measurements	*International Journal of Heat and Mass Transfer*, Vol. 36 (4), 1993, Pp. 1049-1060.	Experimental investigation of the liquid phase turbulent structure in a two phase bubbly upflow in a circular pipe.

Liu, T.J. Bankoff, S.G.	Structure of Air-Water Bubble Flow in a Vertical Pipe--II. Void Fraction, Bubble Velocity and Bubble Size Distribution	*International Journal of Heat and Mass Transfer*, Vol. 36 (4), 1993, Pp. 1061-1072.	Experimental measurements of the radial profiles of void fraction, bubble velocity and bubble size.
Ma, Y.P. Chung, N.M. Pei, B.S. Lin, W.K. Hsu, Y.Y.	Two Simplified Methods to Determine Void Fractions for Two Phase Flow	*Nuclear Technology*, Vol. 94 (1), 1991, Pp. 124-133.	The development and discussion of two techniques to determine void fraction in two phase flows.
Mandhane, J.M. Gregory, G.A. Aziz, K.	A Flow Pattern Map for Gas-Liquid Flow in Horizontal Pipes	*International Journal of Multiphase Flow*, Vol. 1, 1974, Pp. 537-553.	Comparison of flow regime maps for two phase flow in horizontal pipes as well as the presentation of a new flow regime correlation.
Manwell, S.P. Bergles, A.E.	Gas-Liquid Flow Patterns in Refrigerant-Oil Mixtures	*ASHRAE Transactions*, Vol. 96 (2), 1990, Pp. 456-464.	Experimental study of the refrigerant flow patterns that occur in smooth and in micro-fin tubes.
Maron, D.M. Dukler, A.E.	Flooding and Upward Film Flow in Vertical Flow--II: Speculations on Film Flow Mechanisms	*International Journal of Multiphase Flow*, Vol. 10 (5), 1984, Pp. 599-621.	Discussion of different mechanisms for flooding and upward film flow in vertical tubes.
Martin, C.S.	Vertically Downward Two Phase Slug Flow	*Journal of Fluids Engineering*, Vol. 98 (4), 1976, Pp. 715-722.	Experimental investigation of vertically downward slug flow of air-water mixtures in circular pipes.
McAdams, W.H. Woods, W.K. Bryan, R.L.	Vaporization Inside Horizontal Tubes	*ASME Transactions*, Vol. 63, 1941, Pp.545-552.	Experimental study of changes in the coefficient of heat transfer for evaporation of a liquid inside a heated horizontal tube.

McAdams, W.H. Woods, W.K. Heroman, Jr., L.C.	Vaporization Inside Horizontal Tubes--II: Benzene Oil Mixtures	*ASME Transactions*, Vol. 64, 1942, Pp. 193-200.	Experimental investigation of the heat transfer coefficients and the pressure drops for mixtures of benzene and lubricating oils inside heated horizontal tubes.
Mills, A.F.	Condensation Heat Transfer: Comments on Non-Equilibrium Temperature Profiles and the Engineering Calculation of Mass Transfer	*International Journal of Multiphase Flow*, Vol. 6 (1-2), 1980, Pp. 41-50.	Review of a theory on non-equilibrium phase change and of methods by which to calculate mass transfer as they apply to condensation heat transfer.
Nencini, F. Andreussi, P.	Studies of the Behavior of Disturbance Waves in Annular Two-Phase Flow	*The Canadian Journal of Chemical Engineering*, Vol. 60, August 1982, Pp. 459-465.	Experimental investigation of downward annular two phase flow. Development of statistical methods to calculate the flow rates of substrate and large wave flow.
Nicholson, M.K. Aziz, K. Gregory, G.A.	Intermittent Two Phase Flow in Horizontal Pipes: Predictive Models	*The Canadian Journal of Chemical Engineering*, Vol. 56, December 1978, Pp. 653-663.	Extension of a previous model for two phase slug flow to include the entire intermittent flow regime.
Nitheanandan, T. Soliman, H.M.	Influence of Tube Inclination on the Flow Regime Boundaries of Condensing Steam	*Canadian Journal of Chemical Engineering*, Vol. 71, February 1993, Pp. 35-41.	Presentation of experimental data on flow regime of condensing steam in inclined and declined two phase flows.
Persen, L.N.	Stratified Two Phase Flow in Circular Pipes	*International Journal of Heat and Mass Transfer*, Vol. 27 (8), 1984, Pp. 1227-1234.	Discussion of stratified two phase flow in circular pipes and the development of equations for the pressure drop and the shape of the interphase.

Persen, L.N.	On the Stability of Stratified Flow and Its Transition to Other Flow Regimes	*International Journal of Heat and Mass Transfer*, Vol. 36 (7), 1993, Pp. 1969-1980.	Presentation of the determination of the normal depth of stratified two phase flow and the conditions of its stability.
Rahman, M.M. Fathi, A.M. Soliman, H.M.	Flow Pattern Boundaries During Condensation: New Experimental Data	*Canadian Journal of Chemical Engineering*, Vol. 63, August 1985, Pp. 547-552.	Experimental study of flow patterns of condensing steam in horizontal tubes.
Rice, C.K.	The Effect of Void Fraction Correlation and Heat Flux Assumption on Refrigeration Charge Inventory Predictions	*ASHRAE Transactions*, Vol. 93 (1), 1987, Pp. 341-367.	Evaluation of the effect on refrigerant charge inventory predictions of various void fraction correlations and heat flux assumptions.
Richards, W.V.	Some Guides for Safe and Successful Refrigerant Circulation	*ASHRAE Transactions*, Vol. 96 (1), 1990, Pp. 1332-1338.	Presentation of a method to obtain good heat transfer with acceptable pressure drop in multiple tube overfeed evaporators.
Ruskin, R.P.	Calculating Line Sizes for Flashing Steam-Condensate	*Chemical Engineering*, Vol. 82, August 1975, Pp. 101-103.	Presentation of a method for sizing flashing steam-condensate lines and deriving the flow velocities.
Shearer, C.J. Nedderman, R.M.	Pressure Gradient and Liquid Film Thickness in Cocurrent Upwards Flow of Gas Liquid Mixtures: Application to Film Cooler Design	*Chemical Engineering Science*, Vol. 20, 1965, Pp. 671-683.	Development of expressions for liquid film thickness and pressure drop in upwards annular cocurrent annular flow.
Shekriladze, I. Mestvirishvili, S.H.	High Rate Condensation Process Theory of Vapour Flow Inside a Vertical Cylinder	*International Journal of Heat and Mass Transfer*, Vol. 16 (4), 1973, Pp. 715-724.	Analysis of film condensation of a gas flow in a vertical circular pipe.

Shoham, O. Taitel, Y.	Stratified Turbulent-Turbulent Gas Liquid Flow on Horizontal and Inclined Pipes	*AIChE Journal*, Vol. 30 (3), 1984, Pp. 377-385.	Development of a two-dimensional model for stratified turbulent-turbulent two phase flow in inclined pipes.
Simpson, A.R. Wylie, E.B.	Large Water-Hammer Pressures for Column Separation in Pipelines	*Journal of Hydraulic Engineering*, Vol. 117 (10), 1991, Pp.1310-1316.	Investigation of the variation of shape and magnitude of short-duration pressure pulses for a reservoir-valve system.
Sisson, W.	Nomogram Sizes Condensate Return Lines	*Power Engineering*, December 1975, pp. 68.	Presentation of a nomogram for sizing a condensate return line or for finding fluid velocity in existing piping systems.
Spalding, D.B.	Multiphase Flow Prediction in Power System Equipment and Components	*International Journal of Multiphase Flow*, Vol. 6 (1-2), 1980, Pp. 157-168.	A discussion of the requirements for the prediction of multiphase flows in equipment and components.
Spedding, P.L. Spence, D.R.	Flow Regimes in Two Phase Gas-Liquid Flow	*International Journal of Multiphase Flow*, Vol. 19 (2), 1993, Pp. 245-280.	Comparison of experimental results with existing flow regime maps and flow transition maps for co-current air-water horizontal flow.
Stuhmiller, J.H.	The Influence of Interfacial Pressure Forces on the Character of Two Phase Flow Model Equations	*International Journal of Multiphase Flow*, Vol. 3 (6), 1977, Pp. 551-560.	Development of equations for two phase flow based on interfacial pressure.
Suzuki, S. Ueda, T.	Behavior of Liquid Films and Flooding in counter Current Two Phase Flow--Part I. Flow in Circular Tubes	*International Journal of Multiphase Flow*, Vol. 3 (6), 1977, Pp. 517-532.	Experimental study of the flooding gas velocity for counter-current two phase flow in pipes.

Taitel, Y. Barnea, D, Dukler, A.E	A Film Model for the Prediction of Flooding and Flow Reversal for Gas Liquid Flow in Vertical Tubes	*International Journal of Multiphase Flow*, Vol. 8 (1), 1982, Pp. 1-10.	Presentation of a model which predicts the gas flow rate which initiates flooding and flow reversal and the liquid flow rate at which they end for a vertical two phase flow.
Tandon, T.N. Varma, H.K. Gupta, C.P. R22.	An Experimental Study of Flow Patterns During Condensation Inside a Horizontal Tube	*ASHRAE Transactions*, Vol. 86 (2A), 1983, Pp. 471-482.	Experimental analysis of two phase flow patterns during condensation inside horizontal tubes for R12 and
Tandon, T.N. Varma, H.K. Gupta, C.P.	A Void Fraction Model for Annular Two Phase Flow	*International Journal of Heat and Mass Transfer*, Vol. 28 (1), 1985, pp. 191-198.	Development of an analytical model for the prediction of void fraction in two phase annular flow.
Tichy, J.A. Duque-Rivera, J. Macken, N.A. Duval, W.M.B.	An Experimental Investigation of Pressure Drop in Forced Convection Condensation and Evaporation of Oil-Refrigerant Mixtures	*ASHRAE Transactions*, Vol. 92 (2A), 1986, Pp. 461-472.	Comparison of experimental measurements of pressure drop in forced-convection evaporation and condensation of oil-refrigerant mixtures in horizontal tubes to theoretical relationships of frictional pressure drop and void fraction.
Traviss, D.P. Rohsenow, W.M.	The Influence of Return Bends on the Downstream Pressure Drop and condensation Heat Transfer in Tubes	*ASHRAE Transactions*, Vol. 79 (1), 1973, Pp. 129-137.	Investigation of the heat transfer and pressure drop in condensers and the effect of return bends on condenser performance.
Troniewski, L. Ulbrich, R.	The Analysis of Flow Regime Maps of Two Phase Gas Liquid Flow in Pipes	*Chemical Engineering Science*, Vol. 39 (7/8), 1984, Pp. 1213-1224.	Analysis and comparison of two phase flow regime maps for horizontal and vertical flows.

Tutu, N.K.	Pressure Fluctuations and Flow Pattern Recognition in Vertical Two Phase Gas-Liquid Flows	*International Journal of Multiphase Flow*, Vol. 8 (4), 1982, Pp. 443-447.	Experimental study of wall pressure fluctuations and pressure drop fluctuations for bubbly, slug, churn, and annular flows to establish objective methods for determining flow pattern.
Wallis, G.B.	Critical Two-Phase Flow	*International Journal of Multiphase Flow*, Vol. 6, 1980, Pp. 97-112.	Review of the present theories on critical two phase flow and the direction in which research in this area should head.
Wallis, G.B. Crowley, C.J. Hagi, Y.	Conditions for a Pipe to Run Full When Discharging Liquid into a Space Filled with Gas	*Journal of Fluids Engineering*, 1977, Pp. 405-413.	Experimental study of the conditions necessary for a vertical or horizontal tube to run full.
Wallis, G.B. Kuo, J.T.	The Behavior of Gas-Liquid Interfaces in Vertical Tubes	*International Journal of Multiphase Flow*, Vol. 2 (5-6), 1976, Pp. 521-536.	Experimental study on the interface behavior when a gas flows past a stationary liquid in a confined vertical flow.
Whalley, P.B.	Air Water Two Phase Flow in a Helically Coiled Tube	*International Journal of Multiphase Flow*, Vol. 6 (4), 1980, Pp. 345-356.	Experimental study of two phase flow in helically coiled tube, including the study of transition between stratified and annular flows.
White, E.T. Beardmore, R.H.	The Velocity of Rise of Single Cylindrical Air Bubbles Through Liquids Contained in Vertical Tubes	*Chemical Engineering Science*, Vol. 17, 1962, Pp. 351-361.	Correlation of experimental measurements on single cylindrical bubbles rising in a vertical tube.
Zahn, W.R.	A Visual Study of Two-Phase Flow While Evaporating in Horizontal Tubes	*Journal of Heat Transfer*, Vol. 86 (3), 1964, Pp. 417-429.	Experimental study of the flow patterns of evaporationg R-22 in horizontal tubes.

Zekind, J.C.	Reduced Load Dynamics in Steam Heat Exchangers	*ASHRAE Transactions*, Vol. 87 (1), 1981, Pp. 954-962.	Presentation of results of research in the dynamics of steam condensate systems and the interrelationship between load control and the condensate return system.
Zukoski, E.E.	Influence of Viscosity, Surface Tension, and Inclination Angle on Motion of Long Bubbles in Closed Tubes	*Journal of Fluid Mechanics*, Vol. 25 (4), 1966, Pp. 821-837.	Experimental study on the effects of viscosity and surface tension on motion of long bubbles in closed tubes. Also, development of correlation of bubble velocities in vertical flows.

Flow Regime Transition and Slug Initiation

Author	Title	Source	Comments
Ahmed, R. Banerjee, S.	Finite Amplitude Waves in Stratified Two-Phase Flow: Transition to Slug Flow	*AIChE Journal*, Vol. 31 (9), 1985, Pp. 1480-1487.	Study of the effects of the nonlinear instability of finite amplitude interfactial waves on transition to slug flow in horizontal two phase flow
Andreussi, P. Asali, J.C. Hanratty, T.J.	Initiation of Roll Waves in Gas-Liquid Flows	*AIChE Journal*, Vol. 31 (1), 1985, Pp. 119-126.	Investigation of the effect of liquid viscosity on the initiation of roll waves in horizontal flow
Andritsos, N. Bontozoglou, V. Hanratty, T.J.	Transition to Slug Flow in Horizontal Pipes	*Chemical Engineering Communications*, Vol. 118, 1992, Pp. 361-385.	Study of the effects that physical properties and pipe diameter have on the transition to slug flow in horizontal pipes
Andritsos, N. Williams, L. Hanratty, T.J.	Effect of Liquid Viscosity on the Stratified-Slug Transition in Horizontal Pipe Flow	*International Journal of Multiphase Flow*, Vol. 15 (6), 1989, Pp. 877-892.	Study of the effect that viscosity has on the initiation of slug flow in horizontal pipes
Bankoff, S.G.	Some Condensation Studies Pertinent to LWR Safety	*International Journal of Multiphase Flow*, Vol. 6 (1-2), 1980, Pp. 51-67.	Discussion of steady-state turbulent stratified flows and review bubble studies applied to reactor safety
Barnea, D.	On the Effect of Viscosity on Stability of Stratified Gas-Liquid Flow -- Application to Flow Pattern Transition at Various Pipe Inclinations	*Chemical Engineering Science*, Vol. 46 (8), 1991, Pp. 2123-2131.	An analysis of the stability of stratified flows at varying inclinations. Also develops a model to predict the transition to slug and annular flows

Barnea, D. Luninski, Y. Taitel, Y.	Flow Pattern in Horizontal and Vertical Two-Phase Flow in Small Diameter Pipes	*Canadian Journal of Chemical Engineering*, Vol. 61, October 1983, Pp. 617-620.	Experimental study of two phase flow transition in small diameter pipes for vertical and horizontal flows
Barnea, D. Shoham, O. Taitel, Y.	Flow Pattern Transition for Downward Inclined Two Phase Flow: Horizontal to Vertical	*Chemical Engineering Science*, Vol. 37 (5), 1982, Pp. 735-740.	Developed model for transition in downward flowing two phase inclined pipe flow. Model compared with experimental results.
Barnea, D. Shoham, O. Taitel, Y.	Flow Pattern Transition for Vertical Downward Two Phase Flow	*Chemical Engineering Science*, Vol. 37 (5), 1982, Pp. 741-744.	Presentation of results of experiments on flow patterns of vertical downward gas-liquid flows. Also presents transition criteria for flow patterns.
Barnea, D. Shoham, O. Taitel, Y. Dukler, A.E.	Flow Pattern Transition for Gas-Liquid Flow in Horizontal and Inclined Pipes	*International Journal of Multiphase Flow*, Vol. 6, , 1980, Pp. 217-225.	Comparison of experimental measurements of flow patterns for two phase flows with theories of flow pattern prediction.
Barnea, D. Taitel, Y.	Transitional Formulation Modes and Stability of Steady State Annular Flow	*Chemical Engineering Science*, Vol. 44 (2), Pp. 325-332.	Develops criterion for stability in cocurrent and countercurrent two phase annular flows.
Bendikson, K.H. Espedal, M.	Onset of Slugging in Horizontal Gas-Liquid Pipe Flow	*International Journal of Multiphase Flow*, Vol. 18 (2), 1992, Pp. 237-247.	Quantitative examination of the relation between wave appearance, slug formation, and transition to stable slug flow in horizontal pipes.
Hall-Taylor, N. Hewitt, G.F. Lacey, P.M.C.	The Motion and Frequency of Large Disturbance Waves in Annular Two Phase flow of Air Water Mixtures	*Chemical Engineering Science*, Vol. 18, 1963, Pp. 537-552.	Examination of the initiating conditions, velocity, separation, and frequency of large disturbance waves in annular two phase flows.

Ishii, M.	Wave Phenomena and Two Phase Flow Instabilities	*Handbook of Multiphase Systems*, Ed. G. Hetsroni, 1982, Pp. 2.95-2.122	Discussion of wave formation and flow instabilities for two phase flows.
Jayanti, S. Hewitt, G.F. Low, D.E.F. Hervieu, E.	Observation of Flooding in the Taylor Bubble of Co-Current Upwards Slug Flow	*International Journal of Multiphase Flow*, Vol. 19 (3), 1993, Pp. 531-534.	Experimental study of flooding in the Taylor bubble of cocurrent upwards slug flow and its relation to transition to churn flow.
Kordyban, E.S.	The Transition of Slug Flow in the Presence of Large Waves	*International Journal of Multiphase Flow*, Vol. 3, 1977, Pp. 603-607.	Experimental study of wave instability as a cause of slug formation and comparison of experimental transition data to previous theoretical models.
Kordyban, E.S.	Some Details of Developing Slugs in Horizontal Two Phase Flow	*AIChE Journal*, Vol. 31 (5), 1985, Pp. 802-806.	Photographic study of slug development in horizontal two phase flows to explore the physical reasons for slug initiation.
Kordyban, E.S.	Horizontal Slug Flow: A Comparison of Existing Theories	*Journal of Fluids Engineering*, Vol. 112, 1990, Pp. 74-83.	A review of the accuracy of various theories concerning the transition to slug flow in horizontal two phase flow.
Kordyban, E.S. Okleh, A.H.	The Effect of Surfactants on Wave Growth in the Transition to Slug Flow	ASME, HTD-Vol. 260 / FED-Vol. 169, 1993, Pp. 73-84.	Study of the effect of surfactants on the transition to slug flow.
Kordyban, E.S. Okleh, A.H.	Growth of Interfacial Waves and the Transition to Slug Flow: Effect of Fluid Properties	Cavitation and Multiphase Flow Forum, FED-Vol. 135, 1992, Pp. 17-21.	Study of the effects of viscosity and surface tension on wave growth and thus on slug initiation.
Kordyban, E.S. Ranov, T.	Mechanism of Slug Formation in Horizontal Two Phase Flow	*Journal of Basic Engineering*, Vol. 92 (4), 1970, Pp. 857-864.	Theory that transition to slug flow is due to Kelvin-Helmholtz instability.

Minato, A. Ikeda, T. Masanori, N.	Mechanistic Model of Slugging Onset in Horizontal Circular Tubes	*Journal of Nuclear Science and Technology*, Vol. 23 (9), September 1986, Pp. 761-768.	Development of a model of the mechanism of transition from stratified to slug flow in horizontal two phase flows.
Mishima, K. Ishii, M.	Theoretical Prediction of Onset of Horizontal Slug Flow	*Journal of Fluid Engineering*, Vol.102, 1980, Pp. 441-445.	Theoretical derivation of a criterion for the initiation of slug flow in horizontal two phase flow.
Moissis, R.	The Transition from Slug to Homogeneous Two Phase Flows	*Journal of Heat Transfer*, Vol. 85 (4), 1963, Pp. 366-370.	Analysis of the transition from non-homogeneous slug flow to homogeneous frothy flow in two phase vertical flows in pipes.
Moissis, R. Griffith, P.	Entrance Effects in a Two Phase Slug Flow	*Journal of Heat Transfer*, Vol. 84 (1), 1962, Pp. 29-38.	Quantitative description of the developing slug flow regime.
Ruder, Z. Hanratty, P.J. Hanratty, T.J.	Necessary Conditions for the Existence of Stable Slugs	*International Journal of Multiphase Flow*, Vol. 15 (2), 1989, Pp. 209-226.	Experimental investigation of the minimum film heights and gas velocities required to initiate a slug in two phase flows.
Ruder, Z. Hanratty, T.J.	A Definition of Gas-Liquid Plug Flow in Horizontal Pipes	*International Journal of Multiphase Flow*, Vol. 16 (2), 1990, Pp. 233-242.	Experimental study of the transition from slug flow to plug flow for horizontal two phase flows
Spedding, P.L. Spence, D.R.	Flow Regimes in Two Phase Gas-Liquid Flow	*International Journal of Multiphase Flow*, Vol. 19 (2), 1993, Pp. 245-280.	Comparison of experimental results with existing flow regime maps and flow transition maps for co-current air-water horizontal flow.

Taitel, Y.	Flow Pattern Transition in Rough Pipes	*International Journal of Multiphase Flow*, Vol. 3, 1977, Pp. 597-601.	Extension of a previous model for the prediction of flow transition in horizontal pipes to include rough pipes.
Taitel, Y. Barnea, D. Dukler, A.E	Modeling Flow Pattern Transitions for Steady Upward Gas-Liquid Flow in Vertical Tubes	*AIChE Journal*, Vol. 26 (3), 1980, Pp. 345-354.	Development of models for predicting flow transition in steady two phase vertical flows.
Taitel, Y. Dukler, A.E.	A Model for Predicting Flow Regime Transitions in Horizontal and Near Horizontal Gas-Liquid Flow	*AIChE Journal*, Vol.22 (1), 1976, Pp. 47-55.	Presentation of models and a flow regime map for flow transition in horizontal and near horizontal two phase flows.
Taitel, Y. Dukler, A.E.	A Model for Slug Frequency During Gas-Liquid Flow in Horizontal and Near Horizontal Pipes	*International Journal of Multiphase Flow*, Vol. 3. 1977, Pp. 585-596.	Modeling of the frequency of the local liquid film motions during slug formation.
Wallis, G.B. Dobson, J.E.	The Onset of Slugging in Horizontal Stratified Air-Water Flow	*International Journal of Multiphase Flow*, Vol. 1, 1973, Pp. 173-193.	Presentation of a criterion for the transition from stratified to slug or plug flow in horizontal rectangular ducts.

Condensation and Bubble Collapse

Author	Title	Source	Comments
Akagawa, K. Hamaguchi, H. Sakaguchi, T.	Studies on the Fluctuation of Pressure Drop in Two Phase Slug Flow (3rd Report)	*Bulletin of the Japan Society of Mechanical Engineers*, Vol. 14 (71), 1971, Pp.462-469	Study of the pressure recovery behind a bubble rising in still water in a tube
Bankoff, S.G.	Some Condensation Studies Pertinent to LWR Safety	*International Journal of Multiphase Flow*, Vol. 6 (1-2), 1980, Pp. 51-67.	Discussion of steady-state turbulent stratified flows and of bubble studies as applied to reactor safety.
Bendikson, K.H.	An Experimental Investigation of the Motion of Long Bubbles in Inclined Tubes	*International Journal of Multiphase Flow*, Vol. 10, (4), 1984, Pp. 467-483.	Study of the relative motion of single long air bubbles in fluid flows in inclined tubes.
Bendikson, K.H	On the Motion of Long Bubbles in Vertical Tubes	*International Journal of Multiphase Flow*, Vol. 11 (6), 1985, Pp. 797-812.	Examination of the effects of surface tension and external forces on infinitely long bubbles in vertical pipes.
Biasi, L. Prosperetti, A. Tozzi, A.	Collapse of a Condensing Bubble in Compressible Liquids	*Chemical Engineering Science*, Vol. 27 1972, Pp. 815-822.	Analysis of bubble condensation in compressible fluids.
Biesheuvel, A. van Wijngaarden, L.	Two Phase Flow Equations for a Dilute Dispersion of Gas Bubbles in Liquid	*Journal of Fluid Mechanics*, Vol. 148, 1984, Pp. 301-318	Development of first order equations of motion for the dispersion of bubbles in liquids.

Block, J.A.	Condensation Driven Fluid Motions	*International Journal of Multiphase Flow*, Vol. 6 (1-2), 1980, Pp. 113-129.	Study of the interrelationship between condensation processes and fluid motions with references to specific industrial application..
Board, S.J. Kimpton, A.D.	Spherical Vapour Bubble Collapse	*Chemical Engineering Science*, Vol. 29, 1974, Pp. 363-371.	Experimental study of spherical bubble collapse in a subcooled fluid. Development of an incompressible equilibrium model of bubble collapse based on finite difference techniques.
Bornhorst, W.J. Hatsopoulos, G.N.	Analysis of a Liquid Vapor Phase Change by the Methods of Irreversible Thermodynamics	*Journal of Applied Mechanics*, Vol. 34 (4), 1967, Pp. 840-846.	Theoretical development of equations based on irreversible thermodynamics that predict fluid behavior during phase change.
Bornhorst, W.J. Hatsopoulos, G.N.	Bubble Growth Calculation Without Neglect of Interfacial Discontinuities	*Journal of Applied Mechanics*, Vol. 34 (4), 1967, Pp. 847-853.	A theoretical investigation of the importance of the nonequilibrium region at the bubble wall on the growth of a vapor bubble.
Chou, Y. Griffith, P.	Admitting Cold Water into Steam Filled Pipes Without Water Hammer Due to Steam Bubble Collapse	*Transient Thermal-Hydraulics in Vessel and Piping Systems*, PVP Vol. 190, ASME, NY, 1989, Pp. 63-71.	Development of stability maps for various geometries for the addition of subcooled water to steam filled pipes.
Florschuetz, L.W. Chao, B.T.	On the Mechanics of Vapor Bubble Collapse	*Journal of Heat Transfer*, Vol. 87 (2), 1965, Pp. 209-220.	Study of the importance of the effects of liquid inertia and heat transfer during the collapse of a bubble.

Guevara, E. Gotham, D.H.T.	Entrainment in Condensing Annular Flow	*International Journal of Multiphase Flow*, Vol. 9 (4), 1983, Pp. 411-419.	Comparison of experimental measurements of liquid film flow rates in condensing, horizontal, annular flow with correlations for entrainment based on previous studies.
Hawtin, P. Henwood, G.A. Huber, R.A.	On the Collapse of Water Vapour Cavities in a Bubble Analogue Apparatus	*Chemical Engineering Science*, Vol. 25, 1970, Pp. 1197-1209.	Development of a mathematical model to predict the rate of collapse of a vapor cavity in a bubble analogous apparatus.
Hickling, R. Plesset, M.S.	Collapse and Rebound of a Spherical Bubble in Water	*The Physics of Fluids*, Vol. 7 (1), 1964, Pp. 7-14.	Theoretical study of bubble collapse in a compressible fluid.
Hunter, C.	On the Collapse of an Empty Cavity in Water	*Journal of Fluid Mechanics*, Vol. 8, 1960, Pp. 241-263.	Theoretical study of the collapse of a vapor bubble, modeled as a spherical void, in a compressible fluid.
Leung, J.C.	Size Safety Relief Valves for Flashing Liquids	*Chemical Engineering Progress*, Vol. 88 (2), 1992, Pp. 70-75.	Discussion of the homogeneous equilibrium model as a sizing method for flashing liquids
Linehan, J.H. Petrick, M. El-Wakil, M.M.	On the Interface Shear Stress in Annular Flow Condensation	*Journal of Heat Transfer*, Vol. 91 (3), 1969, Pp. 450-452.	Discussion of models used to evaluate the interfacial shear stress in annular flim condensation.
Loyko, L.L.	Hydraulic Shock in Ammonia Systems	Presented at IIAR 11th Annual Meeting, March 12-15 1989.	Discussion of hydraulic shock and the conditions that cause hydraulic shock in ammonia systems

Loyko, L.L.	Condensation Induced Hydraulic Shock	Presented at IIAR 14th Annual Meeting, March 22-25 1992.	A discussion of condensation-induced shock and how to vary system designs to help prevent its occurrence
Moalem, D. Sideman, S.	The Effect of Motion on Bubble Collapse	*International Journal of Heat and Mass Transfer*, Vol. 16 (12), 1973, Pp. 2321-2329	Study of the effects of translational bubble velocity on the rate of bubble collapse.
Rayleigh	On the Pressure Developed in a Liquid During the Collapse of a Spherical Cavity	*Philosophical Magazine*, Vol. 34 (200), August 1917, Pp. 94-98	Theoretical study of the time of collapse of a spherical void in an incompressible fluid.
Trilling, L.	The Collapse and Rebound of a Gas Bubble	*Journal of Applied Physics*, Vol. 23 (1), January 1952, Pp. 14-17.	Theoretical study of the collapse and rebound of a vapor bubble in a compressible fluid.
Wittke, D.D. Chao, B.T.	Collapse of Vapour Bubbles with Translatory Motion	*Journal of Heat Transfer*, Vol. 89 (1), 1967, Pp. 17-24.	Study of the collapse of vapor bubbles where heat transfer is the controlling factor. Includes effects of translatory motion and noncondensable gas

Water Hammer: Causes, Impact, and Prevention

Author	Title	Source	Comments
Akselrod, A.F. Esselman, T.C. Griffith, P.G. Min, E.B.	Condensation Induced Water hammer in Steam Distribution Systems	*Fluid Transients and Fluid-Structure Interaction*, PVP-Vol. 224 / FED-Vol. 126, ASME, NY, 1991, Pp. 29-31.	A study of the effects of pipe inclination on condensation induced water hammer.
Anand, N.K. Schliesing, J.S. O'Neal, D.L. Peterson, K.T.	Effects of Outdoor Coil Fan Pre-Start on Pressure Transients During the Reverse Cycle Defrost of a Heat Pump	*ASHRAE Transactions*, Vol. 95 (2), 1989, Pp. 699-704.	Experimental investigation of the effects on refrigerant pressure transients when the outdoor coil fan is started prior to the termination of defrost
ANSI/ASHRAE	Safety Code for Mechanical Refrigeration	ANSI/ASHRAE 15 - 1992	Sets design and operation standards for mechanical refrigeration systems to promote system safety
ANSI/IIAR	Equipment, Design, and Installation of Ammonia Mechanical Refrigeration Systems	ANSI/IIAR, 1978.	Determines the standards for the design and operation of ammonia refrigeration systems.
Belytschko, T. Karabin, M. Lin, J.I.	Fluid Structure Interaction in Water Hammer Response of Flexible Piping	*Journal of Pressure Vessel Technology*, Vol. 108, 1986, Pp. 249-255.	Analysis of fluid-structure interaction for water hammer type flow conditions assuming incompressible flow.
Bergant, A. Simpson, A.	Quadratic Equation Inaccuracy for Water Hammer	*Journal of Hydraulic Engineering*, Vol. 117 (11), 1991, Pp. 1572-1574.	A comparison of two quadratic solution techniques used to solve the boundary conditions of a piping system..

Bjorge, R.W. Griffith, P.	Initiation of Waterhammer in Horizontal and Nearly Horizontal Pipes Containing Steam and Subcooled Water	*Journal of Heat Transfer*, Vol. 106, 1984, Pp. 835-840.	Presentation of experimental results concerning water hammer in horizontal pipes. Development of an analytical model for the prediction of water hammer initiation.
Bozkus, Z. Wiggert, D.C.	Slug Motion and Impact in a Voided Line	*Fluid Transients and Fluid-Structure Interaction*, PVP-Vol. 224 / FED-Vol. 126, ASME, NY, 1991, Pp. 25-27.	Study of the motion and impact of slugs through a voided line. Measurement of pressure forces exerted during slug impact at an elbow joint.
Budny, D.D. Hatfield, F.J. Wiggert, D.C.	An Experimental Study on the Influence of Structural Damping on Internal Fluid Pressure During a Transient Flow	*Journal of Fluid Mechanics*, Vol. 112, 1990, Pp. 284-290.	An experimental study of the effect that structural damping has on fluid pressure transients.
Cabrera, E. Abreu, J. Perez, R. Vela, A.	Influence of Liquid Length Variation in Hydraulic Transients	*Journal of Hydraulic Engineering*, Vol. 118 (12), 1992, Pp. 1639-1650.	Study of the effect liquid column length has on peak pressure of a system with entrapped air
Chaudhry, M.H Hussaini, M.Y.	Second-Order Accurate Explicit. Finite-Difference Schemes for Waterhammer Analysis	*Journal of Fluids Engineering*, Vol. 107, 1985, Pp. 523-529.	Comparison of three second-order accurate explicit finite-difference schemes used to solve the partial differential equations describing water hammer
Chiu, C. Tuttle, D. Serkiz, A.W.	Water Hammer in a PWR Horizontal Feedwater Line	*Transactions of ANS*, Vol. 52, Reno, Nevada, June 15-19 1986, Pp. 589-590.	Discussion of a water hammer incident in a main feedwater line and an analysis of the conditions needed to initiate water hammer in horizontal feedwater lines

Clarke, D.	Water Hammer: 1	*The Chemical Engineer*, No. 452, September 1988, Pp. 34-35.	Presents procedure on analyzing a system for potential water hammer and suggests some design changes to help prevent water hammer
Clarke, D.	Water Hammer: 2	*The Chemical Engineer*, No. 457, February 1989, Pp. 14-15.	Discussion on the use of surge suppression to avoid water hammer
Fleming, A.J.	Cost-Effective Solution to a Water Hammer Problem	*Public Works*, Vol. 121, July 1990, Pp. 42-44. suddenly stopped.	Discussion of water hammer that occurs when a large pump in a force main is
Gillessen, R. Lange, H.	Water Hammer Production and Design Measures in Piping Systems	*International Journal of Pressure Vessel and Piping Systems*, 1988, Pp. 219-234.	Discussion of methods by which to alter fluid dynamic conditions or piping systems designs so as to reduce the effects of water hammer.
Gray, C.A.M.	Analysis of Water Hammer by Characteristics	*Proceedings, ASCE*, Vol. 79, 1953, Paper 274.	Analysis of the effects of kinetic energy, friction, and change in wave form on the solution to the equations that describe water hammer.
Hatfield, F.J. Wiggert, D.C.	Water Hammer Response of Flexible Piping by Component Synthesis	*Journal of Pressure Vessel Technology*, Vol. 113, 1991, Pp. 115-119.	Presentation of an alternative method of calculating dynamic pressures and pipe displacements for water hammer conditions.
Huber, W.T. Barton, R.N.	Design Considerations for Mechanical Joints in Preinsulated Underground Piping Systems	*ASHRAE Transactions*, Vol. 89 (2B), 1983, Pp. 858-865.	Discussion on the use of certain seals as joints in preinsulated underground piping systems as well as some of the design considerations involved.

International Institute of Ammonia Refrigeration (IIAR)	Bulletin No. 116: Guidelines for Avoiding Component Failure in Industrial Refrigeration Systems Caused by Abnormal Pressure Shock	IIAR, October 31, 1992 (Draft)	Presentation of guidelines for ammonia refrigeration system design and operation in order to decrease the occurrence of pressure transients.
Kim, J.H.	Water-Hammer Prevention, Mitigation, and Accommodation: A Perspective	EPRI, 1987, Pp. 733-734.	Report on the frequency and cost of the occurrence of water hammer in industry.
Kim, J.H.	Two-Phase Water Hammer in Nuclear Power Plants	Cavitation and Multiphase Flow Forum -- 1987, O. Furuya, Ed., Cincinnati, OH, ASME, June 1987, Pp. 117-120.	Discussion of the effects of water hammer on industry and the research needs in this area for the future.
Kroon, J.R. Stoner, M.A. Hunt, W.A.	Water Hammer: Causes and Effects	*American Water Works Association Journal*, Vol. 76, November 1984, Pp. 39-45.	Review of the principles and causes of water hammer.
Loyko, L.L.	Hydraulic Shock in Ammonia Systems	Presented at IIAR 11th Annual Meeting, March 12-15 1989.	Discussion of hydraulic shock and the conditions that cause hydraulic shock in ammonia systems
Loyko, L.L.	Condensation Induced Hydraulic Shock	Presented at IIAR 14th Annual Meeting, March 22-25 1992.	A discussion of condensation-induced shock and how to vary system designs to help prevent its occurrence
Martin, C.S.	Status of Fluid Transients in Western Europe and the United Kingdom. Report on Laboratory Visits by Freeman Scholar	*Journal of Fluids Engineering*, Vol. 95 (2), 1973, Pp. 301-318.	A critique of the research efforts in Western Europe and the United Kingdom in the area of fluid transients.

Moody, F.J.	A Survey of Fluid Transient Studies -- 1991	*Journal of Pressure Vessel Technology*, Vol. 113, 1991, Pp. 228-233.	Discussion of various topics concerning fluid transients
Mosshart, Jr., D.J.	A Contractor's View of HVAC Noise and Vibration Problems	*ASHRAE Transactions*, Vol. 86 (1), 1980, Pp. 559-564.	Discussion of noise and vibration problems that occur in HVAC systems and some fundamental guidelines that can prevent such problems.
Neckowicz, T.S. Murphy, W.E. Goldschmidt, V.W. Johnston, R.C.R.	A Note on One Aspect of the Transient Response of Package Air Conditioners: Flooding of the Liquid Line	*ASHRAE Transactions*, Vol. 96 (2), 1984, Pp. 179-184.	Discussion of the relation of flooding of the liquid line at start-up to the transient response in the evaporator of an air conditioner.
Sibetheros, I.A. Holley, E.R. Branski, J.M.	Spline Interpolations for Water Hammer Analysis	*Journal of Hydraulic Engineering*, Vol. 117 (10), 1991, Pp. 1332-1351.	Investigation of the application of the method of characteristics with spline polynomials for interpolations for numerical water hammer analysis of horizontal pipes.
Singh, R.	Modeling of Fluid Transients in Machines--Part I: Basic Considerations	*Shock and Vibration Digest*, Vol. 12 (6), 1980, Pp. 7-14.	Literature review of the mathematical modeling of fluid transients in machines.
Singh, R.	Modeling of Fluid Transients in Machines--Part II: Advanced Considerations	*Shock and Vibration Digest*, Vol. 12 (7), 1980, Pp. 11-17.	Literature review of the applications and advanced considerations of mathematical models of fluid transients in machinery.
Singh, R. Nieter, J.J. Prater, Jr., G.	An Investigation of the Compressor Slugging Phenomenon	*ASHRAE Transactions*, Vol. 92 (1B), 1986, Pp. 250-258.	Study of the overpressures caused by liquid slugging that occur in refrigeration compressors

Streeter, V.L. Wylie, E.B.	Waterhammer and Surge Control	*Annual Review of Fluid Mechanics*, Vol. 6, 1974, Pp. 57-73.	Analysis of various numerical methods for computing system transients.
Suo, L. Wylie, E.B.	Impulse Response for Frequency-Dependent Pipeline Transients	*Journal of Fluid Engineering*, Vol. 111, 1989, Pp. 478-483.	Presentation of a numerical method for computing transients in piping systems. Frequency-dependent parameters are included.
Swierzawski, T.J. Griffith, P.	Preventing Water Hammer in Large Horizontal Pipes Passing Steam and Water	*Journal of Heat Transfer*, Vol. 112, 1990, Pp. 523-524.	Technical note on preventing water hammer in horizontal pipes having countercurrent flows of steam and subcooled water.
Walker, J.S. Phillips, J.W.	Pulse Propagation in Fluid Filled Tubes	*Journal of Applied Mechanics*, Vol. 44 (1), 1977, Pp. 31-35.	Presentation of a theory on the propagation of pressure pulses in an inviscid compressible pipe flow.
Wang, T. Shah, V.J. Nieh, L.C.S.	Waterhammer in a Stream Line Partially Filled with Trapped Condensate	*Transient Thermal-Hydraulics in Vessel and Piping Systems*, PVP-Vol. 156, ASME, NY, 1989, Pp. 23-27.	Investigation of a water hammer incident in a nuclear power plant and an analysis of the interface between steam and a liquid phase
Wedekind, G.L. Bhatt, B.L. Beck, B.T.	A System Mean Void Fraction Model for Predicting Various Transient Phenomena Associated with Two Phase Evaporating and Condensing Flows	*International Journal of Multiphase Flow*, Vol. 4 (1), 1978, Pp. 97-114.	Presentation of a system mean void fraction model for analyzing transients when complete vaporization or condensation occur in a two phase flow.
Weisman, J. Duncan, D. Gibson, J. Crawford, T.	Effects of Fluid Properties and Pipe Diameter on Two-Phase Flow Patterns in Horizontal Lines	*International Journal of Multiphase Flow*, Vol. 5, 1979, Pp. 437-462.	Presentation of experimental data on transitions in cocurrent, horizontal, two phase flows.

Wiggert, D.C. Otwell, R.S. Hatfield, F.J.	The Effect of elbow Restraint on Pressure Transients	*Journal of Fluids Engineering*, Vol. 107, 1985, Pp. 402-406.	Analysis of the effect that the type of elbow restraint has on the propagation of pressure transients.
Wood, D.J.	A Study of the Response of Coupled Liquid Flow Structural Systems Subjected to Periodic Disturbances	*Journal of Basic Engineering*, Vol. 90 (4), 1968, Pp. 532-540.	An analysis of the coupled responses of liquid flow systems and structural supports to pressure and flow pertubations.
Yeung, W.S Wu, J. Fernandez, R.T. Sundaram R.K.	RELAP5/MOD3 Simulation of the Water Cannon Phenomenon	*Nuclear Technology*, Vol. 101 (2), 1993, Pp. 224-251.	Investigation of the ability of the RELAP5/MOD3 computer code to analyze the transient behavior of water cannon phenomenon.